

ISTANBUL TECHNICAL UNIVERSITY ★ GRADUATE SCHOOL OF SCIENCE
ENGINEERING AND TECHNOLOGY

MODELING OF TLR4 SIGNAL TRANSDUCTION PATHWAY

Ph.D. THESIS

Aylin GÜNEL

Department of Physics Engineering

Physics Engineering Programme

NOVEMBER 2012

ISTANBUL TECHNICAL UNIVERSITY ★ GRADUATE SCHOOL OF SCIENCE
ENGINEERING AND TECHNOLOGY

MODELING OF TLR4 SIGNAL TRANSDUCTION PATHWAY

Ph.D. THESIS
Aylin GÜNEL
(509032100)

Department of Physics Engineering

Physics Engineering Programme

Thesis Advisor : Assoc. Prof. Dr. O. Yavuz EKŞİ
Co-Supervisor : Assoc. Prof. Dr. O. Ugur SEZERMAN

NOVEMBER 2012

İSTANBUL TEKNİK ÜNİVERSİTESİ ★ FEN BİLİMLERİ ENSTİTÜSÜ

TLR4 SİNYAL YOLAĞININ MODELLENMESİ

DOKTORA TEZİ
Aylin GÜNEL
(509032100)

Fizik Mühendisliği Anabilim Dalı

Fizik Mühendisliği Programı

Tez Danışmanı : Doç. Dr. Yavuz EKŞİ
Eş Danışman : Doç. Dr. O. Uğur SEZERMAN

KASIM 2012

Aylin Günel, a Ph.D. student of ITU Graduate School of Science, Engineering and Technology, 509032100, successfully defended the thesis entitled “MODELING OF TLR4 SIGNAL TRANSDUCTION PATHWAY”, which she prepared after fulfilling the requirements specified in the associated legislations, before the jury whose signatures are below.

Thesis Advisor : **Assoc. Prof. Dr. Yavuz EKŞİ**
Istanbul Technical University

Co-advisor : **Assoc. Prof. Dr. O. Uğur SEZERMAN**
Sabancı University

Jury Members : **Prof. Dr. H. Nüzhet DALFES**
Istanbul Technical University

Prof. Dr. Feride SEVERCAN
Middle East Technical University

Prof. Dr. Metin TÜRKAY
Koç University

Prof. Dr. Nazmi POSTACIOĞLU
Istanbul Technical University

Assist. Prof. Dr. Tolga BİRKANDAN
Istanbul Technical University

Date of Submission : 28 September 2010
Date of Defense : 22 November 2012

FOREWORD

This work is partially supported by 2214 TUBITAK research travel grant supplied for one year research period at UCSD, I appreciate TUBITAK for this support otherwise this thesis would never be possible. ITU Graduate School of Institute of Science and Technology supported this computational study by providing a computer at the end of my fifth year in PhD education.

The author appreciates Jose Onuchic for providing affiliate position at UCSD Center of Theoretical Biological Physics.

The author thanks Daniel Schultz, Ahmet Civas, Metin Türkay, Marcus Covert, Michael David, Gideon Schreiber, Metin Arık, Adem Tekin, Feride Severcan, Nüzhet Dalfes for their valuable discussions, Dr. Alexander Hoffmann for his help in the introduction of the author to the problem and his guidance through valuable discussion.

I appreciate Is Bank because I was able conduct my research mostly by loaning to Is Bank.

The auther also thankful to members of ITU Informatics Institute and UYBHM for providing technical support and their friendships.

I dedicate this thesis to my mother and father 20 years after left my home to be able to do science, to the wasted minds under mobbing and with PhD degrees lasting 7-10 years, which is 2-3 times longer than average PhD degree in Europe, finally and mostly to all the our martyrs who sacrificed their lives for these lands.

September 2011

Aylin GÜNEL

TABLE OF CONTENTS

	<u>Page</u>
FOREWORD.....	vii
TABLE OF CONTENTS.....	ix
ABBREVIATIONS	xi
LIST OF TABLES	xiii
LIST OF FIGURES	xv
LIST OF SYMBOLS	xvii
SUMMARY	xix
ÖZET.....	xxi
1. INTRODUCTION.....	1
1.1 Motivations and Main Achievements.....	4
1.2. Background	5
1.2.1 TLR4 pathway	5
1.2.2 Interferon beta pathway	13
1.2.3 NF- κ B circulatory network	16
1.2.4 PKR connection between IFN β and TLR4 pathway.....	19
1.2.5 Biologically important mechanisms.....	22
1.2.5.1 Feedbacks	22
1.2.5.2 Oscillation.....	23
1.2.5.3 Delay times	28
1.2.6 Tools of system biology	28
1.3 Theory	31
1.3.1 Reaction ordinary differential equations	31
1.3.2 Modeling with transfer functions	32
1.3.3 Optimization	35
1.3.3.1 Genetic algorithms.....	37
1.3.3.2 Pattern search.....	38
1.3.3.3 Nelder –Mead algorithm.....	40
1.3.3.4 Stochastic Modeling	40
1.3.3.5 Gillespie’s algorithm	41
2. METHODS	45
2.1 Method I-Transfer Functions and Simulink	45
2.2 Method II- Modeling with Ordinary Differential Equations.....	50
2.3 Method III-Modeling of the Interferon Transcription.....	51
2.4 Method IV-Modeling of the Signaling Cascades	57
2.5 The PKR Connection.....	65
2.6 Method V-Stochastic Modeling of Interferon Pathway	67
3. RESULTS and DISCUSSION.....	73
3.1 Results for the NF κ B-I κ B module	73
3.2 Modeling of TLR4 and IFN β Pathways with Ordinary Differential Equation Based Method	75
3.3 The Results for the PKR Connection	85

4. CONCLUSIONS.....	91
REFERENCES	97
APPENDICES	113
APPENDIX A	114
APPENDIX B	133
CURRICULUM VITAE.....	135

ABBREVIATIONS

ABM	: Agent based models
BMM	: Bone marrow-derived macrophage
B2TB1	: Inactive tuberculosis cells
CA	: Cellular automata
ELISA	: Enzyme-linked immunosorbent assay
EMSA	: Electrophoretic mobility
elf2α	: Eukaryotic initiation factor-2 α
HeLa	: Henrietta Lacks cell line
HMGB1	: High mobility group box 1
HMG-I(Y)	: High-mobility group protein
HL116	: Human fibroblast cells
IFN	: Interferon
IκB	: Inhibitor of κ light chain gene enhancer in B cells
IKK	: I κ B kinase
IL-1R	: Interleukine-1 receptor
IRAK	: IL-1 receptor-associated kinase
IRF	: Interferon regulatory factor
ISGF3	: Interferon-stimulated gene factor 3
ISRE	: Interferon-sensitive responsive element
JAKs	: Janus kinases
GA	: Genetic algorithm
KO	: Knockout
LBP	: LPS binding protein
LPS	: Lipopolysaccharide
MAPK	: Mitogen-activated protein kinase
MEF	: Mouse embryonic fibroblast
MyD88	: Myeloid differentiation primary response gene
MS	: Multiple Sclerosis
NCA	: Network component analyze
NIH3T3	: Mouse embryonic fibroblast cell line
NF-κB	: Nuclear factor- κ B
NRE	: Negative regularity element
NRF	: NF κ B repression factor
ODEs	: Ordinary differential equations
PAMP	: Pathogen-associated molecular patterns
PDE	: Partial differential equation
PIAS	: Protein inhibitor of activated STATs
PERK	: elf2 α kinase
PKR	: Protein kinase R, also known as dsRNA-activated protein kinase
RANTES	: Regulated upon activation, normally T cell-expressed, and secreted
RIP	: Rat insulin promoter
RIP1	: Receptor-interacting protein
SARM	: Sterile alpha and HEAT-Armadillo motifs-containing protein
SIGIRR	: Single immunoglobulin IL-1R-related molecule

SHP	: SH2 containing phosphates
SH2	: src homology 2
STAT	: Protein inhibitor of activated STATs
SOCS1	: Suppressor of cytokine signaling-1
TAK1	: Transforming growth factor- β -activated kinase 1
TANK	: TRAF family member-associated NF- κ B activator
TBK1	: TANK binding kinase 1
TIR	: Toll-Interleukin-1 receptor
TIRAP	: TIR domain-containing adaptor protein
TLR	: Toll-like receptor
TNFα	: Tumor necrosis factor α
TNFR	: TNF receptor
TRAF	: TNF receptor-associated factor
TRIF	: TIR domain-containing adaptor inducing IFN- β
TRAM	: TRIF-related adaptor molecule
UBC13	: Ubiquitin-conjugating enzyme 13
YY1	: Ying yag 1
WT	: Wild type
2fTGH	: Wild-type fibrosarcoma cells

LIST OF TABLES

	<u>Page</u>
Table 3.1: The list of model parameters and sources	86

LIST OF FIGURES

	<u>Page</u>
Figure 1.1: The schematics of the TLR4 and IFN β pathway.....	9
Figure 1.2: TIRAP-MyD88 and TRAM-TRIF interaction with TLR4 receptor.....	11
Figure 1.3: NF- κ B combinatorial structure, NF- κ B, I κ B genes, polypeptides and dimmers.	17
Figure 1.4 : NF- κ B (p50, p65) regulation.	18
Figure 1.5: LPS and IFN β stimulated pathways.	20
Figure 1.6: Under the DNA damage PKR expression induced by P53 and concomitant tumor inhibition mechanisms.	21
Figure 1.7: A sketch of the feedback loops controlling the concentration NF- κ B..	23
Figure 1.8: NF- κ B nuclear localization predicted by a computational model.	24
Figure 1.9: Some of the important part of the NF- κ B regulatory system.	26
Figure 1.10: An equivalent transfer function of single feedback system.....	22
Figure 1.11: A block representation of transfer function.....	32
Figure 1.12: Graphic illustrates the parameters used for determination of transfer function and second order systems.	34
Figure 1.13: I κ B α over expressed NF κ B activation.....	35
Figure 1.15: A comparison of derivative based algorithm and pattern search infinding the minima when a rough surface or when a stochastic noise present.....	39
Figure 1.16: NF- κ B oscillations.	42
Figure 2.1: Transfer functions giving the NF κ B activity profile for I κ B isomorms isolated effects and for wild type cells.	46
Figure 2.2: The output of transfer functions for the model having real time scale...	47
Figure 2.3: Some of the possible models that suits to existing experimental knowledge.....	48
Figure 2.4: Some of the possible models planed to analyze.	49
Figure 2.5: Dependence of $F_{\text{regulatory}}$ on f_{AB} and w values.	56
Figure 2.6: Dependence of IFNmRNA on f_{AB} and w values.	57
Figure 2.7: The schematics of model structure based on feedback mechanisms.....	58
Figure 2.8: The schematics of the TLR4 and IFN β model.	65
Figure 2.9: Schematics of interferon mRNA production.....	68
Figure 3.1: Results of optimization for the total NF κ B profile, gains and delay in the system: (a), (b), (c)..	74
Figure 3.2: <i>In silico</i> simulations of the IRF3 expression profile and dose response curves.....	77
Figure 3.3: The simulation results for IFN β in comparison with experimental values.....	78
Figure 3.4: The proposed LPS-ISGF3 dose response curves.	81
Figure 3.5: The effect of degradation and internalization rate on the transcription factor profile.	82
Figure 3.6: Expression profiles of some othe specific reaction species.....	83
Figure 3.7: PKR activation under the influence of 100 ng/ml LPS.	89

LIST OF SYMBOLS

A, B	: The number of the two types of the transcription factor molecules
Dl	: Diffusion rate of molecules
f_{AB}	: The ‘glue-like’ interaction between polymerase and the union of two transcription factors acting.
f_p	: Binding affinity of P53 to polymerase on specific promoter site of DNA.
f_{pkr}	: Binding affinity of PKR to polymerase on specific promoter site of DNA.
f_x	: The ‘glue-like’ interaction of X transcription factor and polymerase on specific promoter site of DNA.
F_{reg}	: Regulatory factor. A factor reflecting effect of transcription factors on the effective change in the number of RNA polymerases binding to promoter.
K_d	: PKR degradation rate
K_p	: Effective equilibrium dissociation constant of P53
K_{pkr}	: Effective equilibrium dissociation constant of PKR
$K_1, K_2 \dots K_{83}$: Reaction kinetics rates (equation 2.17-2.42, the values are given in Table 1)
k_1, k_2, k_3	: Reaction rates (equation 1.1-1.7)
k, k_p, k_{pkr}	: Regulation factor rate
K_x	: Effective equilibrium dissociation constant for x molecule
NS	: non Specific sites
P	: The number of the two types of the transcription factor molecules.
P_o	: The Boltzmann weight denoted for the polymerase binding to specific site
P_{oo}	: Unoccupied promoter region.
P_{o1}	: NFkB bound promoter.
P_{1o}	: IRF3 bound promoter.
P_{11}	: NFkB and IRF3 bound promoter (the bound form of enchosome)
P_{bound}	: Binding probability of RNA polymerase molecules to promoter of interest both in presence and absence of activators.
P_l	: Boltzmann weight for the RNA polymerase binding to non-specific site.
S	: specific sites
Z	: Partition function
Z_{total}	: Total partition function of the system.
Z_{bound}	: Partition function of RNA polymerase bound states to specific sites.
α	: Boltzmann weight denoted for the activator-a binding to specific site
β	: Boltzmann weight denoted for the activator-b binding to specific site
α_l	: Boltzmann weight for the activator-a binding to non-specific site
β_l	: Boltzmann weight for the activator-b binding to non-specific site
ϵ_{xd}	: Binding energy of molecule X to DNA

$\epsilon_{\text{xd}}^{\text{NS}}$: Average binding energy of molecule X to the genomic background
$\epsilon_{\text{pd}}^{\text{S}}$: Average binding energy of RNAP to the genomic specific sites
$\Delta\epsilon_{\text{xd}}$: Difference of average binding energy of molecule X to specific and nonspecific sites
ω	: Interaction between two transcription factors.
[IFN β]	: concentration of IFN β ,
[IFNAR]	: concentration of IFNAR,
[IFNAR2]	: concentration of dimerized IFNAR,
[IFNAR2IFN β]	: concentration of dimerized IFNAR and IFN β complex,
[IFNAR2JAK]	: concentration of dimerized IFNAR, JAK complex,
[IFNAR2JAKIFN β]	: concentration of dimerized IFNAR, JAK and IFN β complex,
[ISGF3]	: concentration of ISGF3,
[ISGF3N]	: concentration of ISGF3 in the nucleus,
[IFNmRNA1]	: concentration of IFN β mRNA,
[PKRmRNA1]	: concentration of PKR mRNA,
[PKR]	: concentration of PKR,
[LPS]	: concentration of LPS,
[TLR4]	: concentration of TLR4,
[LPS2TLR4]	: concentration of dimerized TLR4 and LPS complex,
[LPS2TLR4TRIFF]	: concentration of dimerized TLR4, LPS and TRIFF complex,
[LPS2TLR4TRAM]	: concentration of dimerized TLR4, LPS and TRAM complex,
[TRAF3]	: concentration of TRAF3,
[TBK]	: concentration of TBK,
[IRF3]	: concentration of IRF3,
[IRF3N]	: concentration of IRF3 in the nucleus,
[IFNmRNA1]	: concentration of IFN β mRNA in the nucleus,

MODELING OF TLR4 SIGNAL TRANSDUCTION PATHWAY

SUMMARY

A principal challenge for life sciences is to understand the organization and dynamics of those components that make up a living system. Understanding the systems of cellular processes is very similar to solving many body problems including complex interactions, in this case among a large number of genes, proteins and other molecules. One way to achieve such an aim is passing through the investigation of signaling pathways by computational Modeling approaches.

Bacterial lipopolysaccharide (LPS) association with their connate receptor TLR4 triggers Type I interferon signaling cascade through its MyD88 independent downstream. Compared to plethora of reported empirical unorganized data on TLR4 and Type I interferon pathways, there is no known model to decipher crosstalk mechanisms between these two crucial innate immune pathogen activated pathways regulating vital transcriptional factors such as nuclear factor- κ B (NF κ B), interferon beta (IFN β), the interferon-stimulated gene factor-3 (ISGF3) and an important cancer drug target protein kinase-R (PKR).

Innate immune system is based on a sensitive balance of many interactions. Attempts restricted to single pathway resulted in misleading Modeling infrastructures in reported models such as introducing conjectural 6 hour delay in single transcription step for PKR, in this aspect, *in silico* combination of immune regulatory systems have great potential to unravel elusive regulatory mechanisms.

In this study we model the NF κ B-I κ B signaling module by control theory approaches and the interactions between two vital pathogen activated pathways, namely the TLR4-MyD88 independent and interferon pathways, overall by utilizing reaction kinetics ODEs and a statistical approach at the transcriptional level. This is the first report joining toll-like receptor-4 (TLR4) and IFN β pathways in a single *in silico* model, analyzing the crosstalk mechanisms, explicitly Modeling the cascade through TLR4-IKK, limiting the transcription of IFN and PKR by introducing a hybrid method including a statistical physics technique and pinpointing the source of delay in PKR late phase activity. The TLR4-IFN β model quite successfully recapitulates published interferon regulatory factor-3 (IRF3) and IFN β data from mouse macrophages and PKR data from mouse embryonic fibroblast cell lines. The simulations end up with an estimate of IRF3, IFN β , ISGF3 profiles for different doses of LPS and IFN β ligands. Involvement of concomitant PKR downstream can reveal elusive mechanisms in specific profiles like NF κ B regulation.

TLR4 SİNYAL YOLAĞININ MODELLENMESİ

ÖZET

Tanı ve tedavi yöntemleri belirlemek için, sisteme ait parçalar hakkında ayrı ayrı bilgiye sahip olmak yeterli gelmemekte ve bu parçaların nasıl etkileştiği bilgisine ihtiyaç duyulmaktadır. Bugün halen bilim dünyası en basit organizmaların bile sistem olarak tüm işleyiş mekanizmasını çözmekten uzaktır. İşte tam bu noktada disiplinler arası bir dal olan sistem biyolojisi önemli bir rol üstlenmektedir. Bu sebeple yaşam ile ilgilenen bilim alanlarının başlıca uğraşısı yaşamsal birimi oluşturan parçaların düzenini ve dinamiğini anlamaktır. Bu uğraş karmaşık etkileşimler içeren çok parçalı problemi çözmeye benzer, ki bu durumda parçacıkların yerini yüksek sayıda gen, protein ve diğer moleküller alır. İşte tam bu noktada disiplinler arası bir dal olan sistem biyolojisi önemli bir rol üstlenmektedir.

Sistem biyolojisinin temelinde DNA, RNA, proteinler ve yağlar gibi biyomoleküller arasındaki dinamik etkileşim mekanizmalarını, metabolik yapının küçük bir parçasından, tüm organizma düzeyine kadar pek çok seviyede inceler. Erken teşhis ve tedavi yöntemleri, önleyici tıbbi yöntemler, enfeksiyona ve enflamasyona karşı özel yöntemler geliştirmek sistem biyolojisinin önemli hedefleri arasında yer alır. Bütün bu çalışmaların bir geri döngüsü de tanı ve tedavi yöntemlerini her kişiyi farklı yapan özellikleri göz önünde bulundurarak, kişiye özel bir şekle dönüştürebilmek olacaktır.

Sistem biyolojisi yinelemeli yöntemler takip eder. İlk aşamada yöntemleri sistem bileşenleri ve bunların bir biri ile etkileşimi belirlenir. Bu sonuçlara göre sistem hakkında öngörülerde bulunmakta kullanılacak modeller geliştirilir.

Biyolojik yapıyı oluşturan temelleri anlayanın etkin yollarından biri de bilgisayar ortamında hesaplamalı modeller oluşturmaktır. Biyolojik sistemlerin matematiksel olarak modellenmesi ve hesaplamalı yöntemlerle çözülmesi mümkün tüm molekülleri denemek yerine içlerinden en iyi adayları ve bunlara en uygun hedefleri göstermedeki potansiyelleri açısından sistem biyolojisi içinde büyük bir öneme sahiptir. Bir ilaç geliştirmek için mevcut olası her kimyasal yöntemi denemek ne zamansal nede maddi açıdan etkin bir yöntem değildir. Biz bu çalışmada vücudun doğal bağışıklık sisteminde önemli rol oynayan NF κ B-I κ B sinyal modülünü kontrol teorisi yöntemleri kullanarak, ve yine hayati açıdan çok önemli TLR4-MyD88, interferon beta sinyal yolağı isimli iki yolağını reaksiyon kinetiği differansiyel denklemleri kullanarak bilgisayar ortamında modelledik. Bağışıklık sistemini sinyal yollarının bu tür bilgisayar modelleri ile kombinasyonu, yollar tek tek incelendiği zaman açıklamanın mümkün olmadığı pek çok olaya çözüm getirebilir. Bu durum göz önünde bulundurularak bu çalışmadaki modeller literatürdeki ilgili yollarının modellerine uyumlu olarak geliştirilmiştir.

Moleküler sinyal yolağı modelleri reaksiyon katsayıları gibi pek çok parametreye bağlıdır. Bu parametrelerin bazıları hassas bir şekilde belirlenebilse de, diğerleri bilinmemekte yada insan genetik farklılıklarının sebep olduğu bireysel farklarla ölçülmesine olanak olmamaktadır. Bu tarz parametrelerin elde edilmesi pek çok durumda sadece, yolak modellerinden elde edilen sonuçların deneysel verilerden elde

edilen sonuçlar ile hesaplamalı yöntemler kullanarak karşılaştırılması ile mümkün olur.

NF- κ B bağışıklık sisteminde planlı hücre ölümü, inflamasyon, kanser, sistemin stres tepkileri gibi pek çok olayda önemli rolü olan bir transkripsiyon faktörüdür. NF- κ B ekspresyonu insan bağışıklık sistemindeki çok sayıda farklı uyarana karşı oldukça ılımlı bir şekilde gerçekleşir. Bu ekspresyondaki ani ve sert değişiklikler ölümcül sonuçlara sebep olabilir. Bağışıklık sistemini enfeksiyon durumunda yaşamsal risk yaratmayacak şekilde tepki verir.

Bu çalışmadaki bir amacımız NF κ B'nin bu ılımlı düzenlenme mekanizmasını, transfer fonksiyonları kullanarak, NF- κ B-I κ B sinyal modülü düzeyinde açıklamaktır. Bu sebeple olası mekanizmaları içeren farklı modeller, her reaksiyon bileşeninin davranışını üreten transfer fonksiyonları ile kurulmuş, bu modellerden doğal mekanizmaya uyumlu olanları optimizasyon yöntemleri ve literatürdeki veriler kullanılarak belirlenmeye çalışılmıştır. Bu yöntemle biyolojik sistem içindeki geri besleme mekanizmalarının nasıl işlendiği incelenmiştir. Çalışma sonucunda deneysel NF κ B ekspresyonu üreten bir model geliştirilip, yöntemin geçerli olduğu limitler literatürdeki uygulamalarla karşılaştırılarak değerlendirilmiştir. Elde edilen model ile deneysel NF κ B zamana bağlı konsantrasyon değişimi verisi, ilk tepenin genliği dışında, genel özellikleri açısından aynen elde etmek mümkün olmuştur. Bu modelden yola çıkarak LPS uyaralı NF κ B regülasyonunu, uyarın seviyesinden itibaren temsil edecek bir model öngörülmüştür. Burada bahsi geçen çalışmada verilen modeller ile sistemin farklı koşullarda nasıl davranacağını öngörmek için, tepkime üyelerinin bu farklı şartlar altında nasıl davranacağını içeren bir veri kütüphanesine ihtiyaç vardır. Zira oluşturulan her transfer fonksiyonu sistemin sadece o koşul için nasıl davranacağını belirten özel bir çözümdür. Bağışıklık sistemi çoğu zaman oldukça doğrusal olmayan davranışlar sergilediği için, bu özel çözümlerin başka sınır koşullarında sistemin gerçek durumunu yansıtmaması ve deneysel sonuçlarını yinelenmemesi kuvvetli bir ihtimaldir. Bu davranışları lineer modelleme yöntemleri ile çözümlemeye çalışmak ancak yoğun bir deneysel verinin varlığında etkin olur, yani her durum için doğru transfer fonksiyonlarının belirlenmesi bu durumlarda sistemin davranışını tanımlayan bilgi gerektirir.

Çalışmanın ikinci aşamasında TLR4 ve IFN β yolları için literatürde yayınlanmış olan fare makrofaj hücrelerinden elde edilmiş IRF3 ve IFN β verilerine uyumlu şekilde adi differansiyel denklemler kullanılarak modeller geliştirilmiştir. Elde edilen denklemler MATLAB ortamında literatürde yer alan veriler doğrultusunda çözülmüştür. TLR4 modelin çıktısı olan IFN β 'nin IFN β yolağındaki interferon reseptörünün tetiklenmesi için kullanılarak bu modeller birleştirilmiştir. Similasyon LPS ve interferonun farklı seviyeleri için ISGF3 ve PKR nin zamana bağlı yoğunluk değişimlerinin elde edilmesi ile sonuçlanır. PKR önemli bir kanser ilaç hedefi olup, literatürde doz tepki eğrileri mevcut olmadığı için, bu çalışma bu verilerin elde edilmesi açısından da önem arz etmektedir. Ayrıca LPS etkisi ile üretilen NF κ B nin uygulanması ile deneysel verilere çok yakın bir IFN β davranışı elde edilmiştir. Deneysel sonuçlarla uyumlu olarak, oluşturulan model de reseptör metabolizmasının transkripsiyon faktörü davranışını düzenleyen başlıca etkenlerden biri olduğunu işaret etmiştir.

Bu çalışmada hayati açıdan çok önemli iki farklı patojen aracılığı ile tetiklenen yolağı literatürde ilk olarak tek bir hesaplamalı model üzerinde birleştirilerek, aralarındaki etkileşim incelenmiştir. Yine ilk kez bu yolların diğer modellerinden farklı olarak gen transkripsiyonu seviyesinde, üretimini üst sınır sağlayabilmek için istatistiksel fizik yöntemlerini içeren melez bir yaklaşım uygulanmıştır. İlâveten PKR

geç fazındaki gecikmeyi üretebilmek için literatürde belirtilen transkripyon seviyesinde 6 saatlik yapay bir gecikme yaratan fonksiyonun yerine, gene ilk olarak iki yolağın etkilesmesinden kaynaklı doğal süreç kullanılmıştır. Bu çalışmada PKR üretimine kadar olan aşamalar modellenmiş olsa da, modelin sonuçlarının kullanılarak genişletilmesi ile NFκB seviyesini düzenleyici diğer mekanizmaların aydınlatılması da olasıdır.

1. INTRODUCTION

Biological signaling cannot be totally understood by ignoring the communication mechanisms between different pathways and the effect of the many positive or negative feedback regulatory mechanisms. Diverse cell response characteristics of mammalian species is a result of interaction networks between over 3000 signaling proteins and 15 secondary messengers (Brandman and Meyer, 2008; Jordan et al., 2000).

The properties of networks such as the World Wide Web, food webs, transportation networks, social, email networks, citation networks, software call graphs and biochemical signaling networks have been drawing attention within the physics community for a while. Interest of physics community to explain life is not only restricted with quite recent network analysis. Schrodinger's discussion about dependence of biological events to individual atoms or molecules has great impact on foundation of molecular biology and his ideas about treating living organisms as purely mechanical systems to explain their behaviour is one of the basis of today's system approach to biology (Schrodinger, 1944; Schrodinger, 1967; Wellstead, 2005). Despite its great contribution, like the other disciplines, physics alone is not enough to resolve whole biological mechanisms. To date, several methods of many disciplines are utilized to understand and model the biochemical signaling pathways. While Schrodinger's system approaches, together with electrical engineering system and signal analysis methods form the early groundwork ushering in prelude systems biology, Wellstead (2005), today broad network of disciplines are integrated under this innovative field to understand the life and contemporary system biology has become a paramount paradigm for life sciences in the last decade.

Systems biology is a recently emerging field with highly multi-disciplinary scope and bursting very promising developments in life sciences. The main interest of system biology is the dynamics of interactions between bio-molecules like DNA, RNA, proteins, lipids and metabolites at various levels ranging from a small part of a metabolic pathway in an organelle to an organism level. To perform this, an iterative

approach is followed. The first step is the determination of system components and their interactions. Consecutively, a predictive model is constructed and its conjectures are tested by present or forthcoming data from experiments which in turn lead to the refinement of the model and construction of new hypotheses. Among the system biology tools, one of the most prominent methods to model cellular dynamics is the use of ordinary differential equations (ODEs) that we also applied in this study.

Developing opportunities for early and accurate diagnosis, preventative strategies, specific treatments for infectious and inflammatory diseases are the important objectives of system biology. One spin off them in prospect is to personalize diagnoses and therapies, by concerning the factors making each individual unique.

Considering its complexity, abundance of interaction and medical significance, one of the ideal application for system biology is immune system. For appropriate immune response various complex interactions, feedbacks, and dynamical behavior is essential as in the case of the innate immune response, which is highly context dependent and according to the context, while pathogen and host factors can be protective, it can also be injurious. For example depending on dose of pathogens, Toll-like receptor (TLR)-2 and myeloid differentiation response gene 88 (MyD88) either defend against spread of Group B Streptococcus in the case of low concentrations or can promote lethality for high doses (Mancuso et al., 2004).

The positive and negative feedback mechanisms are very important in regulation of biological systems. Blurriness in connection of the signaling input-output behavior by known feedback relations can illustrate the presence of missed mechanism (Brandman and Meyer, 2008). Even a very small part of innate immune system like the NF κ B-I κ B signaling module can involve many such mechanisms (Kearn et al, 2006; Basak et al., 2007).

Innate immune system also includes many examples of other types of complex interaction like the ones existing among Toll-like receptors (TLRs: receptors recognizing microbial pathogens signaling) and interferon (IFN) pathways. It is known that the viral by-product double stranded RNAs are sensed via TLR3 pathway and leads production of viral IFNs (Alexopoulou et al., 2001). TLR4 also produces IFN through MyD88 independent pathway that is common both in TLR3 and TLR4 signaling cascade (Kawai et al., 2001; Yamamoto et al., 2003).

At the line of contact in between the pathogens and internal milieu, epithelial cells secrete Type I IFNs as a first defence mechanism facing invading viruses (Jamaluddin et al., 2001). Interferons have important roles in antiviral activities of the cells. It is known that lipopolysaccharide (LPS) stimulation results in IFN β transcription via the MyD88 independent pathway (Kawai et al., 2001; Yamamoto 2003). Thus, there is a close correlation between the responses of the cell in the presence of viral and bacterial infection, and presumably being treated with one of them makes the cell more vulnerable to the other.

Computational models are very effective tools in organizing the correlations and contradictions among the vast amount of data in the literature, pointing to the missed parts and possible other outcomes of the systems. Models of molecular signaling pathways in cells include large numbers of parameters, such as reaction rates. While some of these parameters are known quite accurately, others are either unknown or even impossible to measure, partly because of the fact that human genetic polymorphisms may cause individual variability of some of these parameters. For these reasons, estimation of such model parameters needs to be accomplished by fitting models of pathways involving these parameters to available data. Optimization methods are effective tools to attain the proper fit for the system, but in many case intuitive methods based on biological data are also indispensable because of large search space.

In this study we had searched for the properties of biochemical signaling network regulating the transcription factors such as NF κ B, IRF3 and ISGF3 expression having a role in many vital biological processes. Throughout the last decade an avalanche of research is conducted on these proteins because of their roles in immune response, inflammation, and development. Compared to extensive amount of experimental studies conducted to understand the mechanisms of LPS and IFN β stimulated pathways, at hand only a few comprehensive mathematical or computational models exist for TLR4, even less for the IFN β pathways. We utilized system biology tools and transfer functions in control theory to model these pathways.

1.1 Motivations and Main Achievements

Immune system needs to defend against an infection without risking the organism survival. In immune system NF κ B expression to wide range of stimulation is moderate and harsh changes could be fatal. One of the main motivations in this study is to develop mathematical models explaining such a moderate regulation of NF κ B with methods relayed on reaction kinetics ODEs, transfer functions of control theory and optimization techniques. Still there are many unsolved mechanism for LPS and IFN β stimulated pathways and related NF κ B expression. My purpose is to suggest models illuminating some of these mechanisms and anticipate the illusive parts of stable behavior of the LPS mediated NF- κ B puzzle.

Because of the natural cross correlations and concomitant highly linked outcomes, to simulate the whole picture, it is very important to integrate the pathways. In this sense compatibility in between the models of individual pathways is also very important to consider. With this point of view, we developed computational models for the IFN β and TLR4-MyD88 independent pathways separately, and linked them on a single model that can also be used as part of a more comprehensive structure in combination with other pathogen activated pathway (PAMP) models in the literature. In terms of modelling aspects, this is the first reported attempt to join TLR4 and Interferon beta pathways and to analyze how they communicate with each other.

The ODE model proposed in this study combines reaction kinetics approach for the signal transduction and a probabilistic approach at the transcription level. For TLR4 and IFN β signaling cascade, in parallel with experimental data available in the literature, the results indicated that receptor metabolism like degradation, internalization and complex formation is an important factor in determining the trends of transcription factors' expression profiles. This model successfully reproduced the experimental interferon IRF3 and IFN β expression levels and profiles. Moreover, we propose the possible dose response curves for ISGF3 profiles corresponding to the different levels of LPS and test the results with published dependent PKR expression data.

1.2 Background

1.2.1 TLR4 pathway

TLR4 signal transduction pathway forms an important part in the immune system. Gram-negative bacteria are detected through their LPS regions by transmembrane TLR4 receptors (Carpenter and O'Neill, 2007; Kawai and Akira, 2007). A concomitant signaling cascade via both MyD88 dependent and independent pathways, Kawai et al. (2001), leads to free nuclear factor kappa-light-chain-enhancer of activated B cells (NF κ B) and according to the pathway, interferons and cytokines. Most of the cell types can produce Type I interferon IFN α and IFN β (Barton and Medzhitov, 2003; Meylan et al., 2004; Vivarelli et al., 2004; Katze and He, 2002). Despite the 14 different IFN α genes, IFN β is encoded by single gene (Katze et al., 2002; Kelley and Pitha, 1985; Chen, 2004) and NF κ B and IRFs function together in the transcription of IFN β gene (Thanos, and Maniatis, 1995; Hu et al., 2007).

TLR family members consist of more than 13 members and from TLR1 to TLR10, ten of them have been identified in humans. In mice total twelve TLRs numbered in between 1-9 and 11-13 exist (Takeda, Kaisho, Akira, 2003; Kawai and Akira, 2006). They are component of a wide range of cells in immune system, i.e., macrophages, dendritic cells, neutrophils, B cells and non-immune cells like keratinocytes fibroblast cells and epithelial cells (Kawai and Akira, 2007).

The interaction in between TLR4 and LPS is mediated by a protein called as lymphocyte antigen 96 or MD-2 (Kumar et al, 2009; Kawai and Akira, 2009). The sequence of events after this association remained a mystery for a while. In an early computational study (Selvarajoo, 2006) on MyD88 independent pathway conducted to explain late phase NF κ B activity, the number of intermediates acting through the downstream was claimed as the source of the phase. The reason behind this suggestion was based on the fact that in the models representing MyD88 knockouts, the changes neither in the kinetic rates nor the reaction kinetics equations were not enough to recapitulate the correct NF κ B profile but incorporation of a few unknown intermediates and slowing down the reaction kinetics would lead to the desired expression profile. However another experimental study, Kagan et al., (2008), revealed that the proposed unknown intermediates are not different reaction species but rather endocytosis of TLR4, sequential events during this stage and transportation of the endosome, which are very important in providing the delay necessary to

produce LPS stimulated NFkB profile. The results of the experiment indicate that at the initial stage of TLR4 stimulation, toll-interleukin 1 receptor (TIR) domain-containing adaptor protein (TIRAP)-MyD88 complex interacts with the receptor through its TIR domain. This is followed by internalization of TLR4 by endocytosis (Kagan et al., 2008). Releasing the TIR domain, TRIP- MyD88 complex is not involved in this process, which allows sequential association of TRIF-related adaptor molecule (TRAM) and TIR domain containing adapter inducing interferon- β (TRIF) complex to the remaining empty domain (Kagan et al., 2008). Some *in silico* results indicate a competitive relation between TRAM and the tumour necrosis factor associated factor (TRAF) for the TIR domain (Selvarajoo et al., 2008). The experiment conducted to validate this competitive behaviour illustrates an increase in the early IRF3 expression, Selvarajoo et al. (2008), which is incongruous with the experimental study showing the formation of endosomes and sequential binding to TLR4 (Kagan et al., 2008). However, other evidences in MyD88 knockouts seems to contradict with competitive behaviour and support the sequential binding and endocytosis by indicating a decrease in the level of phosphorylation of down stream molecules like IRF3 (Kawai et al., 2001).

TLRs cause recruitment of a set of adaptor proteins due to the homophilic interactions between their TIR domains and that of adaptor proteins (O'Neill and Bowie, 2007; Kawai and Akira, 2007). Five adaptor proteins contain TIR domain, O'Neill and Bowie (2007), and among all TLRs, TLR4 is the only one known as utilizing all these adaptor proteins (O'Neill and Bowie, 2007). The adaptor proteins are:

- Myeloid differentiation primary response gene 88 (MyD88)
- TIR domain-containing adaptor protein (TIRAP), also named as Mal, MyD88-adaptor- like
- TRIF-related adaptor molecule (TRAM),
- TIR domain-containing adaptor inducing IFN- β (TRIF),
- Sterile Alpha and HEAT-Armadillo motifs-containing protein (SARM) seems to act as an inhibitor of TRIF-mediated signaling in the human HEK293 cell line (Peng et al., 2010). However, the role of SARM in vivo is still unclear (Peng et al., 2010).

Several proteins get involved in LPS stimulation of mammalian cells including the LPS binding protein CD14, (LBP), TLR4 and MD-2 (Gioannini, Weiss, 2007; Miyake, 2007; Lu, Yeh, Ohashi, 2008). LBP is a soluble protein facilitating LPS and CD14 association (Tobias and Soldau, 1986; Wright et al., 1989). CD14 helps the LPS

to be transferred to the TLR4-MD-2 complex (Wright et al., 1990). TLR4 facilitates binding of LPS to MD-2 (Mitsuzawa et al. 2006). In this study, we summarized all of these stages in a single step for the sake of modeling simplicity and because of restricted knowledge about their exact kinetic mechanisms.

TLR4 signals mainly through two pathways (Takeda and Akira, 2004):

- MyD88 Dependent Pathway results in induction of vital proinflammatory cytokines like $\text{TNF}\alpha$, IL-6, SOCS3, JNK, $\text{NF}\kappa\text{B}$, ERK. (Selvarajoo, 2008).
- MyD88 Independent or TRIF Dependent Pathway mainly induces chemokines such as IP-10, Type I interferons (IFNs) (Takeda and Akira, 2004) and dependent proteins through IRF3 and IRF7 in the presence of $\text{NF}\kappa\text{B}$ (Lu et al., 2008).

In addition to activate canonical $\text{NF}\kappa\text{B}$ pathway, both MyD88 and TRIF dependent pathway utilizes distinct signaling cascades defining its unique effectors function.

Despite TLR3, TLR4 additionally triggers MYD88 dependent pathway, which is exclusive to the cell surface membrane (Kumar et al., 2009). TRAM serve at the downstream of TLR4 (Yamamoto et al. 2003a, Yamamoto et al. 2003b). After the association of TLRs with MyD88, the resultant complex recruits death domain of the member IL1 receptor associated kinases family (IRAK) through MyD88 death domain by homophilic interactions (Barton and Medzhitov, 2003). While the family members like IRAK1, IRAK2 and IRAK4 act as TRAF6 activator, IRAK-M blocks this activation by preventing the dissociation of IRAK1 and IRAK4 from MyD88 (Barton and Medzhitov, 2003; Covert et al., 2005; Keating et al., 2007). TRAF6 leads activation of the $\text{I}\kappa\text{B}$ Kinase complex (IKK) and in turn release of $\text{NF-}\kappa\text{B}$ transcription (Covert et al., 2005). The receptor-interactor proteins 1 (RIP1) act together with TRAF6 to enhance cell survival (Covert et al., 2005; O'Neill and Bowie, 2007; Meylan et al., 2004; Vivarelli et al., 2004).

Both IRF3 and IRF7 function synergistically in LPS and virus induced $\text{IFN}\beta$ production (Wathelet et al., 1998; Yang et al., 2004). While this synergistic activity brings maximum efficiency, presence of either IRF3 or IRF7 is sufficient and the redundant roles of this two-transcription factor can bypass virus defence against the immunity (Yang et al., 2004). The effects of IRF3 and IRF7 depend upon the promoter context and even very low levels of IRF7 can lead $\text{IFN}\beta$ expression because of its preferential recruitment to the $\text{IFN}\beta$ promoter (Yang et al, 2004).

LPS treatment does not alter IRF3 protein expression level in both in the presence and absence of MyD88, so the activation of IRF3 is a posttranslational effect and is

required for its transcriptional activity (Kawai, 2001). IRF3 activation occurs through opening of inhibited state closed structure subsequent to multiple phosphorylation of C-terminal serine/ threonine residues (Qin et al., 2003; Honda et al., 2005). Phosphorylation begins at Serine 396 side and proceeds through Ser-404, Ser-405, Ser-386 or 385. Ser-339 and Ser-396 has compensatory mechanism and both have redundant roles on IRF3 transcriptional activity (Clement et al., 2008). While mutation of Serine 396 can cause constitutively active IRF3, Clement et al. (2008), mutation at Ser 386 prevent IRF3 dimerization in the cytoplasm (Mori et al., 2004; McCoy et al., 2008). IRF3 phosphorylation does not only function in positive regulation; it is also needed for negative regulation (McCoy et al., 2008). After virus invasion into cell, IRF3 degrades rapidly (Wathelet et al., 1998; Marie et al., 1998). The transportation of IRF3 through nucleus is regulated via the nuclear localization and nuclear export amino acid sequences. Even though both sequences are constitutively active, prior to the infection nuclear export is dominant nuclear import, thus IRF3 accumulates at cytoplasm. Serine/threonine phosphorylation effects the ability of IRF3 association with CBP/p300 in the nucleus, which inverts previous balance in the direction of IRF3 nuclear accumulation (Kumar et al., 2000).

Although presence of either IRF3 or IRF7 is necessary, it is not enough for IFN β expression. The other three transcriptional factors which take part in the transcriptional activation are AP-1 (ATF-2-c-Jun), NF- κ B, and the architectural protein HMG-I(Y) (Thanos and Maniatis 1995; Thanos and Maniatis, 1992; Agaloti et al., 2000; Merika and Thanos, 2001). For IFN β induction by infection, these four proteins need to form an ensemble called as enhanceosome (Thanos and Maniatis, 1995; Yie et al., 1999). It was shown that rather than protein-protein interactions, conformational changes following sequential interactions with DNA are the source of cooperative binding of these activators (Panne et al., 2004).

The main factors in the TLR4 pathway is depicted in the schematics given in Figure 1.1 and their main characteristics can be summarized as:

IRAK (IL-1 receptor associated kinase):

- Among four members of vertebrates IRAK family, namely IRAK-1, IRAK-2, IRAK-4, IRAK-M, IRAK-M is the only one not having a kinase activity (Kawagoe et al., 2008; Gosu et al., 2012). IRAK-4 comprises a central kinase and an N-terminal death domain (Suzuki et al., 2002).
- MyD88 activates IRAK4 through its death domain and concomitantly leads

activation of IRAK1 by phosphorylation (Kawai and Akira, 2007).

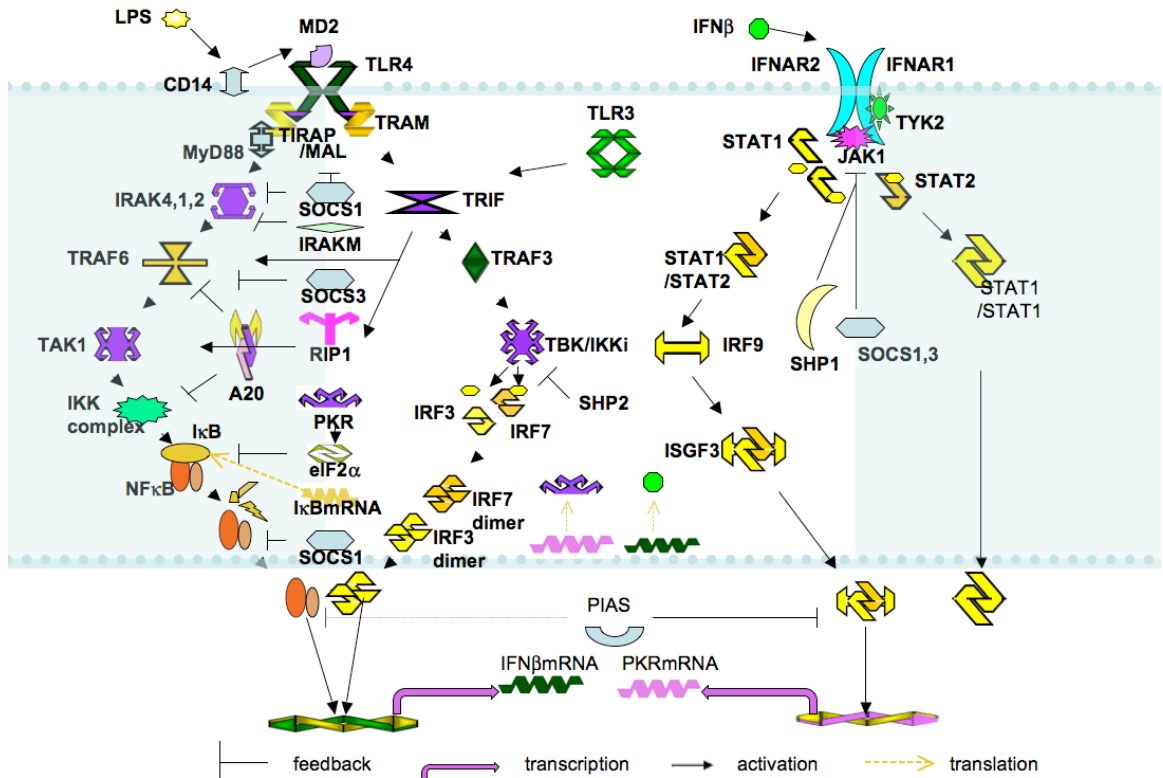


Figure 1.1: The schematics of the TLR4 and IFN β pathway.

- IRAK-4 deficiency results with resistance to most viruses. Among 28 known IRAK-4-deficient patients, Ku et al. (2007), no one suffered from severe viral disease and resist normally to most viruses independent of whether the event occurs by means of TLR3-dependent but IRAK-4-independent responses to dsRNA, TLR3- and IRAK-4-independent responses to dsRNA or responses to other viral intermediates through IRAK-4-independent pathways (Zhang et al., 2007).

- Mouse and human IRAK is 84% identical and 87% similar to each other (Li et al., 2002).

- IRAK-M prevents the dissociation of IRAKs and inhibits signaling through MyD88 (Lu, Yeh, Ohashi, 2008; Kobayashi et al., 2002)

- IRAK2 function is unknown (Kawai and Akira, 2007).

TRAF6 (TNF receptor-associated factor 6):

- It is in the structure of ring-domain E3 ubiquitin ligase (Kawai and Akira, 2007).
- TRIF binds TRAF6 by its N terminal region TRAF6-binding motifs and without these motifs, TRIF is not be able to activate NF κ B (Kawai and Akira, 2007).
- Normally the absence of TRAF6 in TLR3 pathway results in a decrease in NF κ B

expression, Kawai and Akira (2007), however, in macrophages this is not the case, which indicates cell specific contribution of TRAF6 (Gohda et al., 2004).

TAK1:

- Distinct regions of TRIF interact with TRAF6 and RIP1 and result in polyubiquitinated RIP1 and TRAF6 complex, activating TAK1. Such a cooperative functioning of TRAF6 and RIP1 in a complex causes robustness in NF κ B expression (Kawai and Akira S., 2007).
- TAK1 deficiency in TLR3 pathway results in impaired cell response (Sato et al., 2005)

TLR4 and TRAM:

- TRAM and TLR4 exist both at cell membrane and on true endosomes (Kagan et al., 2008) .
- In contrast to TLR4, independence of the localization of TRAM to dynamin illustrates that TRAM can target endosomes via different channel than plasma membrane (Kagan et al., 2008) .
- The action of TLR4 and TRAM via different mechanism can be sign of not transporting together after internalization (Kagan et al., 2008) .

Comparison of TIRAP and TRAM functioning.

- Both TIRAP and TRAM act as a sorting adaptor controlling the initiation stage of the TRIF-dependent signaling pathway from the endosomal compartment (Kagan et al., 2008) .
- TRAM exist at both plasma membrane and early endosomes, but TIRAP are not observed at endosomes (Kagan et al., 2008).
- Both TIRAP and TRAM has polybasic domains which are common motifs found in proteins having binding ability to acidic phospholipids. While TRAM and many acidic phospholipids binds to each other in detectable amounts, TIRAP rather bind with PtdIns(4,5)P2 (Kagan and Medzhitov, 2006). Possibly myristate group provide a nonspecific binding ability to TRAM, so it does not require specific phospholipids binding domain on it.
- Both TRAP-MyD88 and TRAM-TRIF adaptor pair can bind to the same site on the TIR domain of TLR4 , Nuez et al. (2007), but bind sequentially (Figure 1.2).

TRAM:

- TRAM is expressed both in early endosomal compartments and at the plasma membrane (Kagan et al., 2008).

- Mutant cells having no TRAM at the plasma surface can also produce type I interferon (Kagan et al., 2008).
- Disruption of TLR4 endocytosis by dynasore (inhibitor of dynamin) interrupts the TRAM-TRIF-dependent phosphorylation of IRF3 and so IFN- β (Kagan et al., 2008).

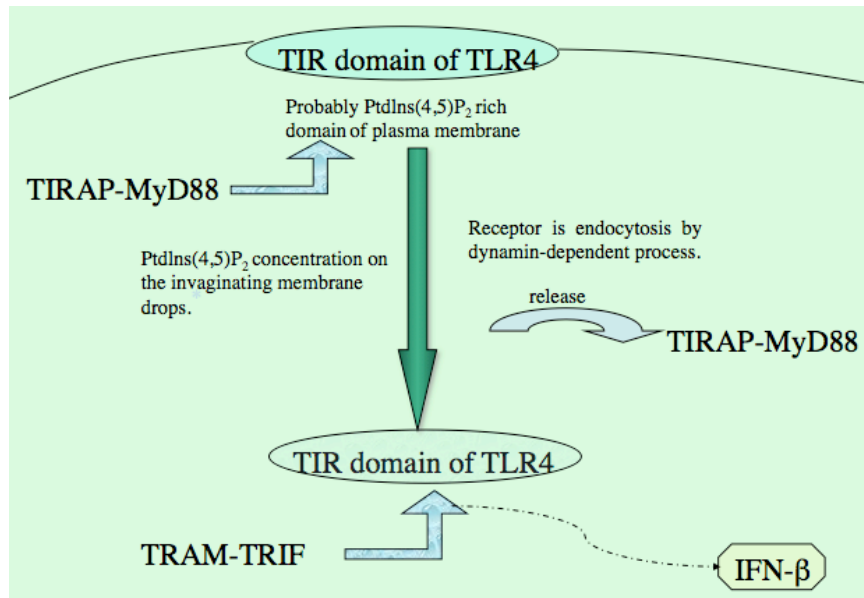


Figure 1.2: TIRAP-MyD88 and TRAM-TRIF interaction with TLR4 receptor¹.

- TRAM-TRIF-dependent signaling pathway is induced consequent to the endosomal localization of TLR4 (Figure 1.2) and from the endosome (Kagan et al., 2008).
- TRAM has bipartite motif (composed of myristate group subsequent to polybasic domain), both of which is essential for plasma membrane targeting but for endosomal localization only myristoylation is required (Kagan et al., 2008).

TRIF:

- Leads to chemokines such as IP-10 (Doyle et al, 2002)
- Downstream is common both in TLR4 and TLR3 cascades (Yamamoto et al., 2003).
- Responsible for late NF κ B activation (Sato et al., 2003).
- Associates with TRAF6 via its TRAF6-binding motifs in its N terminal region and lack of this region hinders TRIF dependent NF κ B activation (Sato et al., 2003).

¹Figure is drawn to summarize the receptor metabolism reported by Kagan et al., (2008).

RIP:

In TLR3 pathway it is shown that RIP1 combine with TRAF6 and TAK1 by polyubiquitination than their complex cooperatively facilitate TAK1 and result in robust NF κ B activation (Kawai and Akira, 2007).

TRAF3:

- TRAF3 is only common component in TLR7, TLR9 (signals via MyD88-dependent IRF7 activation, Honda et al. (2005); Kawai et al. (2004)), TLR3 and TLR4 (signals via TRIF-dependent IRF3 activation (Doyle et al., 2002; Oshiumi et al., 2003)). MyD88 independent pathway includes TRAF3 and its downstream.
- Dissimilar to the TRIP and TRAM, it is rather localized in the intra cellular compartments and it can not involved the cell surface as a part of TLRs pathway (Kagan et al., 2008).
- It can act at plasma membrane by engaging with CD40. TLRs and CD40 downstream are different (Xu, Cheng and Baltimore, 1996; Hostager, Catlett and Bishop, 2000).
- To interact with TRAF3, endosomal internalization of TLR4 is required (Kagan et al., 2008).
- Production of type one interferons via TRAF3 can only be triggered by internal TLRs (Kagan et al., 2008).
- Despite endosome located TLR3, TLR4 signaling is mediated by TRAM for the activation of TRIF-TRAF3 (Kagan et al., 2008).
- TRAF3 form a connection between TRIF and TBK1 (Hacker et al., 2006; Oganessian et al., 2006; Kawai and Akira 2007)

TANK-TBK-IKKi Complex:

TBK1 and IKKi is required for IFN β activation, Kawai and Akira (2007), but not for NF- κ B in TLR mediated activation (Hemmi et al., 2004; Kawai and Akira, 2007). TBK1 and IKKi role in MyD88 independent pathway is phosphorylation of IRF3. IKKi deficiency does not alter IRF3 and IFN activity in the presence of TBK1, Hemmi et al. (2004), but increase the effect of TBK1 absence and ceases IRF3 and IFN β activity (Hemmi et al., 2004; Kawai and Akira, 2007).

IRFs:

The IRFs are protein families having extremely important roles in infections and the host responses (Barnes, Lubyova and Pitha, 2002). IRF1 acts as transcriptional activator and IRF2 as repressor (Katze et al., 2002). IRF 1, IRF3, IRF5 and IRF7 are

transducers of immune response to viruses. (Katze et al., 2002). IRF3 has an important role in LPS stimulation. IRF3 activation is controlled by TRIF dependent pathway and not by MyD88 (Kawai et al., 2001). Before bacterial and viral stimulation, IRF3 is present in cytoplasm in an active form. Infection trigger TBK1 and IKKi to phosphorylate C- terminal region of IRF3 and phosphorylated IRF3s form a homodimers than goes to nucleus (Kawai and Akira, 2007). Over there IRF3 combine with NF- κ B and ATF2/c-Jun to form a complex namely enhanceosome and target the promoter-enhancer side of the IFN β gene (Honda et al., 2006). In general IRFs that enter the nucleus can either take role in activation or repression of the IFNs/IFN-regulated genes (Katze et al., 2002).

There are numerous other factors regulating the TLR4 pathway (Lu et al, 2008). But from the computational aspect, constitutive activity of these regulators can be ignored in the case of either not being induced or showing no change by induction originating from the activity of pathways that we concern.

Inhibitory proteins like A20, IRAK-M, I κ B α can be induced by the effect of LPS. A20 can inhibit ubiquitination of TRAF6, in turn down stream signaling (Lu, Yeh, Ohashi, 2008). Targeting of RIP1 by A20 in TNF signaling pathway, Wertz et al. (2004), indicates a similar possibility for RIP1 in TLR4 signaling (Lu, Yeh, Ohashi, 2008). A recent study indicates induced expression is critical for the functioning of I κ B α in NF κ B expression but not for that of A20 (Werner et al., 2008).

IRAK-M inhibits MyD88 downstream by preserving IRAKs-MyD88 complex (Kobayashi et al., 2002; Janssens and Beyaert, 2003).

1.2.2 Interferon beta pathway

IFNs are mainly classified in to three groups as Type I, Type II and Type III IFNs (Katze et al., 2002; Gad et al., 2009). Inspired from their induction in response to viral products like double stranded RNA, Type I IFNs also called as viral IFNs (Katze et al., 2002) and they play active role in mucosal immunity to viral infection (Smieja et al., 2008). Especially IFN β is very important among type I IFN because of being secreted by epithelial cells first encountering with viruses. IFN β discovered in chick cells after infection of heat inactivated influenza virus (Isaacs and Lindenmann, 1957).

After the detection by their cell-surface specific receptors (IFNAR1/2), Type I Interferons result a signaling cascade through the IFNAR associated tyrosine kinases

phosphorylation of the signal transducers and activators of transcription (STATs) via Janus kinases (JAKs) (Katze et al., 2002). Phosphorylated STAT1–STAT2 forms homo and heterodimers and heterodimers are recruited to ISRE, Taniguchi and Takaoka (2001), sequences together with IFN-regulatory factor 9 (IRF9) by forming ISGF3. STAT1 dimers and ISGF3 function as active transcription factors upon their transport into the nucleus (Smieja et al., 2008). Most of the STAT1-STAT2 heterodimers form the ISGF3 complex, thus the contribution of the isolated heterodimers to the signaling pathway can be neglected (Smieja et al., 2008). STATs dephosphorylation occurs both in the nucleus and cytoplasm. Dephosphorylation causes destruction of the complex and removal of STATs from the nucleus, STATs in the cytoplasm are again available for phosphorylation and process goes so on so forth (Smieja et al., 2008). In our model we represent this process simply by activation and deactivation of ISGF3 both in the cytoplasm and nucleus. In the model increase in the phosphorylation after IFN β treatment correlated with the higher internalization rate introduced by IFN β . Even constitutively active phosphate exists, additional phosphates induced by IFN β function in the regulation of STAT1 homodimers (Smieja et al., 2008). Such a change can also be a matter of fact for STAT1-STAT2 heterodimer and so ISGF3 regulation, but in this preliminary model it is kept out of concern.

To prevent overshooting endogenous regulation of Type I IFN includes negative feedbacks at multiple points provided by suppressors of cytokine signaling (SOCS), Schmitz et al. (2000); Qin et al. (2008); Song and Shuai (1998); Pauli et al. (2008); Starr et al. (1997); Endo et al. (1997); Yasukawa et al. (1999); Yamamoto et al. (2003); Dalpke et al. (2008); Giordanetto and Kroemer (2003), protein inhibitor of activated STATs (PIAS) and SH2 containing phosphates (SHP) proteins (Wormald and Hilton, 2004). SOCS-1 and SOCS-3 are important in Stat 1 and STAT 3 regulation and act on different nodes (Schmitz et al., 2000; Qin et al, 2008; Song and Shuai, 1998; Pauli et al., 2008). SOCS-1 and SOCS-3 are also suppressors of TLR mediated responses and can be triggered by signals from TAM -Tyro3, Axl, and Mer - receptors (Kawai and Akira et al., 2009; Starr et. al, 1997). While SOCS-1 exerts negative feedback on the tyrosine kinase activity of JAKs and concomitantly suppress activation of STATs, Starr et al. (1997); Endo et al. (1997); Yasukawa et al. (1999), SOCS-3 can also act at the cytokine receptor level regulating JAK-STAT pathway activation (Schmitz et al., 2000; Yamamoto et al., 2003). SOCS1 is a critical factor in the downstream of TLR4 pathway, its deficiency leads mice to be very vulnerable to

LPS mediated septic shock (Nakagawa et al., 2002; Kinjyo et al., 2002). TLRs directly induce SOCS but SOCS proteins interfere with IFN- β signaling and prevent TLR dependent overshooting in an indirect way (Dalpke et al., 2008). SOCS-1 exerts negative feedback on JAK2 either by protruding toward the catalytic region and inhibiting kinesis activity or by letting proteasomal degradation (Giordanetto and Kroemer, 2003). Some experiments indicated that SOCS1 is not induced in IFN β stimulated cells (Smieja et al., 2008). Despite SOCS1, SOCS-3 transcribed at early stages of virus attack in a type I IFN independent manner. SOCS-3 deficient cells show a prolonged STAT1 activity resulting with increased levels of corresponding genes. Thus early response of SOCS3 has a possible role in suppression of the antiviral response (Rothlin et al. 2007; Kinjyo et al., 2002). Many of PIASs can sumoylate STATs and upon this sumoylation block its transcriptional activity (Schmitz et al., 2000). SHP1 can also be a limiting factor in JAK1 and STAT1 activation restricting both the amount and duration. SHP1 have also role in basal level regulation of JAKs (David et al., 1995).

While TLR4 pathways trigger interferon pathway via IRFs activation and concomitant IFN- β production, induction of IRFs by IFNs also enhances the response of IFN-stimulated cells to TLRs (Smieja et al., 2008; Sato et al. 1998).

ISGF3 acts on ISRE side of promoter region and function in transcription of PKR (Taniguchi and Takaoka, 2001).

Early and late genes in this pathway evolve distinctly and are controlled by distinct transcription factor. Binding of STAT1 homodimers to the GAS site of the promoter region and the resulting expression of IRF1 gene form the early response of the system (Smieja et al., 2008). Primary transcription factor for IRF1 gene is STAT1 homodimers and STAT1 homodimers mainly affect late system response through IRF1 gene. The heterodimers has weaker affinity to GAS region and if it binds, block the functioning of GAS. However, amount of free the heterodimers is very restricted in the nucleus (Smieja et al., 2008). This mechanism negatively regulated by dephosphorylation of the homodimers in the nucleus and the control mechanism on the early gene expression is independent to the blocking of STATs dephosphorylation at the level of IFNAR (Smieja et al., 2008).

Upon its synthesis, IRF1 enters to the nucleus and consequently controls late gene expression such as TAP1/LMP2 and STAT1 (Smieja et al., 2008). There is a significant delay, about two hours, between the peak of IRF1 in the nucleus and that of

transcription of genes (Smieja et al., 2008). IRF2 have a negative regulator role in IRF1 gene transcription, Harada et al. (1994); Kroeger et al. (2002), and as a transcriptional attenuator by interfering with ISGF3 mediated ISGE activation, Taniguchi and Takaoka (2001); Hida et al. (2000), which in turn affects ISGF3 dependent PKR activity. Induction of IRFs by IFNs also enhances the response of IFN-stimulated cells to TLR and RIG-I pathways (Sato et al., 1998; Smieja et al., 2008). In the late response of this signaling pathway IRF1 transportation to the nucleus is blocked (Smieja et al., 2008).

1.2.3 NF- κ B circulatory network

An important cellular signaling network is that of the nuclear factor- κ B (NF- κ B). The NF- κ B family of transcription factors and signaling components exist in almost every differentiated cell types (Hoffmann and Baltimore, 2006; O'Dea and Hoffmann, 2009; Oeckinghaus and Ghosh, 2009). They have important roles in regulation of cellular survival signals, immunity, i.e., immune cell differentiation, organogenesis, inflammation and is subject to multilevel control mechanism (Li and Verma, 2002; Hoffmann and Baltimore, 2006). In response to the triggering signals, NF- κ B targets over 150 genes (Pahl, 1999). NF- κ B mediates cellular responses to lipopolysaccharide (LPS), interleukin IL and Tumor necrosis factor α (TNF α) stimulation in different ways. Activation of NF- κ B dimer is induced by phosphorylation of the inhibitor protein canonical I κ B isoforms, namely, I κ B α , - β , and - ϵ and the precursor proteins p105 and p100, thereby destruction of NF- κ B-I κ B complex (Ghosh et al., 1998, Hoffmann and Baltimore, 2006). Five different proteins form NF- κ B family. i.e., cRel, RelA, RelB, p50, and p52 (Figure 1.3A) (Ghosh et al., 1998; Hoffmann and Baltimore, 2006). Functionally they form dimers and the confirmation, in turn binding ability to DNA is determined by binding partner (Hoffmann and Baltimore, 2006). The conformational change introduced by I κ B effect the DNA-binding activity of NF- κ B (Hoffmann and Baltimore, 2006; Kearns et al, 2006). NF- κ B nuclear accumulation is also controlled by I κ B isoforms (Ghosh et al., 1998).

Hoffmann et al., (2002) developed a heuristic mathematical model based on ordinary differential equations and the role of I κ B protein family feedback mechanisms in the fine tuning of time-varying NF- κ B expression, due to the harmony in their activation and degradation mechanisms (Cho et al., 2003; Hoffmann 2002). The model supplied precious information about the roles of I κ B isoforms, the bimodal nature of NF- κ B

signal, and the gene expression specificity (Cho et al., 2003). Another ODEs model for TNF α was performed by complementing the enzyme kinetics to map the whole stages in retrieving concentration of reaction species at the steady state into a graphical form and transforming each stages into mathematical language via bunch of ODEs. Ensemble of the kinetic ODEs finally was resulted in a computable model explaining the signaling cascade regulating NF- κ B through TNF α (Cho et al., 2003). Utilization of this kind of methodology for the LPS mediated NF- κ B signaling can also result in well-designed and easliy traceable mathematical models for TLR4 pathway.

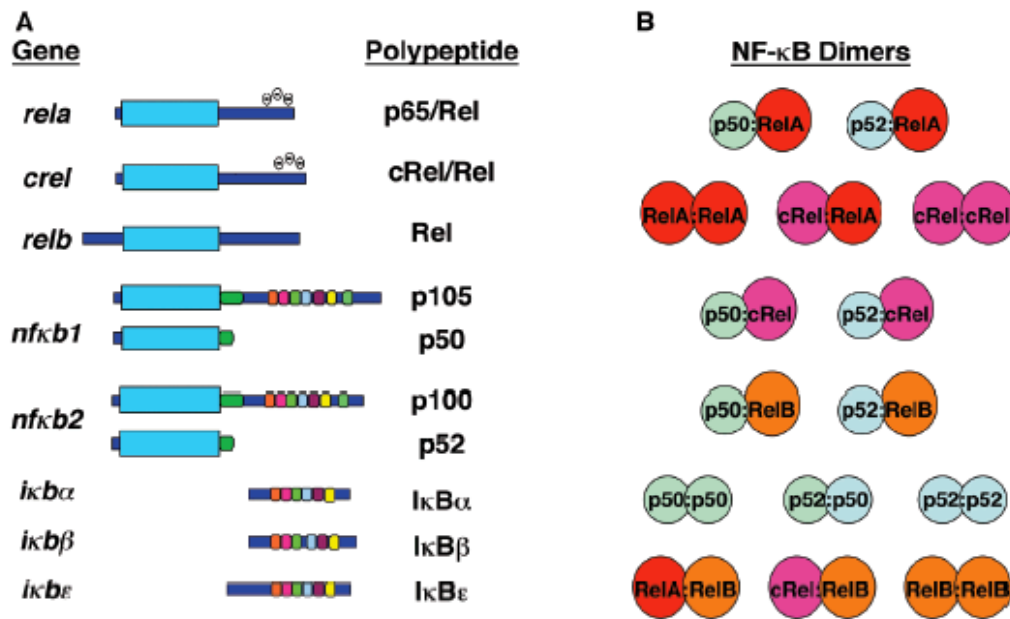


Figure 1.3: NF- κ B combinatorial structure, NF- κ B, I κ B genes, polypeptides and dimmers (Hoffmann and Baltimore, 2006). Among 15 transcription factors (B) formed by hetero- and homo-dimerization of five different NF- κ B polypeptides (A), only nine dimers at the top four rows can act as transcriptional activators in addition to having DNA binding ability. The fifth row represents dimers not having domains for transcriptional activation and the last row for dimers without DNA binding ability. The light blue boxes indicates Rel homology domains of NF- κ B monomers that function in NF- κ B dimerization and in binding to DNA and I κ B proteins. (Hoffmann and Baltimore, 2006).

Despite its damped oscillatory nature in response to TNF α , NF- κ B expresses stable behaviour to LPS stimuli in wild-type cells. LPS triggers immune signals through TLR4 and downstream comprises two branches of signaling cascade both resulting in TNF α type damped oscillatory NF- κ B activity through the canonical pathway of NF- κ B, namely MyD88-dependent and MyD88 independent pathways (Covert et.al, 2005). TNF α triggers the canonical pathway of NF- κ B only once, however, LPS activates it once directly through MyD88 and once as secondary response following

the transcription of $\text{TNF}\alpha$ through MyD88 independent pathway (Covert et.al, 2005; Lee et al., 2009). A computational model elucidated that coupling of two antiphase oscillatory signals coming through MyD88-dependent and MyD88 independent pathways with a 30 min time lag is the one of the sources of LPS dependent stable early NF- κ B activity. The delay originates from the time elapses to induce $\text{TNF}\alpha$ through MyD88-independent pathway (Covert et.al, 2005).

In a recent study, it is shown that another reason behind the stable behavior of NF κ B in LPS stimulated pathway hides in the delay of induced activation of $\text{I}\kappa\text{B}\epsilon$ with respect to that of $\text{I}\kappa\text{B}\alpha$. This late negative feedback on NF- κ B activation prevents the long term oscillations in the system and regulates the cell type specific NF- κ B activity (Kearns et. al, 2006).

NF- κ B is a vital transcription factor and such a critical immunoregulator naturally needs to be controlled by complex network of interactions to sustain a robust innate immunity. The following schematic (Figure 1.4) represents such a network of interaction regulating NF- κ B (p50, p65) between cascades triggered by LPS, IL,IFN β and $\text{TNF}\alpha$ stimulations.

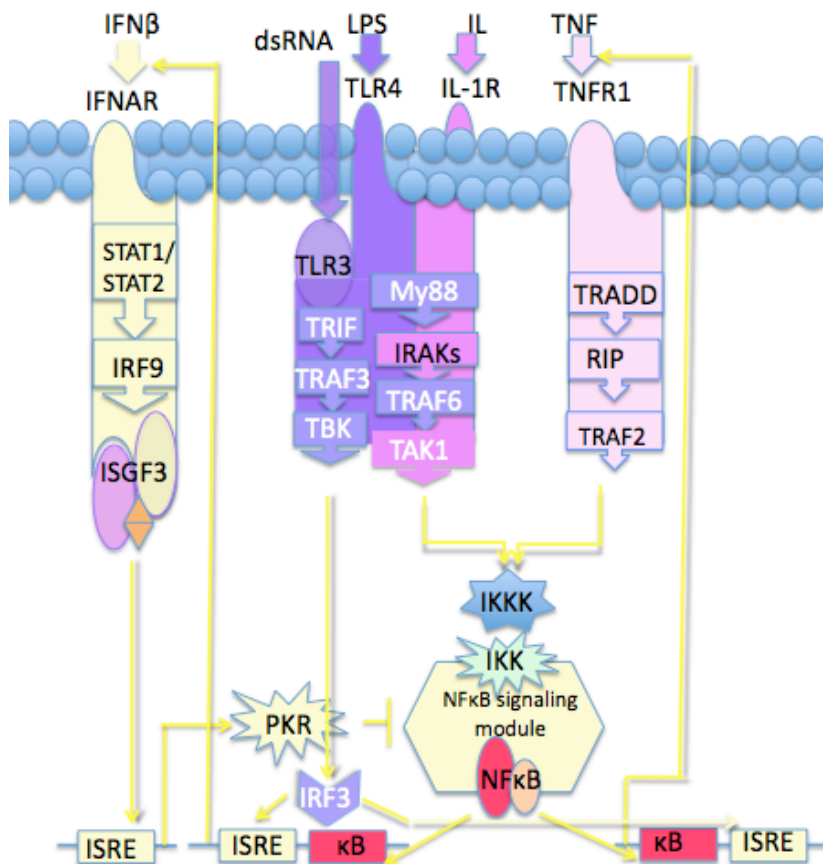


Figure 1.4 : NF κ B (p50, p65) regulation.

As previously mentioned, the characteristic of NF κ B response strongly depends on the duration of stimuli, even very brief signal leads to significant amount of transient NF- κ B and if the stimulus is longer than one hour, NF- κ B is sustained in an extent proportional to the duration of stimulus (Hoffman et al, 2002). This characteristic is not only restricted to NF- κ B expression but it also can be observed in various gene expressions (Hoffman et al, 2002).

1.2.4 PKR connection between IFN β and TLR4 pathway

There is some evidence indicating TLR4 and IFNAR pathways are connected through dsRNA-activated protein kinase (PKR) activity, Horng, Barton and Medzhitov (2001), and in turn through the translational inhibition of I κ B (Levy and Garcia-Sastre, 2001; O'Dea et al., 2008). It is known that LPS activates IFN β transcription through the TRIF dependent pathway, Kawai et al. (2001); Yamamoto et al. (2003), and PKR is a crucial factor in the antiproliferative effects and antiviral defense regulated by interferon (Katze, 1995; Balachandran et al., 2000). PKR impinge on upstream of IKK, Zamanian-Daryoush et al. (2000), and activates NF- κ B by binding IKK β irrespective of its kinase activity (Chu et al, 1999; Bonnet et al, 2000). A justification for NF- κ B activation under the influence of PKR is the induction NF- κ B dependent survival genes (Wang et al, 1998; Karin and Lin, 2002). Induction of NF- κ B as concomitance of eIF-2a phosphorylation cause a delay in PKR induced apoptosis (Donze et al., 2004).

Viruses utilize the host defense system against itself by producing cellular stress response that blocking PKR activation and resisting initiate IFN response (Katze et al., 2002). It is indicated that PKR is also a mediator in cell differentiation and growth control, Koromilas et al. (1992); Donze 'et al. (1995); furthermore, since its overexpression causes apoptosis, Balachandran et al. (1998); Donze et al. (1999), it can be effective in tumor suppression (Meurs et al, 1993; Barber et al, 1995; Donze et al., 2004).

In summary PKR works as a molecular clock in two distinct and opposite phase in sequential manner, Donze O. (2004); namely an early enhancement of cell survival by acting on IKK β , Zamanian-Daryoush et al. (2000); Bonnet et al. (2000), and inducing NF κ B, Chu et al. (1999); Bonet et al. (2000), and as a result of viral replication cycle a late induction of apoptosis by its kinase activity (Lee et al, 1997; Donze 'et al, 1999;

Donze O., 2004).

One striking example that forms the basis of our research for PKR expression is the translational inhibition of I κ B as a result of stress responses induced by UV radiation and ribotoxic agents. According to the existing evidence, translational inhibition of I κ B in response to the UV radiation results from the phosphorylation of eukaryotic initiation factor-2 α (eIF2 α) by the effect of eIF2 α kinase (PERK) (Jiang and Wek, 2005; Wu et al., 2004). Similarly protein kinase PKR activity induced by IFN β results the phosphorylation of eIF2 α , which indicate a possible translational inhibition process of I κ B and so increased NF κ B activity (Figure 1.5).

Although the study first performed for UV radiation, it is also shown that the presence of other ribotoxic agents can also have similar effects and the surplus I κ B synthesis and degradation seems to be evolved so that I κ B provides resistance of NF κ B signaling module to such kind of agents (O'Dea et al., 2008).

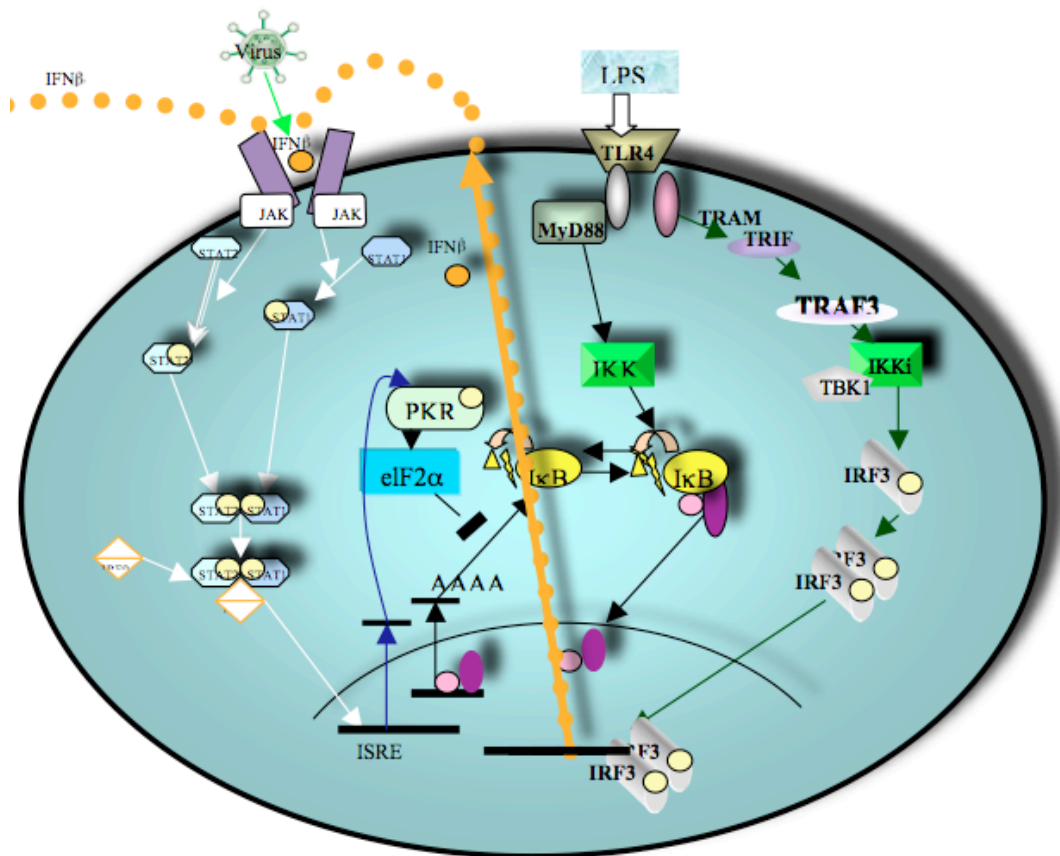


Figure 1.5: LPS and IFN β stimulated pathways.

It has been *in silico* demonstrated that the change in the NF κ B level according to translational inhibition depends also on the I κ B degradation rate. When the turnover rate of I κ B increases, sensitivity of NF κ B activation to the translational inhibition of I κ B increases. In addition this sensitivity also depends on IKK activity, if IKK is not

activated there is no such sensitivity and increasing activity rate of IKK increase the sensitivity further. So while the maximum level of NF κ B activity is determined by IKK activity, it is fine tuned by both I κ B degradation and translational inhibition rates, O'Dea et al., 2008, which can be depended up on to PKR activity.

p53 cause induction of PKR, Yoon et al. (2009), and PKR activates NF κ B (Donze et al., 2004). While the previously mentioned sequential program on cell survival triggered through NF κ B and planned cell death by phosphorylation of eIF-2 α is regulated by PKR, PKR is regulated by outcomes of this sequential activity.

DNA damage cause p53 induction and p53 leads cell apoptosis, so tumor-suppression (Amundson et al., 1998; Yoon et al., 2008). Genotoxic stress dependent p53 activation results with a significant level of PKR synthesis though the cis-acting element (ISRE) (Yoon et al., 2008). p53 induced PKR resulting from the stress of DNA damage is significant in the intracellular network part of the tumor-suppressor function of p53 (Yoon et al., 2009). A resistance to apoptosis arises in the absence of p53 target genes (Villunger, et al 2003).

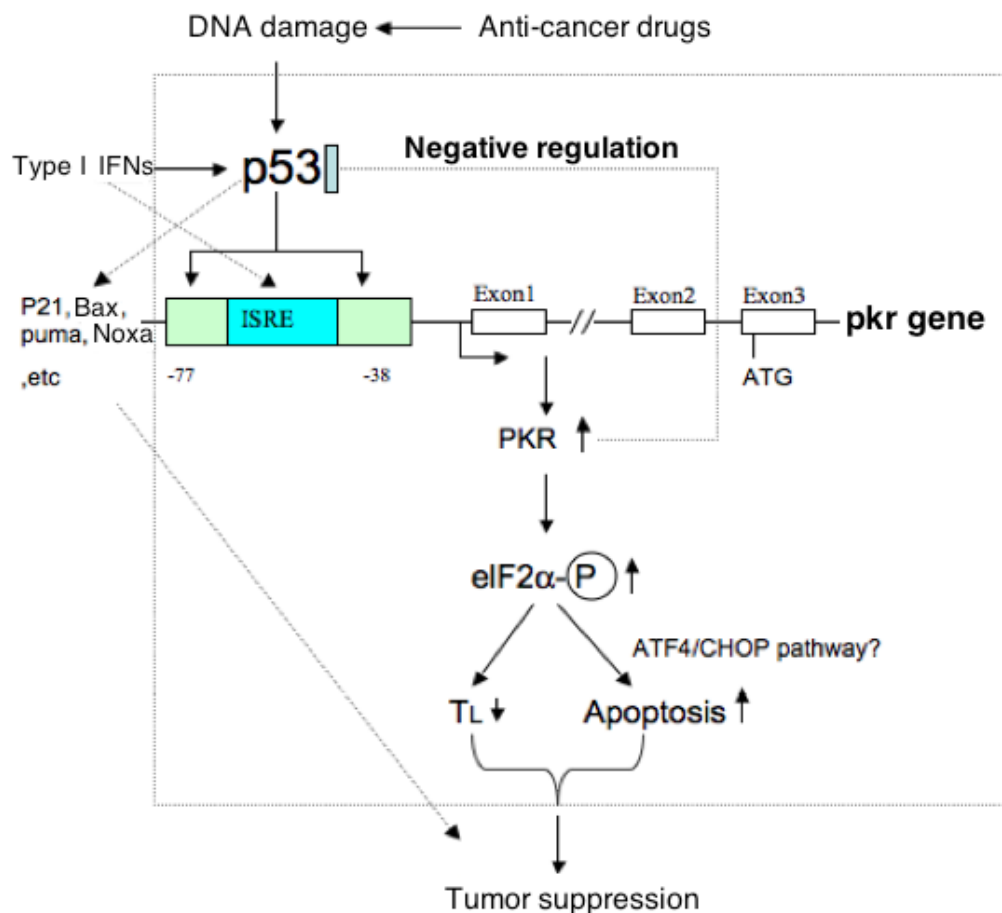


Figure 1.6: Under the DNA damage PKR expression induced by P53 and concomitant tumor inhibition mechanisms (Yoon et al., 2000). Redrawn based on the original figure.

As a homeostatic control mechanism PKR exerts a negative feedback on p53. Under genotoxic conditions this negative feedback may not be enough to overwhelm p53-induced apoptosis (Yoon et al., 2009). Knocking out PKR results with cells faster growing cells both in vivo and in vitro. Human tumor tissues having undetectable levels of P53 usually have lower PKR expression relative to normal ones (Yoon et al., 2009). Figure 1.6 summarises the mechanisms under the DNA damage how PKR expressed and tumor suppression.

1.2.5 Biologically important mechanisms

1.2.5.1 Feedbacks

Many natural biological systems utilized feedbacks. Without feedbacks, control systems are highly sensitive to disturbances and parameter changes of the processes or transfer functions. Continuous response, following the decay of transient response suffers from errors called as steady state errors. Closed loop feedback systems reduce the steady state error by continuously monitoring it and applying actuating signal. They are also used in the adjustment of transient response (Dorf and Bishop, 2008).

A single negative feedback loop (Figure 1.10) can function as basal homeostat, adaptation, transient generator and output limiter (Brandman and Meyer, 2008). These four different function are consequences of its the initial conditions and characteristics (Brandman and Meyer, 2008). Depending on same reasons a single positive feedback motif can function as signal amplifier, bistable switches creator, and timing adjuster of a signaling response (Brandman and Meyer, 2008). Mixed feedback motifs containing both positive and negative feedbacks can provide systems with oscillations or polarization (Brandman and Meyer, 2008).

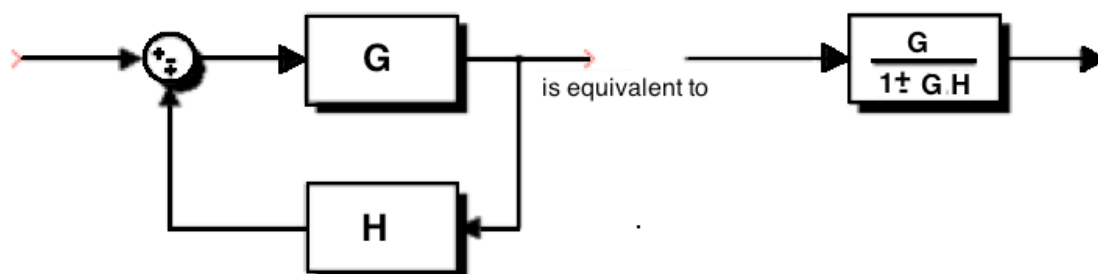


Figure 1.10: An equivalent transfer function of single feedback system.

Even though, adding feedback to the control systems provides several advantages, it also brings some cost like increasing the number of components and complexity. In addition, it can result with instability in the system. One handicap arose from the loss

of gain by a factor of $1/(1+G_c(s)G(s))$, which is exactly corresponding to previously mentioned sensitivity decrease to parameter changes and disturbances. However, mostly utilities provided by feedbacks overweight these disadvantages (Dorf and Bishop, 2008).

1.2.5.2 Oscillation

The mechanisms of regulatory and signal transduction networks do not only rely on shifts in protein concentration between steady states, temporal variation propagating through networks in a complex manner also carries information (Tina et al., 2007). There can be many roles of oscillating signals in biological network so it is important to find answers to question like: how cellular processes utilize temporally varying signals? how are oscillations generated through the network? (Tina et al., 2007), why does oscillations start up in response to some agent or damage and what are the sufficient conditions? (Tina et al., 2007), are oscillations only a by product of adaptation or has evolutionary significance? (Cheong and Levchenko, 2010), is there an information decoded in oscillations or a non-oscillating system can work equally well? (Cheong and Levchenko, 2010).

As mentioned before $I\kappa B$ has isoforms inactivating $NF-\kappa B$ both in the nucleus as well as in the cytoplasm. These isoforms have different profiles and differently function on expression. Some of them transcriptionally activated by $NF-\kappa B$ and provide a negative feedback. A simple sketch of the feedback loops controlling the concentration $NF-\kappa B$ is given in Figure 1.7.

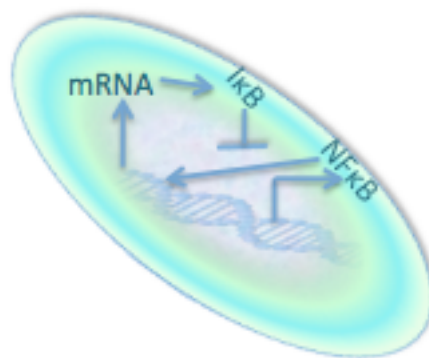


Figure 1.7: A sketch of the feedback loops controlling the concentration $NF-\kappa B$ (Tiana et al., 2007). Redrawn based on original figure.

Experiments on wild-type cells and knockouts expressing only $I\kappa B\alpha$ (knockout $I\kappa B\alpha$ mutants are not viable) with damped oscillatory behavior (Figure 1.8) illustrated the potency of this feedback loop in generating oscillations in the nuclear import and

export of NF- κ B (Hoffmann et al., 2002; Tiana et al., 2007). These results suggest that the NF- κ B oscillations arise due to the fast activation and regulation with the intense negative feedback (Hoffmann et al., 2002).

The effect of $I\kappa B\alpha$ deficiency observed as non-oscillatory NF- κ B behaviour. $I\kappa B\beta$ and $I\kappa B\epsilon$ give slower response to IKK. During the long term stimulations they function to suppress the oscillations. Different behaviors of $I\kappa B\alpha$, $I\kappa B\beta$ and $I\kappa B\epsilon$ let them act together to give substantially fast response to sudden changes in triggering signal such as start up or end of IKK activity and lead to stable NF- κ B concentrations in the case of long-lasting stimuli (Hoffmann et al., 2002).

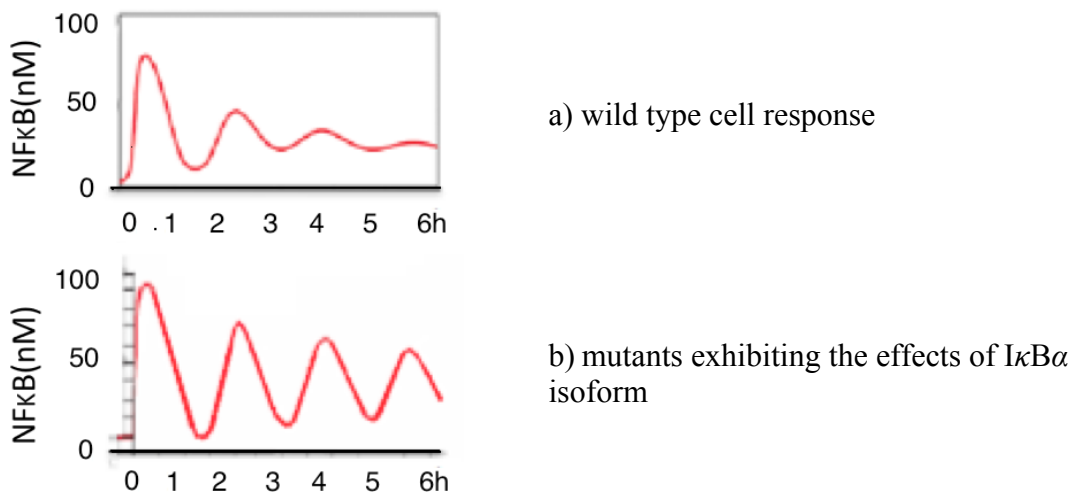


Figure 1.8: NF- κ B nuclear localization predicted by a computational model. (Hoffmann et al., 2002)

In monotone two variable systems having negative feedback loops, either explicit time delay or giving up monotonicity is necessary condition on the oscillations (Tiana et al., 2007). Requirement for explicit time delay can be compensated by introducing a finite minimum time for processes and by introducing intermediate steps (Tiana et al., 2007). If such a system is resolved by rate equations, the time elapsed between two binding reaction assumed to obey Poisson distribution, in other words it is less than the average time separating the reactions (Tiana et al., 2007). On the other hand, molecular processes can require some time and before this time is reached output can be taken as 0 and after 1 (Tiana et al., 2007). In addition to that a constraint restricting the degradation rate of one species with an upper limit, namely saturated degradation, can produce an effective time delay in the system. These kinds of mechanisms are widespread in biological systems and a good example is NF- κ B regulation (Tiana et al., 2007). If there exist a positive feedback of a molecule on its own production

(autocatalysis), oscillations can also occur. Autocatalysis is a necessary condition for oscillations in two variable systems having no explicit time delay (Guantes and Poyatos, 2006; Conrad, 1999; Tiana et al., 2007). Presence of autocatalysis results in non-monotonic system behavior (Tiana et al., 2007). Moreover, a nonlinearity in the reaction equations allows some of the variables to give sharper response to changes than that in linear fashion and in turn can lead to oscillations (Tiana et al., 2007).

Negative feedbacks are one of the prominent ways in adaptation to persistent environmental signals, response time to adapt depends on the strength of the feedback and according to which either an overshooting or oscillation can occur (Cheong and Levchenko, 2010).

An oscillating signal can transmit more information than a steady signal, and oscillations, particularly spiky oscillations, have many useful properties to ameliorate the efficiency and to increase the speed of signaling and response systems (Tiana et al., 2007). A prominent example of the networks exhibiting spiky oscillations is the NF- κ B network given in Figure 1.9. Despite the views on the effect of NF- κ B oscillations on consecutive cell responses, Nelson et al. (2004), many aspects of these effects are still not clear (Barken et al., 2005). Many ubiquitous eukaryotic signaling molecules also demonstrate spiky behavior (Tiana et al., 2007). Being continuously subjected to a high constant level of hormones and other chemicals might have undesirable results for the biological system and such a constant level can lead to saturation of a common receptor that is also used by other signals. However, this problem can be overwhelmed in the case of spikes and oscillations (Tiana et al., 2007). The oscillatory activation of a gene expression can initiate different cascades depending on the sensitivity of the gene to the oscillations. For example, it is possible for a single downstream gene to have a role as low-pass filter (Tiana et al. 2007; Krishna et al. 2006). There can be interaction between different oscillators and one of them can entrain the other as in the case of day-night periodicity and circadian rhythm (Cheong and Levchenko, 2010).

In biological systems, with the same logic of Fourier transform, a particular frequency response can be attained by regulatory circuits with a suitable number of multiple components.

Figure 1.9 illustrates some of the important interactions in the NF- κ B system, Tiana et al. (2007), which can be summarized as:

- I κ B forms a complex with NF- κ B both in cytoplasm and nucleus.

- The NF κ B-I κ B complex cannot be transported into, but can go out from the nucleus.
- IKK cause proteolytic degradation of the cytoplasmic NF κ B-I κ B. Only I κ B degrades as a result of this process (this degradation does not occur for free I κ B) and NF- κ B releases.
- Free NF- κ B transposed in to the nucleus via an active transport process, however, wise verse is not true.
- NF- κ B in the nucleus, stimulate transcription of the I κ B α gene which is the source of the I κ B mRNA in the cytoplasm.
- The I κ B protein is synthesized by translation of the I κ B mRNA in the cytoplasm.
- The I κ B protein transportation can be in both directions from the membrane of the nucleus.

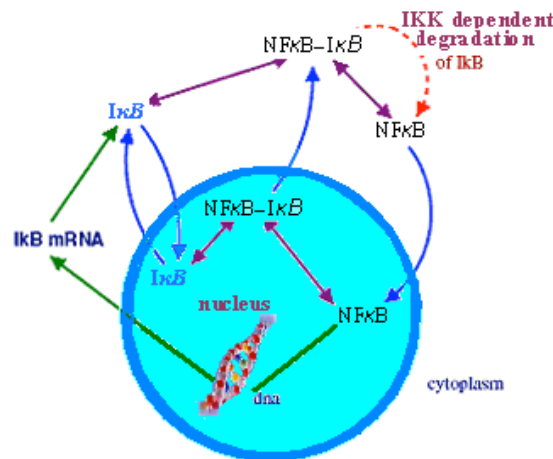


Figure 1.9: Some of the important part of the NF- κ B regulatory system. Transcription and translation represented by green arrows, transport processes by blue, complex formation purple, and degradation of I κ B from NF κ B-I κ B complex by red dashed ones (Tiana et al., 2007).

Other important characteristics for the signaling module can be summarized as:

- Even short stimulations cause substantial NF- κ B responses; correspondence of initial NF- κ B response to duration and dose is very low (Cheong et al., 2006).
- NF- κ B activation shows high sensitivity in response to an extremely wide range of TNF concentrations (Cheong et al., 2006).
- IKK activity can both induce and reduce (via the phosphorylation of RelA by IKK itself) NF- κ B expression (Hoffmann and Baltimore, 2006; Lawrence et al., 2005).

- NF- κ B has ‘bimodal signaling characteristic’; while showing only one peak for stimulations shorter than one hour, activity of it directly proportional to the duration of a longer stimulus (Hoffmann et al., 2002).
- I κ B α exerts negative feedback on NF- κ B expression (Hoffmann et al., 2002).
- I κ B β insert a positive feedback in NF- κ B activity inside nucleus, by preventing nuclear export (Suyang et al., 1996; Phillips and Ghosh, 1997).
- I κ B ϵ produce late feedback on NF κ B expression and a negative deviation in I κ B ϵ level allow prolonged activity of NF- κ B but this not valid in presence of over expressed I κ B α (Hoffmann et al., 2006).
- Substantial amount of NF- κ B is activated even in the case of very short stimulus (Hoffmann et al., 2002).
- One of the reasons behind stable behavior of NF κ B in LPS stimulated pathway hide in the about 45 minute delay of induced activation of I κ B ϵ with respect to that of I κ B α (Hoffmann et al., 2006).
- Different behaviors of I κ B α , I κ B β and I κ B ϵ let them act together to reply substantially fast to changes in the amount of IKK and let to stabilization in NF- κ B activity in long-term (Hoffmann et al., 2002).
- Feedback mechanisms controlled by NF- κ B, A20 and IRF3 in the whole LPS and TNFR signaling pathway, let time dependents expression of IKK activity characteristic to the stimulus and to the pathway, which result in NF- κ B activities and gene expressions specific to each particular case (Hoffmann et al., 2005).
- Binding ability of NF- κ B shows variation according to the constituting dimers and this can change transcriptional activity (May and Ghosh, 1998; Udalova et al., 2000; Li and Verma, 2002).
- Amplitude of initial IKK activity does not have an influence on NF- κ B concentration and duration (Hoffmann et al., 2005).
- The duration of the initial peak in IKK activity changes NF- κ B activity profiles (Hoffmann et al., 2005).
- IKK activation rates alter that of NF- κ B. Deactivation rates has little influences on NF- κ B activation and only become apprehend by increasing towards the late activity of the NF- κ B profile and leads no change in initial peak (Hoffmann et al., 2005).

- Sudden sharp impulses of IKK lead only little NF- κ B activity. The effect of such a short but high increase is very similar to that of a long in duration but a small in amplitude. Both result in an NF- κ B activity profile that persists much longer than the duration of the transient pulse of IKK activity (Hoffmann et al., 2005).
- The level of NF- κ B concentration at late activity is mainly determined by that of IKK and presence of a second plateau in IKK activity has an important role in the late NF- κ B activity and biphasic nature of it (Hoffmann et al., 2005). Experiments indicate such a two altered level of activity behavior for IKK (Cheong et al., 2006).
- The free NF- κ B leads transcription of the ubiquitination enzyme A20 which act as catalyzer inhibiting IKK transformation to an inactive form (Lee et al., 2000; Lipniacki et al., 2004).

1.2.5.3 Delay times

In biological systems delay times can be originated by time necessary for transport of mass or energy and by the addition of time lags to each other due to the series connection of many low-order systems (Normey-Rico, 2007). In standard feedback controllers introduction of dead or delay times to the process brings difficulties in the control. Until considerable time has passed concomitance of disturbances can not be felt and errors caused by a previous situation is tried to be corrected at a later time after losing its validity. Delay time leads further decrease in the phase of system and so that of transfer function gains margin and in return results in instability (Normey-Rico, 2007).

1.2.6 Tools of system biology

Before proceeding further inside into methods that will utilized in this study, it worth to overview different methods used in computational system biology. They can be summarized as (Materi and Wishart, 2007):

- ODEs: In this method sets of ordinary differential equation type reaction rate equation are numarically solved. The advantages of this technique are its having well-defined formalism, its speed, deterministic and mathematically robust nature. The disadvantages are being brittle and restricted to temporal

modeling, presuming high concentrations and uniform distribution (Materi and Wishart, 2007).

- Stochastic Modelings: Stochastic time evolution of a system is Modeled by an algorithm (Gillespie algorithm), Gillespie (1977), including a numerical approach to traditional stochastic differential equation formalism of chemical kinetics called as “master equation” (McQuarri, 1967). The algorithm based on Monte Carlo type methodology and utilizes random number generators. It is fast and robust method effective in modeling trace amounts of reaction members. On the other hand it is nondeterministic and restricted to time dependent modeling (Materi and Wishart, 2007).
- S-system formalism or power law equations: It utilizes Taylor approximation to recast non-linear ODEs model and deciphers the biological systems by transforming the related steady state DEs to easily solvable linear equations with considerable simplifications. It is fast and allows rapid parameter testing. It is circumscribed to events and processes pertaining to time (Materi and Wishart, 2007).
- PDE or molecular dynamics: It represents a system on spatiotemporal basis by means of solving partial derivatives with numerical approaches. The outputs are in numeric form given as concentrations and cartesian coordinates. It has a clear formalism, can be fast, robust in mathematical aspect and let the system model in a dimension of both space and time. However, it is complex, generalization is difficult, also tough to put into practice and brittle. It is not suitable for discontinuous state transitions (Materi and Wishart, 2007).
- Petri nets: It is executable graphical alternative of ODEs for modeling time-dependent and discrete processes based on flowcharting technique between places (states), transitions (actions) and directional connections (D’Angelo, 1983; David and Alla, 2005; Materi and Wishart, 2007). There exist also continuous and hybrid versions of them (David and Alla, 2005). In the case of multiple inputs, signals from different branch of input weighed to activate the down stream of events. It is a promising tool for asynchronous occasions, operation synchronization, concurrent operations, resource allocation and conflicts (Zurawski and Zhou, 1994). It has subclasses as colored petri nets, hybrid Petri nets, stochastic petri nets and timed Petri nets. It immitates telephone switchboard or load management in power-grids. It is suitable for

implementing nonmathematical and allows both qualitative and quantitative models. It also has the same problem of limiting to temporal modeling as previously mentioned ones. In addition to being less developed than ODEs, is widely applied in non linearization (Materi and Wishart, 2007).

- Cellular automata (CA): This technique models time and space processes on a grid based approach in which simple Boolean logic rules out the neighboring objects interactions. It gives animated and numerical results. It permits both qualitative and quantitative modeling of time and space processes, simple to implement, and non mathematical but has the disadvantage of computational cost for large number of objects and having no basic conversion from rate constants. It is not as mature technique as ODEs and PDEs (Materi and Wishart, 2007).
- Agent based models (ABM): Each model member, i.e., proteins, drugs, cells, designed as agents that can spatiotemporally interact with each other according to some predetermining rules. While the rules can have either physical or complex knowledge basis, agents can have Brownian type or directed motions. It has similar properties with CA methodology but with a difference of not having formally essential spatial grids or synchronized time steps. However, in terms of practical aspects these constraints are widely employed in coding stage (Materi and Wishart, 2007).
- Pi calculus: It examines concurrent computational processes interacting with transfer of synchronized messages and having dynamical interconnections evolving with the interactions. In origin, it has algebraic form but can also be designed with graphical syntax. This method is less developed than all other modeling schemas (Materi and Wishart, 2007).
- Hybrid models: Let to utilize the advantage of different techniques in a single model. One of the primary benefits is the ability to integrate processes that happens on different time scales, e.g., integrating diffusion (a fast process) and tumor growth, metastasis (relatively slow and can take days) (Materi and Wishart, 2007).

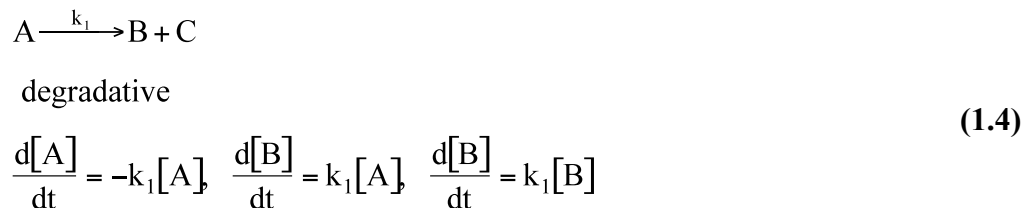
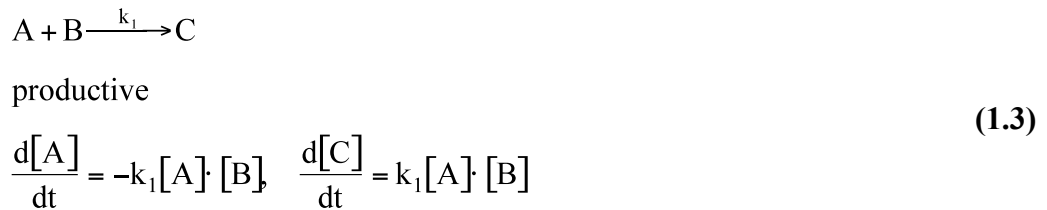
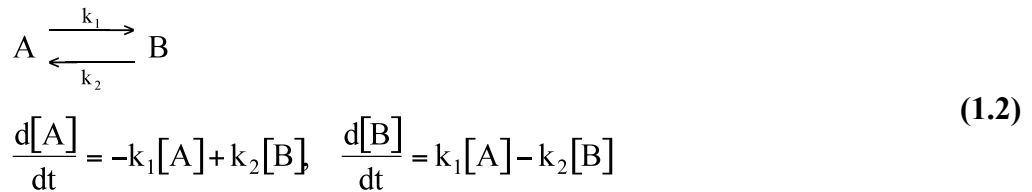
1.3 Theory

1.3.1 Reaction ordinary differential equations

Since our models will rely on reaction kinetics and ordinary differential equations, in this text emphasizes will be given on the ODEs techniques in the following part of the text.

As mentioned before ODEs represents chemical reactions. If they are simple enough ODEs can have exact solutions; in other case must be solved numerically. For the computation of reactant concentrations numerical methods utilize linear approximations via smooth curves having small time intervals based on methods first derived by Newton and Gauss (Materi and Wishart, 2007). To improve the computational accuracy of it, several algorithms like Runge–Kutta are developed.

The main reaction ODEs, Materi and Wishart (2007), can be given as :



$$\begin{aligned}
& A + B \xrightleftharpoons[k_2]{k_1} C + D \\
& \frac{d[A]}{dt} = \frac{d[B]}{dt} = -k_1[A] \cdot [B] + k_2[C] \cdot [D], \\
& \frac{d[C]}{dt} = \frac{d[D]}{dt} = k_1[A] \cdot [B] - k_2[C] \cdot [D]
\end{aligned} \tag{1.5}$$

$$\begin{aligned}
& A + B \xrightarrow{k_1} C \\
& \text{including diffusion rate } D_1 \text{ of molecules} \\
& \frac{d[A]}{dt} = D_1 \nabla^2[A] - k_1[A] \cdot [B], \quad \frac{d[C]}{dt} = -D_1 \nabla^2[C] + k_1[A] \cdot [B]
\end{aligned} \tag{1.6}$$

and for enzymatic reactions

$$\begin{aligned}
& A + B \xrightleftharpoons[k_2]{k_1} AB \xrightarrow{k_3} A + C \\
& \frac{d[A]}{dt} = -k_1[A] \cdot [B] - (k_2 + k_3)[AB], \\
& A_{\text{initial}} = [A] + [AB],
\end{aligned} \tag{1.7}$$

1.3.2 Modeling with transfer functions

The transfer functions firstly used as an elementary component of classical control engineering and nowadays widely used in nearly all fields of engineering. A transfer function can be used to recapitulate the way of how a signal evolves through the system. Having a known transfer function makes it possible to predict the output under a certain stimuli and vice versa. $X(s)$ and $Y(s)$ is usually represents the input and output of the system, respectively. $G(s)$ and $H(s)$ often indicate transfer functions (Figure 1.11). These are Laplace transforms of corresponding time-dependent functions $x(t)$, $y(t)$.

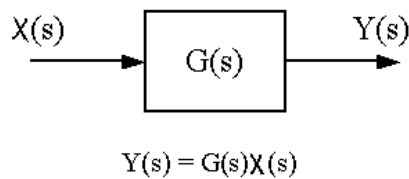


Figure 1.11: A block representation of transfer function $X(s)$ refers input, $Y(s)$ is output.

In mathematical terms, if $x(t)$ and $y(t)$ are input and outputs in phase space respectively, the linear mapping to s domain (the Laplace transform) basically given as (Ogata, 1990):

$$\begin{aligned} X(s) &= L\{x(t)\} = \int_0^{\infty} x(t)e^{-st} dt, \\ Y(s) &= L\{y(t)\} = \int_0^{\infty} y(t)e^{-st} dt, \\ Y(s) &= G(s)X(s). \end{aligned} \tag{1.8}$$

The general form of the transfer function for first order systems, which refers to systems modeled by first order differential equations are given by $G(s)=K/(\tau s+1)$ where K is gain, τ is the time constant for $G(s)$. Transfer functions of second order system are $G(s)=K\omega_n^2/(s^2+2\xi\omega_n s+\omega_n^2)$, where K , ξ , ω_n represents gain, damping parameter and undamped natural frequency, respectively (Ogata, 1990; Oppenheim, Willsky and Nawab, 1997). Higher order systems usually can be modeled as the combination of first and second order systems (Oppenheim, Willsky and Nawab, 1997).

For $K=1$ and a unit step input $X(s) = 1/s$, by taking the inverse Laplace Transform of a second order transfer function one can obtain unit step response as (Ogata, 1990):

$$y(t) = 1 - \frac{e^{\xi\omega_n t}}{\sqrt{1-\xi^2}} \sin(\omega_n \sqrt{1-\xi^2} t) + \tan^{-1} \frac{\sqrt{1-\xi^2}}{\xi} \tag{1.9}$$

In the equation unit step response $\omega_n \sqrt{1-\xi^2} t$ is defined as transient oscillations frequency. Both percentage over shoot and transient equation can be obtained from step response as given in Figure 1.12 at the next page. For $K=1$, one can determine transfer function from this quantities.

The other important parameters which can be obtained by step response are the rise time and settling time. The interval that step responses undergo the most significant changes is called as rise time which can be in the range %0 to %100, %5 to %95, %10 to %90 according to the application, Ogata (1990), and the length of time that takes the system to reach and settle in the vicinity of final value is called the settling time (Ogata, 1990).

In spite of single cell stochastic nature, in average a population can have predictable behaviour that can be explained by simple linear rules (Selvarajoo, Tomita and Tsuchiya, 2009). According to this view, perturbations in first order mass action

response equations can help to resolve network structure of this kind of complex systems by linear principles (Selvarajoo, Tomita and Tsuchiya, 2009). Based on the evidences indicating the resemblance to linear systems and some previous applications, Covert et al. (2005), we used transfer functions to apply the methods of control theory to model the system by representing the systems in frequency domain.

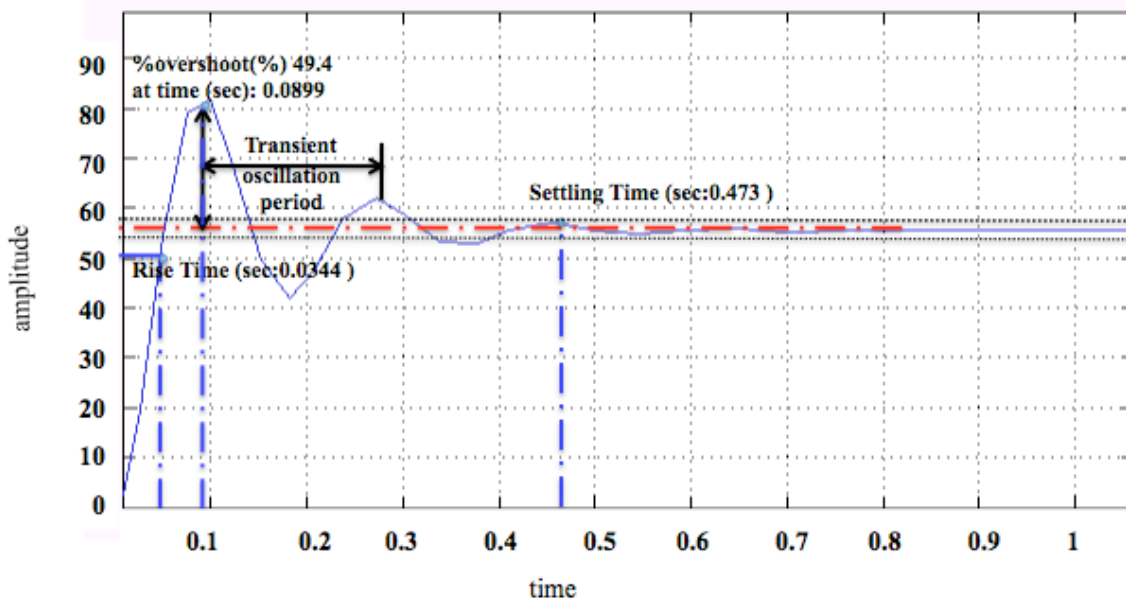


Figure 1.12: Graphic illustrates the parameters used for determination of transfer function and second order systems.

The transfer function of the graph is $G(s) = \frac{5000}{0.07s^2 + 1.1s + 90}$. Overshoot, settling time and rise time is demonstrated on it.

For example in Figure 1.13 a transfer function produces a signal very close to the previously given graph of NF- κ B activity for I κ B α over expressed mutants. The related model illustrated below the graphs. As can be seen from the model, the source is a step function.

Transfer function method was also used to model TLR4 mediated NF κ B-I κ B regulatory network, Covert et al. (2005), and provided clues about time delay in the Trif part of the pathway.

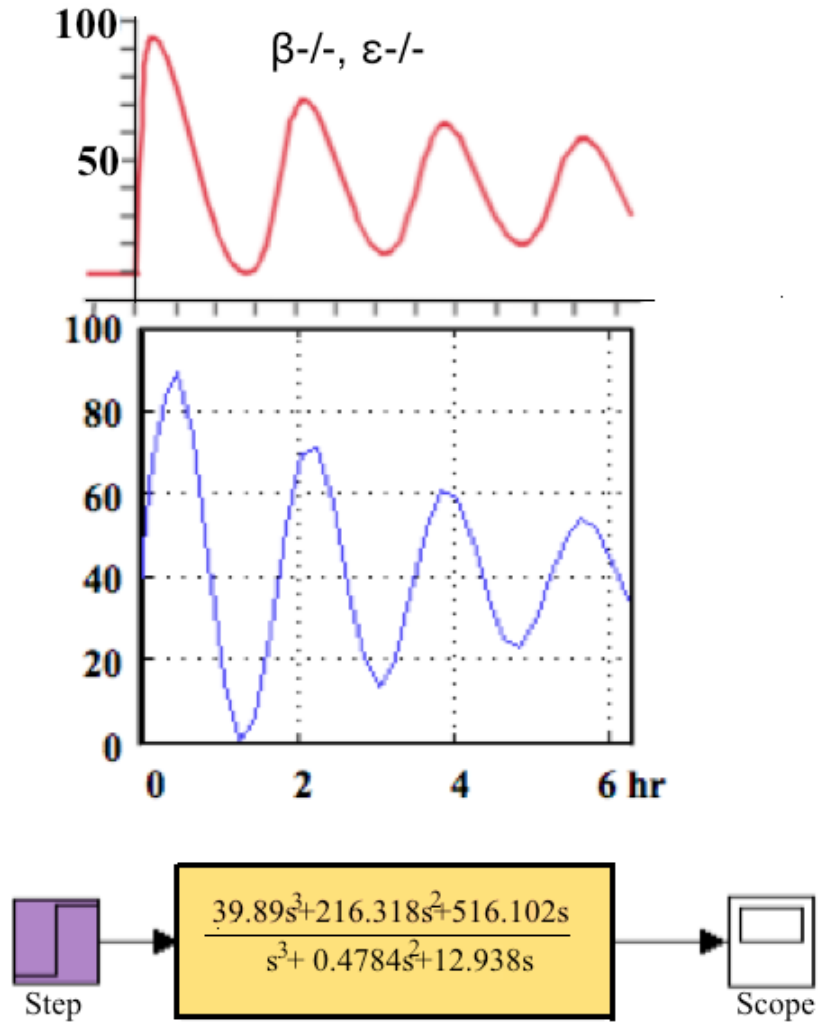


Figure 1.13: The graph given in the left part of the figure, Hoffmann et al., (2002), is the simulation output for IkB α over expressed NF κ B activation. The right graph indicates the step response of the transfer function given by the yellow box in the below part of the figure.

1.3.3 Optimization

To solve most of the real-world problems, optimization of multiple objectives is required. Here optimization refers to just obtaining solutions such that all objective functions have values in acceptable limits, because of exact achievements of each objectives are almost impossible. These kinds of problems requiring the achievement of multiple goals are in general named as multi-objective, multi-criteria, or multi-performance optimization problems and many heuristic search algorithms including artificial immune systems, memetic algorithms, simulated annealing, scatter search, tabu search, particle swarm optimization, and evolutionary algorithms are employed to solve them (Carlos, Gary, and David, 2007; Hamidreza and Christopher, 2008). Among all these optimization strategies, evolutionary approaches have been applied as

the primary tool during the last decades and several variations of multi-objective evolutionary algorithms are developed. In this study we also have a multi-objective problem and we mainly utilize genetic algorithms to minimize our cost functions serving these different objectives. By concerning the need of further refinement of the results, pattern search and Nelder –Mead algorithm are used as a hybrid function in the optimization process.

The approaches to optimize multiple-objective problems can be separated in two general classes namely as Pareto techniques or non-Pareto techniques also known as classical, traditional techniques (Konak, Coit and Smith, 2006):

The traditional approaches work by adding the multiple objectives into a single scalar one, by assigning a weight to each normalized objective function or by moving the objectives into constraint sets (Srinivas and Deb, 1994; Konak, Coit and Smith, 2006). The weights are expected to be supplied by users and only a single solution can be obtained by these weights. If the problem is solved repeatedly by using different combinations of the weights, than multiple solutions attained (Konak, Coit and Smith, 2006). Automation of this process and achieving multiple solutions in a single trial is also possible by use of genetic algorithms if the related weights are placed in each chromosome (Hajela and Lin, 1992). Other possibility is the generation of normalized weight vectors randomly. While it makes possible to search for multiple directions in single run and having the advantage of computational efficiency, it may not work when the solutions distributed uniformly over concave (convex for maximization problems) trade off surface. (Zitzler et al., 2000; Konak, Coit and Smith, 2006). In addition, if the variable space is discontinuous, traditional approaches may function inadequately (Hamidreza and Christopher, 2008).

In the general other class, it is possible to solve the multi objective problem without reducing it to a single objective one, by only finding the all feasible non-dominating solution set, also known as non-inferior, Pareto efficient or Pareto optimal set, or a representative subset of it. A Pareto optimal, Pareto (1896), is a solution such that further improvement in the objectives can not be performed without making at least one of them worse off. The name of non-dominated is originated from the property that the Pareto optimal solution can not be dominated by the other solutions in the search space. In mathematical terms:

For a minimization multi objective problem let two decision variable vectors in the space R^m are given such that $a=a_1, a_2, \dots, a_m$ and $b=b_1, b_2, \dots, b_m$

Two objective variable vectors in the solution space R^n is represented by

$$f(a)=(f_1(a), f_2(a), f_3(a), f_3(a), \dots, f_n(a)) \text{ and}$$

$$f(b)=(f_1(b), f_2(b), f_3(b), f_3(b), \dots, f_n(b))$$

$$a \text{ dominate } b \Leftrightarrow f_i(b) \leq f_i(a) \quad \forall i \in \{1, 2, 3, \dots, m\} \quad (1.10)$$

$$f_j(a) > f_j(b) \quad \exists j \in \{1, 2, 3, \dots, m\},$$

In other words a dominate b , if the solution a is not worser than b for all objective functions and for at least one solution a there is an objective function better than b . If there is no b solution such that b dominates a , than a is called as Pareto optimal solution (Srinivas and Deb, 1994; Zitzler et al., 2000).

The values in objective space corresponding to values of Pareto optimum set form an image (for two dimension simply a curve) called as the Pareto frontier.

Depending on the number of objectives, the size of Pareto optimal sets usually shows variation and obtaining whole Pareto optimal set for many problems is practically impossible on account of its size. Most of the time proof of solution optimality is not computationally cost efficient and to get rid of size problems one frequently applied method is investigating a good representative set of solutions (Zitzler et al., 2000; Konak, Coit and Smith, 2006). A proper set should be equally spaced in Pareto frontier and should reflect the entire trade off, especially at extreme ends (Zitzler et al., 2000; Konak, Coit and Smith, 2006).

Evolutionary algorithms are well tailored to solve multi-objective optimization problems, because they simultaneously handle a set of possible good solutions rather than a single solution (Deb, 2001; Srinivas and Deb, 1994). Dealing with sets of solutions has advantage of exploring the search space within a smaller number of runs, by determining several members of the Pareto optimal set in a single trial and also makes them faster relative to point to point local search procedures like tabu search or simulated annealing (April et al., 2003). Evolutionary algorithms can cope with non-convex and discontinuous Pareto fronts because of being less sensitive to the shape and continuity of it (Ikonen et al., 1997; Coello Coello, Lamont, and Veldhuisen, 2007). Moreover, dependence on initial conditions is lower and definition of neighborhood is not required in this kind of algorithm (April et al., 2003).

1.3.3.1 Genetic algorithms

Genetic algorithms (GA) are widespread meta-heuristics also applicable to multiobjective optimization problems by mimicking the natural process of genetic

duplication (Jones et al., 2002; Konak et al., 2006). Like in the nature better adopted members have more chance to survive and mate. In GA environmental conditions to be adopted are provided by fitness criteria. Population in each generation represents candidate solutions and members of this solution sets (chromosomes) selected to reproduce according to their fitness values. There are two reproduction mechanisms to evolve through new generations called as crossover and mutation. The crossover operator enables transfer and fuse of two parents' best genes in the offsprings and the mutation operator facilitates the population diversity by providing random changes generally at the gene level and so into characteristics of chromosomes. Without mutation, repetition of crossover multiple times results with convergence of population members with indistinguishable chromosomes and one possible concomitant handicap of this is getting stuck in to local minima (Konak et al., 2006). In reproduction, the fitness of an individual determines its likelihood to be inherited to the next generation. Some of the best members of the population can be transferred to the next generation not to lose already found good solutions. The number of good parents kept from previous generations is called as elite count. How fitness of genes is used for selection is determined by different selection mechanisms and most popular mechanisms are proportional selection, tournament selection and ranking (Konak et al., 2006). In the current study we obtained our best results with fitness scaling function of rank, crossover function of two points, pattern search as hybrid function and with the MATLAB default values for all the other functions.

1.3.3.2 Pattern search

Pattern search methods do not use derivatives or approximations of them for optimization as in the case of other direct search algorithms (Kolda et.al, 2003). For this reason they are appropriate for non-smooth, discontinuous systems and for the system including stochastic noise. In many case they are more efficient and deterministic than genetic algorithm but it is needed to provide a right starting point for convergence.

A pattern search algorithm repetitively scan the region around existing best point by evaluating the objective functions in each iteration, to get closer to the desired optimal value. All of points in this search region called as mesh. Size of the region is determined by multiplying a fixed set of vectors known as pattern with a scalar named as mesh size (Url-1). An example of pattern in two dimension is the set of unit vector

of four direction: $[1\ 0]$, $[0\ 1]$, $[-1\ 0]$ and $[0\ -1]$. As soon as algorithm finds a point fitting better to the criteria, the search continues around that new one and this type of search algorithm called as polling. As a next step mesh size is increased. If the results of trial are positive the process goes so on, otherwise mesh size decreased. If the mesh sizes less than a tolerance value, the process is ended. Other standard stopping criteria can also be applied.

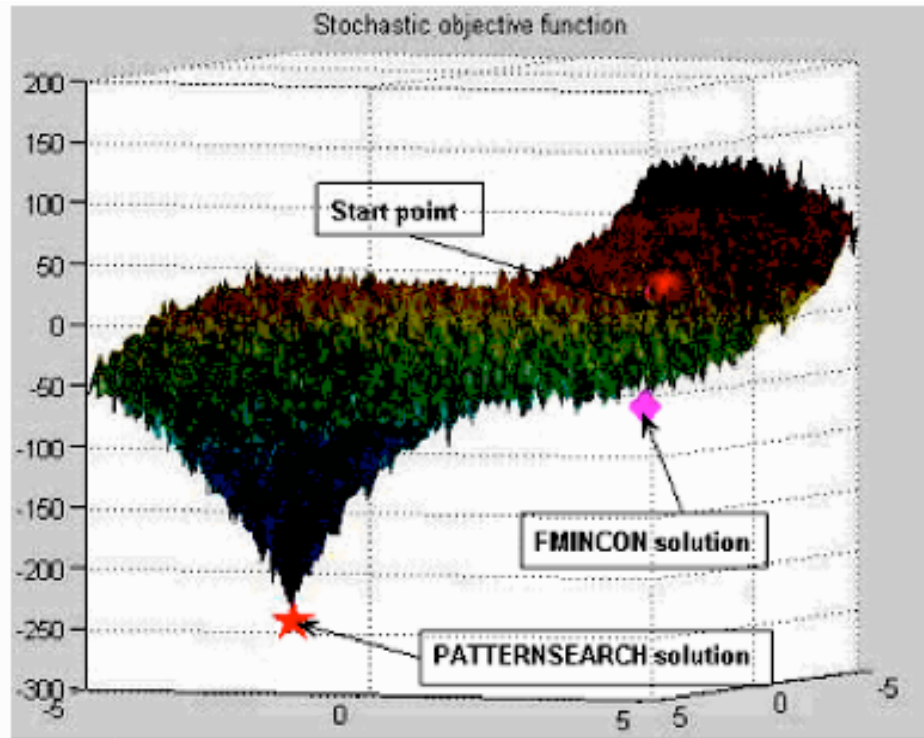


Figure 1.15: A comparison of derivative based algorithm and pattern search in finding the minima when a rough surface or when a stochastic noise present (Url-2).

Pattern search methods are quite appropriate for the incorporation of heuristic procedures. With heuristic algorithms (such as genetic algorithm), very fast achievement of a point near to optimum is possible. On the other hand desired convergence requires many more evaluations. Pattern search alone suffer from convergence to stationary point with polling but the flexible step size let to escape from local minimums. Incorporation with appropriate heuristics makes them well in determination of global minimums (Wetter and Wright, 2003; Ismail, Vaz and Vicente, 2007). Thus, by using the near optimum output from genetic algorithm as input for a pattern search, it is possible to utilize pattern search as a efficient local search tool to refine the results. Figure 1.15 indicates a comparison of derivative based

algorithm and pattern search in finding the minima when a rough surface or when a stochastic noise is present.

1.3.3.3 Nelder –Mead algorithm

The Nelder-Mead algorithm, Nelder and Mead (1965), or simplex search is also an optimization method in the class of direct search methods. It suits very well to N dimensional space and especially designed for unconstrained optimization. This method is one of the oldest one and works well if a function alters smoothly. In an N dimensional space a simplex is determined by N+1 distinct vectors forming the vertices between N+1 points, Lagarias et al., (1998), and is in the shape of a polytope, basically a triangle in two dimensions and a polyhedron in three, a polycrone for four dimension and so forth. There are four main parameters for a simplex algorithm, namely expansion, contraction, shrinkage and reflection (Lagarias et al., 1998). Their default values are standard for most of the algorithms and are 1, 2, 1/2, 1/ 2 respectively (Lagarias et al., 1998).

To converge to desired simplex, the algorithm first determines a new point near to or in the existing one. If this new point has a better score in objectives than another current point of the simplex, then the old worse one is discarded (Lagarias et al., 1998). One of the methods to form a new candidate polytype is reflecting the worst point from the centroid of the vertices of other points (Lagarias et al., 1998). According to the fitness of new point, either it is stretched exponentially along the vertices connecting this point or an shrinkage in the direction of the best point is provided.

One of the main problems related with the algorithm is getting stuck in rut, thus initialization with a right simplex is important. Restarting the algorithm from existing best value with a new simplex is one option that works in many circumstances.

1.3.3.4 Stochastic Modeling

In the deterministic ODE approach, dependences on spatial positioning other than being compartmentally separated (i.e. being in cytoplasm or in nucleus) are ignored (Hayot and Jayaprakash, 2008). This method usually works well for large number of molecules allowing the occurrence of any two reaction at the same time and changes in number of molecules can be solved differentially. But this approach breaks down for small amount of molecules, in which case reactions happens randomly with

temporal separation rather than simultaneous occurrence (Hayot and Jayaprakash, 2008).

For small number of molecules, like in single cell applications, a method based on probability of states for each given time function much better and mostly inevitable, especially in determining oscillations in the single cell experiments which are poorly occurs in reaction ODES method and in determining role of noise. One of the well-known methods to implement the probabilistic, stochastic Modeling techniques is Gillespie's algorithm (Gillespie, 1997). This approach converges to ordinary differential equation method when the results are averaged over population (Hayot and Jayaprakash, 2008).

1.3.3.5 Gillespie's algorithm

The Gillespie's algorithm simply try to represent the collision of molecules within a reaction vessel with randomly generated reaction and time steps. In this aspect, Gillespie's algorithms is a diversification of dynamical Monte Carlo algorithm. Despite well mixed environment with many collisions, the collisions leading reactions are rare, thus are assumed to merely take place between two molecules and can be modeled as collection of binary reactions.

The algorithm basically includes four step as given below:

Initialization: Initialization of system parameters (i.e. the number of molecules, reactions constants).

Monte Carlo step: random number generation to pick the time interval and the next reaction.

Update: The number of molecules and time step are updated according to the reaction that occur and the randomly generated time interval, respectively.

Iterate: First three steps are repetitively applied until go beyond simulation time or number of the reactants ceases.

Figure 1.16, Hayot and Jayaprakash (2006), illustrates results of an application of Gillespie's algorithm on a simplified version of the NF- κ B model proposed by Hoffmann et al. (2002). The solid curve represents an average NF- κ B expression in response TNF α over 1000 single cell for initial amount of IKK having a Gaussian distribution with average number 30,000 and width (σ) equal to 5000. The dashed lines are for single cell with 25,000 and 35,000 IKK molecules. As this study

illustrates, average over many cells inadequately describe the single cell behaviour in terms of oscillations and phase.

Depending on how strong the transcription rate and fluctuations on IKK molecules, this study also indicates that population average either can represent oscillations like in Hofmann 2002 model or oscillations can be sweep out in average because of the extent of variability in single cell behaviour (Nelson et al. 2004; Hayot and Jayaprakash, 2006).

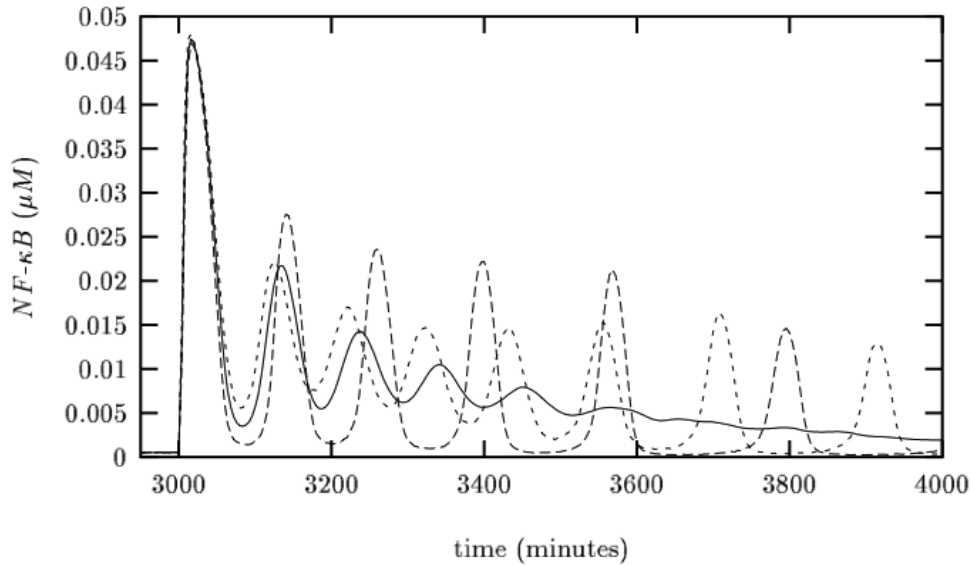


Figure 1.16: NF- κ B oscillations (Hayot and Jayaprakash, 2006).

According to recent findings, Tay et al. (2009), it is possible to reproduce many single cell NF- κ B profile in response to TNF α data obtained by micro fluidic studies by utilizing an upgraded version of previously developed stochastic model (Lipniacki et al., 2007). The new model differs from previous one according to some model parameters. These models include stochasticity at the level of receptor and at the transcription of A20 and I κ B α genes by NF- κ B. Stochasticity at the level of receptor supports the assumption that activation of single TNF α ligand complex is sufficient to induce substantial amount of NF- κ B translocation to nucleus and activation of related genes.

In another recent study on LPS stimulated NF- κ B activation, Lee et al. (2009), to recapitulate single cell data, stochasticity is introduced by application of a set reaction rates to the reported NF- κ B model (Covert et al., 2005). In the study while %50 of single cells show a late phase activity, the rest of the population do not. As a source of this behaviour, paracrine TNF α activation in response to MYD88 dependent pathway and resultant secondary NF- κ B activation is indicated. It seems there are still

missing points in explaining this late phase activity because the computational results and experimental data difference in the late phase which is possibly due to ignoring other crosstalk mechanism in between interferon and LPS pathway via PKR activity. Deterministic model is more effective at the initial stage for such a model examining the crosstalk mechanisms. But after indicating such an affect, utilization of stochastic Modeling approaches is important to be able to explain some single cell data.

2. METHODS

2.1 Method I-Transfer Functions and Simulink

The biochemical signaling networks of nuclear factor κ B (NF- κ B) family of proteins have important functions in immune response, inflammation, development and cell survival. This family of transcription factors is subject to multilevel control mechanism. In this part of the study we proposed a computational model relying on control theory and demonstrating the role of NF- κ B inhibitor proteins (IkB isoforms) in NF- κ B regulation. IkB α , IkB β and IkB ϵ (the isoforms) act differently in NF- κ B regulation and this difference allow rapid response to changes in the stimulus and long term moderate concentration of NF- κ B. We calculated transfer functions for each isoforms and for the overall effect to reproduce the temporal damped oscillation profiles given by the models of Hoffmann's group in literature. By utilizing direct search algorithms the multi-objective optimization problem of fitting the parameters in transfer functions, gains and delays are solved in 15 dimensional search space. Our preliminary optimization works on a simplified model of the system performed by MATLAB genetic algorithm toolbox with pattern search as hybrid method. We attained the main attributes of the reference signals, then refined the results by Nealder- Mead Algorithm. The resultant best profiles for the total effect of the IkB isoforms fit around eighty percent in amplitude to the reference signal for the initial peak and almost exactly in the later two peaks without any phase shift.

Procedure:

- After gathering the data from the reference model, we determined the transfer functions for each IkB isoforms (Figure 2.1 and Figure 2.2)

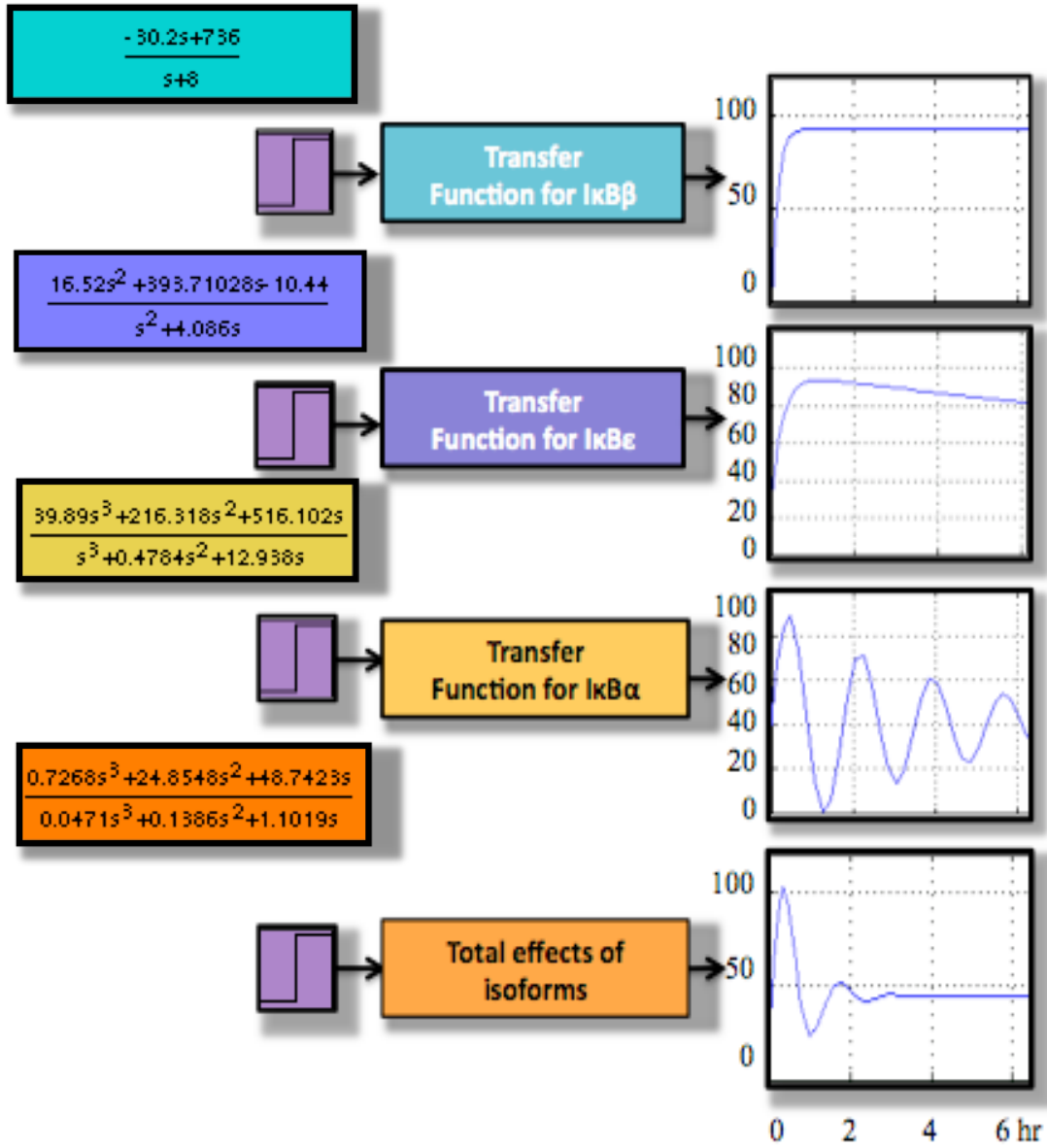


Figure 2.1: Transfer functions giving the NF κ B activity profile for IkB isoforms isolated effects and for wild type cells.

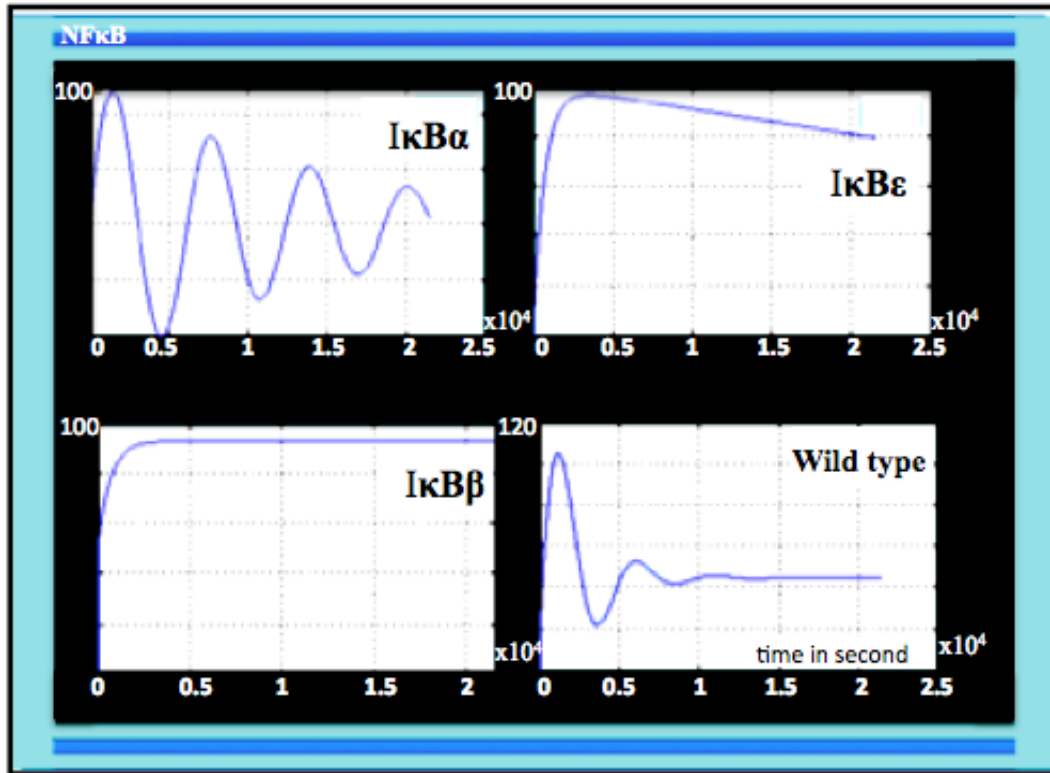
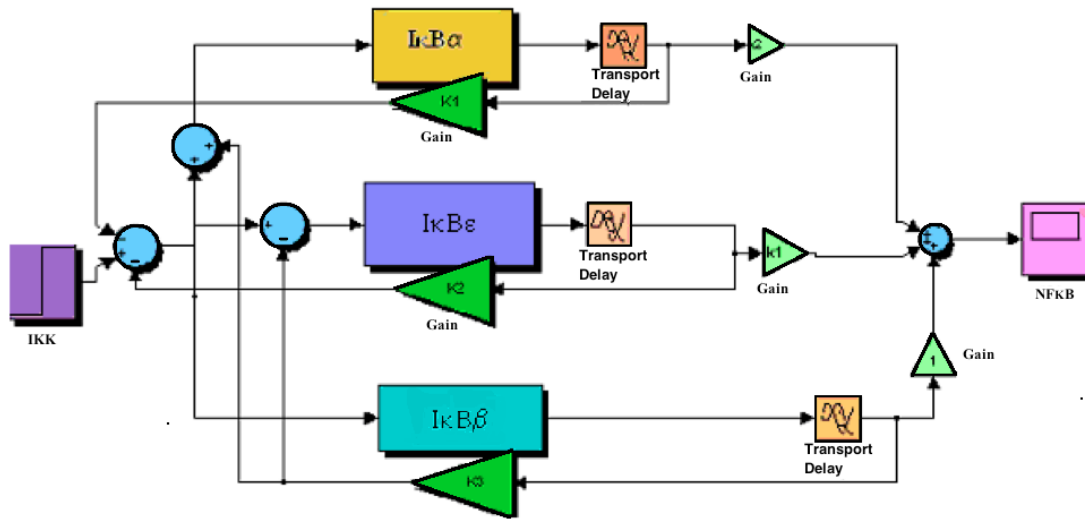


Figure 2.2: The output of transfer functions for the Model having real time scale.

- By using the experimental results in literature we selected the possible feedback relations between IκB isoforms and NFκB (Figure 2.3 and Figure 2.4).
- We constructed several models in Simulink including these possible interactions and let 15 parameters free to fit the reference data.
- These parameters are optimized by minimizing the least mean square error between reference signals of each isoform+their total affect and signals that we produced. In first stage of the optimization process Matlab Genetic algorithm toolbox is used.
- Pattern search is utilized as hybrid algorithm in genetic algorithm to refine our results.
- The best result is obtained from this hybrid search transferred to pattern search toolbox for further refinement with hybrid Nelder-Mead algorithm.

a)



b)

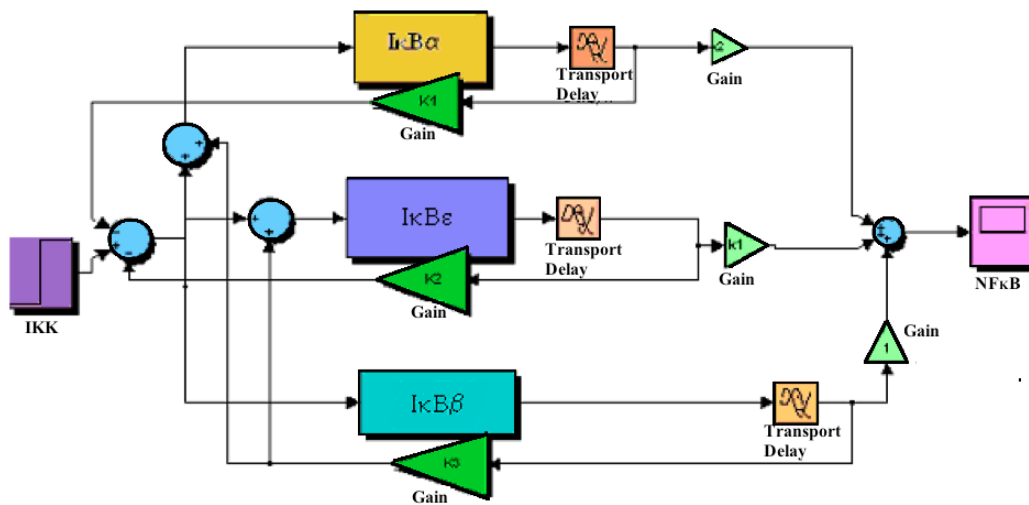


Figure 2.3: Some of the possible models that suits to existing experimental knowledge. a) signal coming from $I\kappa B$ site induces negative feedback, b) signal coming from $I\kappa B$ site induces positive feedback.

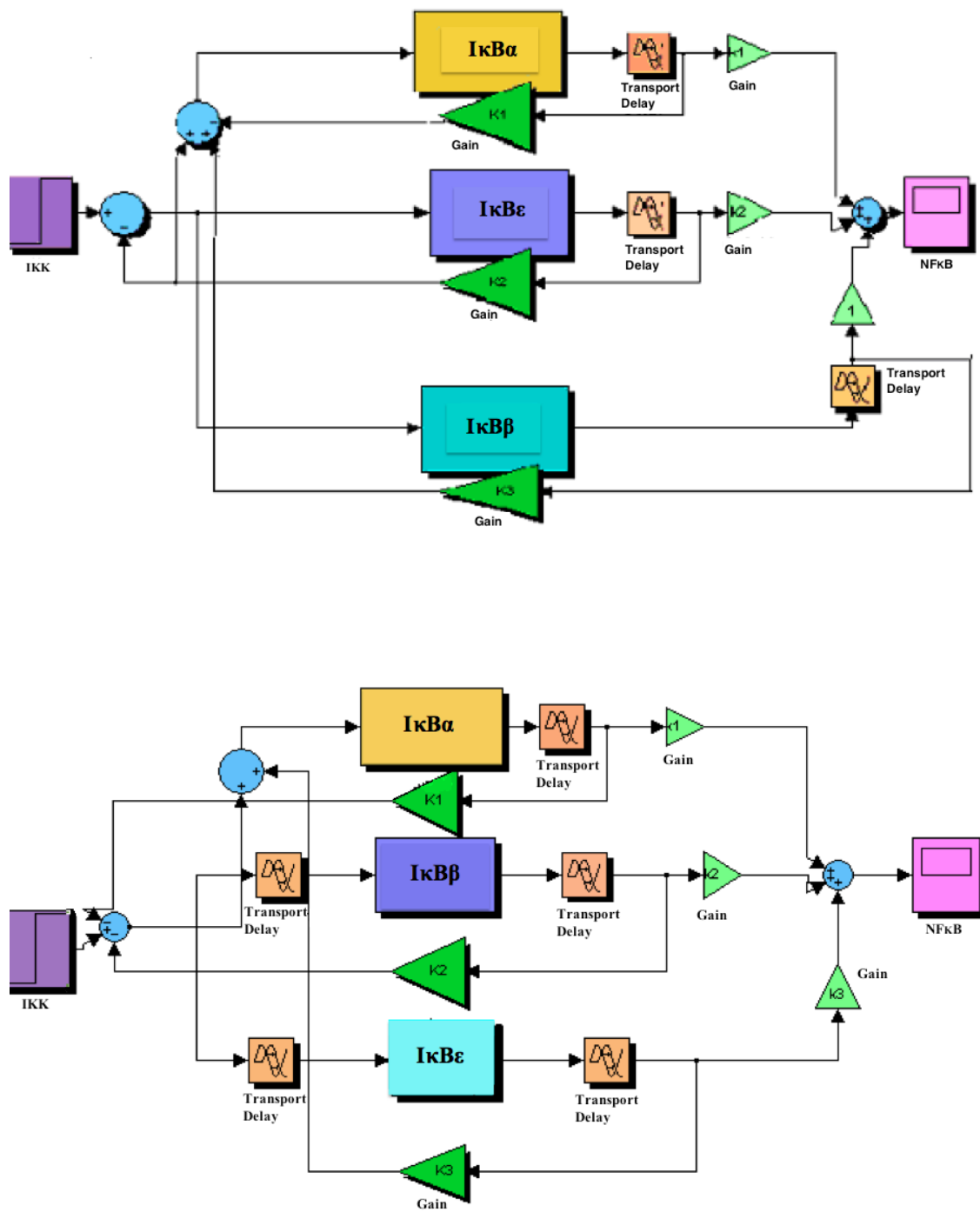


Figure 2.4: Some of the possible models planned to analyze.

2.2 Method II- Modeling with Ordinary Differential Equations

The attempts to explain LPS stimulated pathways and late phase activity of LPS stimulated NF κ B expression resulted in a few mathematical models of the system. While some of them were based on only one method like reaction ODEs or agent based approaches, An (2009), hybrid methods utilizing both transfer functions and reaction ODEs were also applied on the system. The main difficulty in these models is the lack of knowledge especially for the upstream MyD88 pathway and in determining the source of required delays. To achieve the expected NF κ B profiles either intermediates were introduced, Selvarajoo (2006), by just predicting the number of steps for required outcome or in place intermediates mediating signal through the upstream, a transfer function recapitulating this part of the system by an output in conjunction with experiments were used (Covert et al., 2005). Assigning such transfer function for upstream of MyD88 dependent and independent pathways were not enough to explain the experimental results. By bringing stochasticity to the system with a probabilistic approach at the stage of Triff dependent TNF α production, it was possible to obtain NF κ B late phase expression within relatively feasible limits (Lee et al., 2009). The other approach to estimate the number of intermediates in between receptor and downstream was not supported by the experiments indicating the receptor internalization as the source of the events in that region of the signaling cascade (Kagan et al., 2008). A rule-based model with crude estimate of reaction rates suggested various dose response curves and tolerance dynamics for LPS stimulated A20 and TNF α expression profiles (An and Faeder, 2009). This study also indicated the requirement of dual feedback mechanism exerted by both A20 at the TRAF6 and IKK level and I κ B at the NF κ B level and claimed A20 as an important source for providing delay and I κ B as the source of tolerance (An and Faeder, 2009). Rather than negative crosstalk interactions, signaling flux redistribution is suggested as a possible regulatory mechanism by another ODEs model and competition, conformational changes and physical blocking are proposed as the source of flux redistribution. This model utilized to evaluate the flux distribution at the different nodes after introducing perturbation to input. However especially at the receptor level proposed flux redistribution is not

validated by the subsequent experiments clarifying sequential occurrence of reactions at this level (Selvarajoo et al., 2008).

The only comprehensive IFN β pathway ODEs model in the literature was developed to enlighten the early and late responses of the system in the epithelial cells. In the study, while main emphasis was on the transcription from the GAS site like IRF1 regulation and STAT1 homodimers were taken as the primary transcription factor in this process, detailed analysis of the part acting through ISGF3, ISRE and dependent gene expressions were left to later studies. It mainly concentrated on the mechanisms of STATs (STAT1, STAT2) phosphorylation, STATs homo and heterodimer regulation, IRF1 regulation and tested several negative feedback mechanisms including SOCS1, PIAS, activation of dormant phosphatases, hypothetical molecules producing results commensurate with experiments (Smieja et al., 2008). One kind of these hypothetical molecules is supposed to be present at the nucleus, activated by ISGF3 and acts on STATs dimers and the other one is present in the cytoplasm and acts on IRF1. The system responses at the early stages were explained by phosphates activity and the late ones were based on IRF1 deactivation and accumulation at cytoplasm (Smieja et al., 2008). To determine the transcription factor behaviour, in this study we also tested the feedback mechanism, but we realised that receptor metabolism, i.e., degradation, complex formation and internalization, is the determining factor on the general tendency (Figure 3.5). In the previous study, it was claimed that transcription rate can be simply proportional to transcriptional factor concentration, however for the cases blocking the nuclear export with concomitant accumulation of transcription factors in the nucleus, they suggested to insert a nonlinearity, limiting the transcription by a function having a peak at the theoretical maximum transcription rate and given as: (Theoretical maximum transcription rate) \times (Transcriptional factor concentration) / (parameter to be determined + Transcriptional factor concentration) (Smieja et al., 2008).

2.3 Method III-Modeling of the Interferon Transcription

In this study, to limit transcription at a certain extent we employed an alternative method based on the probability of desired states that is widespread in statistical physics and also recently well described for the transcription event (Bintu et al., 2005). The binding probability to specific site can be written as the number of the

possible states that allow desired transcription divided by the number of all possible states of the system. Main assumptions of this approach are that transcription becomes possible if one of the RNA polymerase bound to specific side, the remaining ones distributed among the nonspecific sides on DNA and nonspecific sides act as the reservoir (Bintu et al., 2005). In our system the presence of both type of transcription factor at the same time enhances the transcription, in other words, NFκB and IRF3 act as AND gate for the transcription. The enhancement of transcription factors appears as a multiplier in the probability equation and is called as the regulatory factor (Bintu et al., 2005). The measure of transcription factors' effects on gene expression relative to the absence of transcription factors is given by fold change and it is approximately equal to the regulatory factor in the case of weak promoters controlling the transcription (Bintu et al., 2005). By using these definitions and the methodology, we derived the equations matching with the AND gate property of the transcription factors in our system.

To determine the probability of the statistical weights for the cases at which the promoter occupied are added up after the weight of each case is calculated by multiplying the number of arrangements and the Boltzmann factor for each state and the result is divided by the total statistical weight of all the possible states of the system, namely the partition function of the system. For this part of the model, just for simplification we ignored the whole mechanism of the enhanceosome formation and mainly concentrated on the effect of transcription factors and according to this assumption there are four possible cases for the binding of the polymerase molecules to specific sides: 1) only the polymerase bind to promoter and activator site is unoccupied, 2) only RNA polymerase and NFκB bind to specific sites 3) only the polymerase and IRF3 bind to specific sites 4) both of the activator sites and the promoter site are occupied. In addition to these four eventualities, the partition function includes four other cases very similar to the above but with versions in which the promoter is unoccupied so transcription is not an issue. In the direction of these descriptions, the partition function for the system in our concern can be written as follows:

$$\begin{aligned}
 Z_{\text{Total}} = & Z(P, A, B) + Z(P, A - 1, B)\alpha + Z(P, A, B - 1)\beta \\
 & + Z(P, A - 1, B - 1)\alpha\beta + Z(P - 1, A, B)P_o + Z(P - 1, A - 1, B)P_o\alpha f_A \\
 & + Z(P - 1, A, B - 1)P_o\beta f_B + Z(P - 1, A - 1, B - 1)P_o\alpha\beta f_{AB}\omega,
 \end{aligned} \tag{2.1}$$

where P represents the number of RNA polymerases, A and B represent the number of transcription factor molecules. The Boltzmann weights are denoted as:

$$\begin{aligned} e^{-\varepsilon_{pd}^S/k_B T} &= P_o, & e^{-\varepsilon_{ad}^S/k_B T} &= \alpha, & e^{-\varepsilon_{bd}^S/k_B T} &= \beta, \\ e^{-\varepsilon_{ap}/k_B T} &= f_A, & e^{-\varepsilon_{bp}/k_B T} &= f_B, \\ \omega &= e^{-\varepsilon_{ab}/k_B T}, & f_{AB} &= e^{-\varepsilon_{(ab)p}/k_B T}, \end{aligned} \quad (2.2)$$

and binding probability is:

$$P_{\text{bound}} = \frac{Z_{\text{bound}}}{Z_{\text{total}}} \quad (2.3)$$

where

$$\begin{aligned} Z_{\text{bound}} &= Z(P-1, A, B)P_o + Z(P-1, A-1, B)P_o \alpha f_A \\ &\quad + Z(P-1, A, B-1)P_o \beta f_B \\ &\quad + Z(P-1, A-1, B-1)P_o \alpha \beta f_{AB} \omega. \end{aligned} \quad (2.4)$$

Before the infection the IFN β secretion is very low and because of the fact that both the presence of IRF3 and NF κ B is required for the transcription of IFN β in remarkable amounts, Yie et al. (1999), we assumed that although IRF3 and NF κ B can bind to specific site, the adhesive energies, ε_{ap} , ε_{bp} between only one kind of transcription factor and the polymerase on the promoter is very low, close to zero, so the resultant f_A , f_B can be approximated as 1. In addition, we assumed the enhanceosome including IRF3 (A) and NF κ B (B) has a binding energy $\varepsilon_{(ab)p}$ and resultant Boltzmann weights is denoted by f_{AB} . We also accepted that this two transcription factor can not be on their specific sites without interacting with each other in enhanceosome ensemble based on reported data indicating completion of enhanceosome formation only become possible by the protein-protein interactions between IFN β activators (Yie et al., 1999).

Simply:

$$\begin{aligned} \varepsilon_{ap} &= 0; \quad f_A = 1; \\ \varepsilon_{bp} &= 0; \quad f_B = 1; \end{aligned} \quad (2.5)$$

In explicit form Z_{bound} can be written as:

$$\begin{aligned}
Z_{\text{bound}} = & \frac{N! \alpha_1^A \beta_1^B P_1^{P-1} P_o}{(P-1)! A! B! (N-P-A-B+1)!} \\
& + \frac{N! \alpha_1^{A-1} \beta_1^B P_1^{P-1} \alpha P_o}{(P-1)! (A-1)! B! (N-P-A-B+2)!} \\
& + \frac{N! \alpha_1^A \beta_1^{B-1} P_1^{P-1} \beta P_o}{(P-1)! A! (B-1)! (N-P-A-B+2)!} \\
& + \frac{N! \alpha_1^{A-1} \beta_1^{B-1} P_1^{P-1} \beta P_o \alpha f_{AB} \omega}{(P-1)! A! (B-1)! (N-P-A-B+2)!}
\end{aligned} \tag{2.6}$$

and in explicit form Z_{total} is :

$$\begin{aligned}
Z_{\text{total}} = & \frac{N! \alpha_1^A \beta_1^B P_1^P}{P! A! B! (N-P-A-B)!} + \frac{N! \alpha_1^{A-1} \beta_1^B P_1^P}{P! (A-1)! B! (N-P-A-B+1)!} \\
& + \frac{N! \alpha_1^A \beta_1^{B-1} P_1^P \beta}{P! (A-1)! B! (N-P-A-B+1)!} \\
& + \frac{N! \alpha_1^{A-1} \beta_1^{B-1} P_1^P \alpha \beta \omega}{P! (A-1)! B! (N-P-A-B+2)!} \\
& + \frac{N! \alpha_1^A \beta_1^B P_1^{P-1} P_o}{(P-1)! A! B! (N-P-A-B+1)!} \\
& + \frac{N! \alpha_1^{A-1} \beta_1^B P_1^{P-1} \alpha P_o}{(P-1)! (A-1)! B! (N-P-A-B+2)!} \\
& + \frac{N! \alpha_1^A \beta_1^{B-1} P_1^{P-1} \beta P_o}{(P-1)! A! (B-1)! (N-P-A-B+2)!} \\
& + \frac{N! \alpha_1^{A-1} \beta_1^{B-1} P_1^{P-1} \beta P_o \alpha f_{AB} \omega}{(P-1)! A! (B-1)! (N-P-A-B+2)!}
\end{aligned} \tag{2.7}$$

and the bounding probability is found to be

$$\begin{aligned}
P_{\text{bound}} = \frac{Z_{\text{bound}}}{Z_{\text{total}}} = & \left(\frac{N! \alpha_1^A \beta_1^B P_1^{P-1} P_o}{(P-1)! A! B! (N-P-A-B+1)!} \right. \\
& + \frac{N! \alpha_1^{A-1} \beta_1^B P_1^{P-1} \alpha P_o}{(P-1)! (A-1)! B! (N-P-A-B+2)!} \\
& + \frac{N! \alpha_1^A \beta_1^{B-1} P_1^{P-1} \beta P_o}{(P-1)! A! (B-1)! (N-P-A-B+2)!} \\
& \left. + \frac{N! \alpha_1^{A-1} \beta_1^{B-1} P_1^{P-1} \beta P_o \alpha f_{AB} \omega}{(P-1)! A! (B-1)! (N-P-A-B+2)!} \right) / \dots
\end{aligned} \tag{2.8}$$

$$\begin{aligned}
& \left(\frac{N! \alpha_1^A \beta_1^B P_1^P}{P! A! B! (N - P - A - B)!} + \frac{N! \alpha_1^{A-1} \beta_1^B P_1^P}{P! (A - 1)! B! (N - P - A - B + 1)!} \right. \\
& + \frac{N! \alpha_1^A \beta_1^{B-1} P_1^P \beta}{P! (A - 1)! B! (N - P - A - B + 1)!} \\
& + \frac{N! \alpha_1^{A-1} \beta_1^{B-1} P_1^P \alpha \beta \omega}{P! (A - 1)! B! (N - P - A - B + 2)!} \\
& + \frac{N! \alpha_1^A \beta_1^B P_1^{P-1} P_o}{(P - 1)! A! B! (N - P - A - B + 1)!} \\
& + \frac{N! \alpha_1^{A-1} \beta_1^B P_1^{P-1} \alpha P_o}{(P - 1)! (A - 1)! B! (N - P - A - B + 2)!} \\
& + \frac{N! \alpha_1^A \beta_1^{B-1} P_1^{P-1} \beta P_o}{(P - 1)! A! (B - 1)! (N - P - A - B + 2)!} \\
& \left. + \frac{N! \alpha_1^{A-1} \beta_1^{B-1} P_1^{P-1} \beta P_o \alpha f_{AB} \omega}{(P - 1)! A! (B - 1)! (N - P - A - B + 2)!} \right)
\end{aligned} \tag{2.8}$$

simplification results with

$$\begin{aligned}
P_{\text{bound}} = & \left(\frac{\alpha_1 \beta_1 P_o}{A \beta N} + \frac{\beta_1 \alpha P_o}{\beta N^2} + \frac{P_o B \alpha_1}{A N^2} + \frac{P_o B \alpha f_{AB} \omega}{N^3} \right) \\
& / \left(\frac{P_1 \beta_1 \alpha_1}{P A \beta} + \frac{P_1 \beta_1 \alpha}{P \beta N} + \frac{P_1 \alpha_1 B}{P A N} + \frac{P_1 \alpha B \omega}{P N^2} + \frac{\alpha_1 \beta_1 P_o}{A \beta N} \right. \\
& \left. + \frac{\beta_1 \alpha P_o}{\beta N^2} + \frac{P_o B \alpha_1}{A N^2} + \frac{P_o B \alpha f_{AB} \omega}{N^3} \right)
\end{aligned} \tag{2.9}$$

and

$$P_{\text{bound}} = \frac{1}{1 + \frac{P_1}{P_o} \frac{N}{P} \frac{1}{\frac{\alpha_1}{A} \frac{\beta_1}{\beta} + \frac{\alpha}{N} \frac{\beta_1}{\beta} + \frac{\alpha_1}{A} \frac{B}{N} + \frac{B}{N} \frac{\alpha}{N} f_{AB} \omega}} \tag{2.10}$$

by rearrangements

$$P_{\text{bound}} = \frac{1}{1 + \frac{P_1}{P_o} \frac{N}{P} \frac{1}{1 + \frac{A}{N} \frac{\alpha}{\alpha_1} + \frac{B}{N} \frac{\beta}{\beta_1} + \frac{B}{N} \frac{A}{N} \frac{\alpha}{\alpha_1} \frac{\beta}{\beta_1} f_{AB} \omega}} \tag{2.11}$$

$$\begin{aligned}
\Delta \varepsilon_{\text{ad}} &= \varepsilon_{\text{ad}}^S - \varepsilon_{\text{ad}}^{\text{NS}} & \frac{\alpha}{\alpha_1} &= e^{-\Delta \varepsilon_{\text{ad}}} & a &= \frac{A}{N} e^{-\Delta \varepsilon_{\text{ad}}} \\
\Delta \varepsilon_{\text{bd}} &= \varepsilon_{\text{bd}}^S - \varepsilon_{\text{bd}}^{\text{NS}} & \frac{\beta}{\beta_1} &= e^{-\Delta \varepsilon_{\text{bd}}} & b &= \frac{B}{N} e^{-\Delta \varepsilon_{\text{bd}}}
\end{aligned} \tag{2.12}$$

after simplifications, the equation reduces to the form,

$$P_{\text{bound}} = \frac{1}{1 + \frac{N}{PF_{\text{regulatory}}} e^{\Delta\epsilon_{\text{pd}}/k_B T}} \quad (2.13)$$

and $F_{\text{regulatory}}$ is obtained as

$$F_{\text{regulatory}} = \frac{1 + a + b + abf_{AB}\omega}{1 + a + b + ab\omega} \quad (2.14)$$

or

$$F_{\text{regulatory}} = \frac{1 + \frac{[A]}{K_A} + \frac{[B]}{K_B} + \frac{[A][B]}{K_A K_B} f_{AB}\omega}{1 + \frac{[A]}{K_A} + \frac{[B]}{K_B} + \frac{[A][B]}{K_A K_B} \omega} \quad (2.15)$$

$$K_B = [B]/b, K_A = [A]/a$$

where $[A]$, $[B]$ are the concentrations and K_A , K_B are the effective equilibrium dissociation constants of the transcription factors, f_{AB} is a factor which represents adhesive interactions in between union of transcription factors and RNA polymerase on the promoter and ω is the interaction between two transcription factors.

In our model we utilize the regulatory factor in the reaction ODE for transcription as in the following equation:

$$\frac{d(\text{IFNmRNA})}{dt} = k \cdot (F_{\text{reg}} - 1) - k_{\text{deg}} \text{IFNmRNA} \quad (2.16)$$

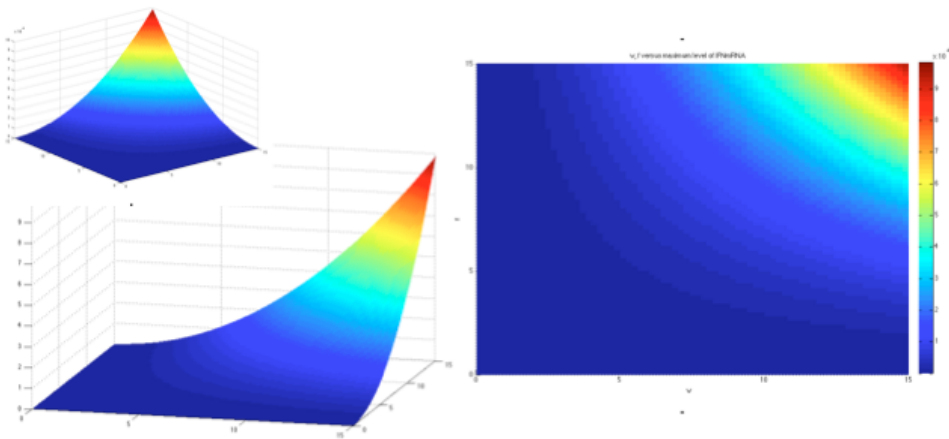


Figure 2.5 : Dependence of $F_{\text{regulatory}}$ on f_{AB} and ω values.

This equation gives one in the absence of one of the transcription factors. Either NF κ B or IRF3 is not present in the system, to obtain zero production rate, we need to subtract one from the regulatory factor value. Figure 2. 5 depicts the how how ω and

f values effect the $F_{\text{regulatory}}$ factor value for a change in between 0 and 15 and and Figure 2.6 indicates the dependencies of IFNmRNA values to these factors with w and f_{AB} values ranging between 0 and 6 with an interval of 0.5.

At the transcription level epigenetic is another factor determining IFN β regulation (Génin et al., 2009). Histone modifications at local sides, chromatin remodeling complexes and so DNA folding can be also introduced in a more advanced statistical transcriptional model than the one used in this work. Unfortunately histone modifiers recruited by IRF3 and IRF7 are not known, Génin et al. (2009), and so are not involved in our model.

2.4 Method IV-Modeling of the Signaling Cascades

For the remaining part of the problem we formulated reaction ODEs for the each form of the reaction species represented in the Figure 2.8 and solved these equations with Matlab ode15s solver. Based on reaction ODEs method, I design two models for IFN pathway one taking account of IFNAR internalization and PKR feedback (Figure 2.8) and one assumes constant amount of total receptor but includes negative feedbacks like SOCs1 and SOCs3 to obtain required decrease of ISGF3 (Figure 2.7). Despite the model including the receptor metabolism stages, the model including the SOCs feedbacks have a single phase not involving a stage to reach basal values.

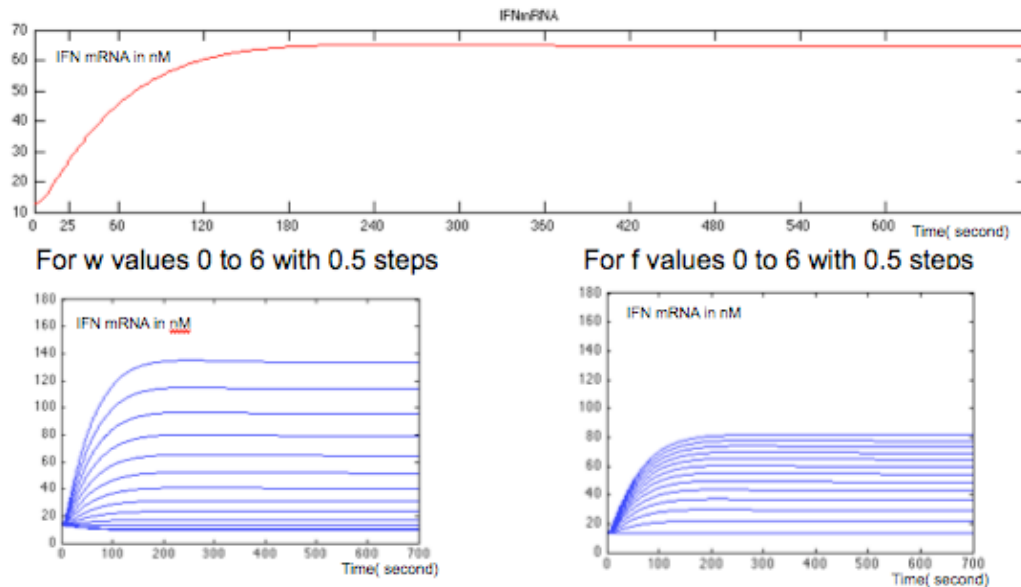


Figure 2.6 : Dependence of IFNmRNA on f_{AB} and ω values.

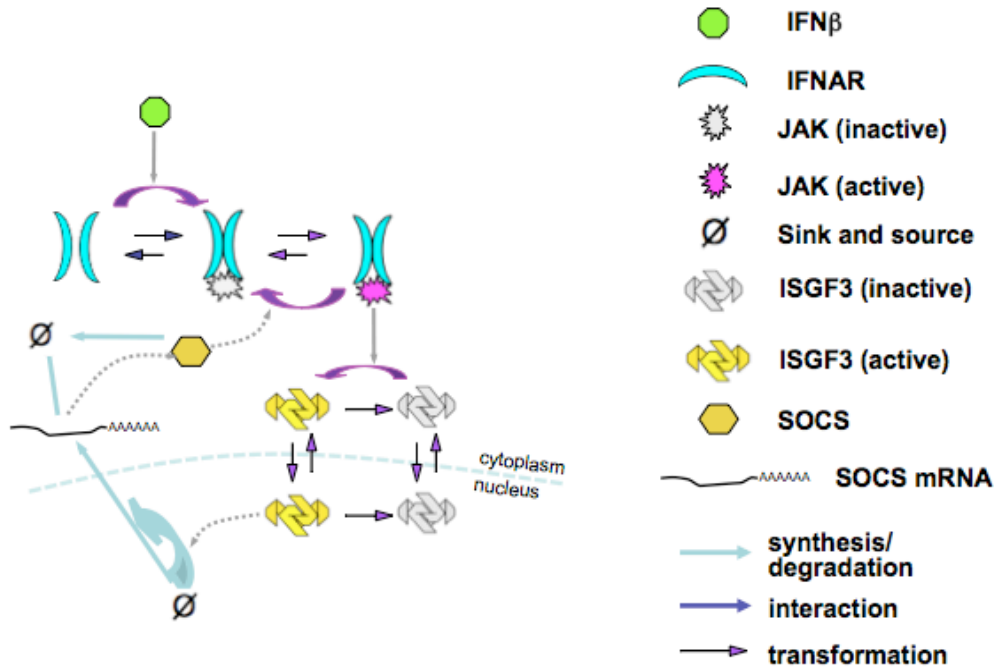


Figure 2.7: The schematics of model structure based on feedback mechanisms.

If sinks and sources are included, the models consist of 22, 12 species and 15, 9 ODE sets for the two interferon models, respectively. In the validation stage of these models, we observe that receptor internalization is very important in ISGF3 expression and down regulation. As a result we eliminated the second model that assumes the total amount of receptor on the cell surface as constant.

Because of the receptor internalization is a very important stage in IFN β pathway and by considering the number of the possible steps for the metabolism mechanism at the receptor level, we proposed a modified model based upon the TNF α -NF κ B model, Werner et al. (2008), including receptor complex formation, internalization and degradation steps. This approach brought a very favourable reduction in the number of reaction kinetic rates needed to be determined, either by directly employing the same value or setting a reference point in search space. We also made use of the reference model's two phases working principle, Werner et al. (2008); before ligand equilibrium basal levels of reactants are achieved and then by the ligand application time course data of the species are obtained. For the interferon pathway the reaction in the receptor level separated in to two parts for IFN β bound and unbound forms of receptor. The combined model includes 65 parameter and 28 ODE equations in total. While most of the parameter values are

taken from the data in the literature some of them adjusted to fit the published IFN β and IRF3 profile in the reference experimental study (The parameter list and their sources are in the supplementary materials).

From 37 parameters of the Interferon model, 8 of them are inherited directly from the reported TNF α -NF κ B model. Very similar to interferon pathway receptor metabolism is also characteristic part of the TLR4-MyD88 independent pathway determining the timing of end products (Figure 3.5). For this part of the model we tried a rather reduced model and ignored the many steps assumed to spontaneously occur without ligand, which are involved at left part of the IFN β receptor level. As a result the TLR4 pathway model in this study involves 28 parameters 2 of which originated from the reference TNF α -NF κ B model. After TLR4 forms dimer in the presence of LPS, MyD88 and Trif bind to the complex sequentially and before Trif, MyD88 leaves the TIR domain (Kagan et al., 2008). This simplified model was also very efficient to produce similar results with the more comprehensive one including the unbound receptor steps. In the model Trif receptor complex activate TRAF3 and concomitantly TBK1-IKK ϵ complex, IRF3 and IRF7 activated in sequential manner. Since the activation of IRF3 is a posttranslational effect and responsible for transcriptional activity, in the model IRF3 represented in four different forms given as: inactive, active cytoplasmic and nuclear forms, while the dimerization ignored in the nucleus, Kumar et al. (2000); Tsuchida et al. (2009), causes transcription of IFN β in collaboration with NF κ B (Thanos and Maniatis, 1995; Yie et al., 1999). Resultant IFN β triggers Type I interferon receptor.

The equations in two models can be given as:

$$\begin{aligned}
 d[\text{IFN}\beta]/dt = & -K_1.[\text{IFN}\beta] + 0.51.K_{50}.[\text{IFNmRNA1}] \\
 & -K_{15}.[\text{IFNAR}].[\text{IFN}\beta] \\
 & -K_{16}.[\text{IFNAR2}].[\text{IFN}\beta] \\
 & +K_{17}.[\text{IFNAR2IFN}\beta] \\
 & +K_{27}.[\text{IFNAR2JAKIFN}\beta] \\
 & -K_{28}.[\text{IFNAR2JAK}].[\text{IFN}\beta] \\
 & +K_{29}.[\text{IFNAR2JAKIFN}\beta \text{ a}] \\
 & -K_{30}.[\text{IFNAR2JAKa}].[\text{IFN}\beta];
 \end{aligned} \tag{2.17}$$

While [IFNAR2JAKIFN β] indicates concentration of dimerized IFNAR, JAK and IFN β molecules' inactive complex, [IFNAR2JAKIFN β a] indicates active form of

this complex. [IFNAR2JAK], [IFNAR2JAKa] are assigned for inactive form of two IFNAR molecule, JAK complex and active form of the same complex, respectively. Similarly [IFNAR2IFN β] represents dimerized IFNAR and JAK complex and [IFNmRNA1] refers to IFN β mRNA concentration.

$$\begin{aligned} d[\text{IFNAR}]/dt = & +K_2 - K_3.[\text{IFNAR}] + 2.K_4.[\text{IFNAR}] \\ & + 2.K_5.[\text{IFNAR2}] \\ & - 2.K_{15}.[\text{IFNAR}].[IFN\beta]; \end{aligned} \quad (2.18)$$

[IFNAR] is IFNAR receptor concentration,

$$\begin{aligned} d[\text{IFNAR2}]/dt = & + K_4.[\text{IFNAR}] - K_5.[\text{IFNAR2}] \\ & - K_6.[\text{IFNAR2}] - K_7.[\text{IFNAR2}] \\ & + K_8.[\text{IFNAR2JAK}] \\ & + K_9.[\text{IFNAR2JAK}]; \end{aligned} \quad (2.19)$$

[IFNAR2] is dimerized IFNAR receptor concentration,

$$\begin{aligned} d[\text{IFNAR2IFN}\beta]/dt = & - K_{18}.[\text{IFNAR2IFN}\beta] \\ & + K_{16}.[\text{IFNAR2}].[IFN\beta] \\ & - K_{17}.[\text{IFNAR2IFN}\beta] \\ & + K_{15}.[\text{IFNAR}].[IFN\beta] \\ & - K_{19}.[\text{IFNAR2IFN}\beta] \\ & + K_{20}.[\text{IFNAR2JAKIFN}\beta]; \end{aligned} \quad (2.20)$$

$$\begin{aligned} d[\text{IFNAR2JAK}]/dt = & +K_7.[\text{IFNAR2}] - K_8.[\text{IFNAR2JAK}] \\ & -K_9.[\text{IFNAR2JAK}] \\ & +K_{11}.[\text{IFNAR2JAKa}].[SOCS3] \\ & +K_{11}.[\text{IFNAR2JAKa}].[SOCS1] \\ & + K_{10}.[\text{IFNAR2JAKa}] \\ & + K_{27}.[\text{IFNAR2JAKIFN}\beta] \\ & - K_{28}.[\text{IFNAR2JAK}].[IFN\beta]; \end{aligned} \quad (2.21)$$

$$\begin{aligned} d[\text{IFNAR2JAKa}]/dt = & - K_{12}.[\text{IFNAR2JAK}] \\ & + K_9.[\text{IFNAR2JAK}] \\ & - K_{10}.[\text{IFNAR2JAKa}] \\ & - K_{11}.[\text{IFNAR2JAKa}].[SOCS3] \end{aligned} \quad (2.22)$$

$$\begin{aligned}
& - K_{11} \cdot [\text{IFNAR2JAKa}] \cdot [\text{SOCS1}] \\
& - K_{14} \cdot [\text{IFNAR2JAKa}] \\
& + K_{29} \cdot [\text{IFNAR2JAKIFN}\beta \text{ a}] \\
& - K_{30} \cdot [\text{IFNAR2JAKa}] \cdot [\text{IFN}\beta] ;
\end{aligned}$$

$$\begin{aligned}
d [\text{IFNAR2JAKIFN}\beta \text{ a}] / dt = & - K_{24} \cdot [\text{IFNAR2JAKIFN}\beta] \\
& + K_{21} \cdot [\text{IFNAR2JAKIFN}\beta] \\
& - K_{22} \cdot [\text{IFNAR2JAKIFN}\beta \text{ a}] \\
& - K_{23} \cdot [\text{IFNAR2JAKIFN}\beta \text{ a}] \cdot [\text{SOCS3}] \\
& - K_{23} \cdot [\text{IFNAR2JAKIFN}\beta \text{ a}] \cdot [\text{SOCS1}] \quad (2.23) \\
& - K_{26} \cdot [\text{IFNAR2JAKIFN}\beta \text{ a}] \\
& - K_{29} \cdot [\text{IFNAR2JAKIFN}\beta \text{ a}] \\
& + K_{30} \cdot [\text{IFNAR2JAKa}] \cdot [\text{IFN}\beta];
\end{aligned}$$

$$\begin{aligned}
d [\text{IFNAR2JAKIFN}\beta] / dt = & + K_{19} \cdot [\text{IFNAR2IFN}\beta] \\
& - K_{20} \cdot [\text{IFNAR2JAKIFN}\beta] \\
& - K_{21} \cdot [\text{IFNAR2JAKIFN}\beta] \\
& + K_{22} \cdot [\text{IFNAR2JAKIFN}\beta \text{ a}] \\
& + K_{23} \cdot [\text{IFNAR2JAKIFN}\beta \text{ a}] \cdot [\text{SOCS3}] \quad (2.24) \\
& + K_{23} \cdot [\text{IFNAR2JAKIFN}\beta \text{ a}] \cdot [\text{SOCS1}] \\
& - K_{25} \cdot [\text{IFNAR2JAKIFN}\beta] \\
& - K_{27} \cdot [\text{IFNAR2JAKIFN}\beta] \\
& + K_{28} \cdot [\text{IFNAR2JAK}] \cdot [\text{IFN}\beta];
\end{aligned}$$

$$\begin{aligned}
d[\text{ISGF3}]/dt = & + K_{33} \cdot [\text{ISGF3a}] \\
& + K_{37} \cdot [\text{ISGF3N}] \\
& - K_{31} \cdot [\text{ISGF3}] \cdot [\text{IFNAR2JAKa}] \quad (2.25) \\
& - K_{32} \cdot [\text{ISGF3}] \cdot [\text{IFNAR2JAKIFN}\beta \text{ a}] \\
& - K_{38} \cdot [\text{ISGF3}];
\end{aligned}$$

[ISGF3] and [ISGF3a] is inactive and active ISGF3 concentration, respectively,

$$\begin{aligned}
d[\text{ISGF3a}]/dt = & + K_{35} \cdot [\text{ISGF3Na}] \\
& + K_{31} \cdot [\text{ISGF3}] \cdot [\text{IFNAR2JAKa}] \quad (2.26)
\end{aligned}$$

$$+K_{32} \cdot [ISGF3] \cdot [IFNAR2JAKIFN\beta a] \\ - K_{33} \cdot [ISGF3a] - K_{36} \cdot [ISGF3a];$$

[ISGF3N], [ISGF3Na] are inactive and active ISGF3 concentration in the nucleus,

$$d[ISGF3N]/dt = +K_{34} \cdot [ISGF3Na] \\ +K_{38} \cdot [ISGF3] \\ -K_{37} \cdot [ISGF3N]; \quad (2.27)$$

$$d[ISGF3Na]/dt = -K_{34} \cdot [ISGF3Na] \\ -K_{35} \cdot [ISGF3Na] \\ +K_{36} \cdot [ISGF3a] \quad (2.28)$$

For TLR4 pathway the equations are:

$$d[LPS]/dt = -K_{51} \cdot [LPS] \\ -K_{57} \cdot [TLR4] \cdot [LPS]; \quad (2.29)$$

[LPS] is the ligand (LPS) concentration,

$$d[TLR4]/dt = -K_{53} \cdot [TLR4] \\ +K_{52} - 2 \cdot K_{57} \cdot [TLR4] \cdot [LPS]; \quad (2.30)$$

[TLR4] is TLR4 receptor monomer concentration,

$$d[LPS2TLR4] / dt = -K_{58} \cdot [LPS2TLR4] \\ +K_{57} \cdot [TLR4] \cdot [LPS] \\ +K_{64} \cdot [LPS2TLR4TRIF] \\ + K_{60} \cdot [LPS2TLR4TRAM] \\ -K_{59} \cdot [LPS2TLR4]; \quad (2.31)$$

[LPS2TLR4] is concentration of LPS and dimerized TLR4 receptor complex,

$$d[LPS2TLR4TRIF] / dt = +K_{61} \cdot [LPS2TLR4TRAM] \\ - K_{62} \cdot [LPS2TLR4TRIF] \\ - K_{66} \cdot [LPS2TLR4TRIF] \\ - K_{64} \cdot [LPS2TLR4TRIF]; \quad (2.32)$$

[LPS2TLR4TRAM] is concentration of LPS, TRAM and dimerized TLR4 receptor complex,

$$d[LPS2TLR4TRAM] / dt = -K_{61} \cdot [LPS2TLR4TRAM] \\ + K_{62} \cdot [LPS2TLR4TRIF] \\ -K_{65} \cdot [LPS2TLR4TRAM] \\ + K_{59} \cdot [LPS2TLR4] \\ - K_{60} \cdot [LPS2TLR4TRAM]; \quad (2.33)$$

$$\begin{aligned} d[\text{TRAF3}]/dt &= -K_{69} \cdot [\text{TRAF3}] \cdot [\text{LPS2TLR4TRIF}] \\ &\quad + K_{70} \cdot [\text{TRAF3a}]; \end{aligned} \quad (2.34)$$

[TRAF3] is TRAF3 concentration,

$$\begin{aligned} d[\text{TRAF3a}]/dt &= +K_{69} \cdot [\text{TRAF3}] \cdot [\text{LPS2TLR4TRIF}] \\ &\quad - K_{70} \cdot [\text{TRAF3a}]; \end{aligned} \quad (2.35)$$

[TRAF3] is active TRAF3 concentration,

$$\begin{aligned} d[\text{TBK}]/dt &= -K_{69} \cdot [\text{TBK}] \cdot [\text{TRAF3a}] \\ &\quad + K_{70} \cdot [\text{TBKa}]; \end{aligned} \quad (2.36)$$

[TBK] is TBK concentration,

$$\begin{aligned} d[\text{TBKa}]/dt &= +K_{69} \cdot [\text{TBK}] \cdot [\text{TRAF3a}] \\ &\quad - K_{70} \cdot [\text{TBKa}]; \end{aligned} \quad (2.37)$$

[TBKa] is active TBK concentration,

$$\begin{aligned} d[\text{IRF3a}]/dt &= +K_{74} \cdot [\text{IRF3Na}] \\ &\quad + K_{71} \cdot [\text{IRF3}] \cdot [\text{TBKa}] \\ &\quad - K_{72} \cdot [\text{IRF3a}] - K_{73} \cdot [\text{IRF3a}]; \end{aligned} \quad (2.38)$$

[IRF3a] is active IRF3 concentration,

$$\begin{aligned} d[\text{IRF3}]/dt &= -K_{71} \cdot [\text{IRF3}] \cdot [\text{TBKa}] \\ &\quad - K_{76} \cdot [\text{IRF3}] + K_{72} \cdot [\text{IRF3a}] \\ &\quad + K_{77} \cdot [\text{IRF3N}]; \end{aligned} \quad (2.39)$$

[IRF3] is IRF3 concentration,

$$\begin{aligned} d[\text{IRF3Na}]/dt &= +K_{73} \cdot [\text{IRF3a}] \\ &\quad - K_{74} \cdot [\text{IRF3Na}] \\ &\quad - K_{75} \cdot [\text{IRF3Na}]; \end{aligned} \quad (2.40)$$

[IRF3Na] is active IRF3 concentration in the nucleus,

$$\begin{aligned} d[\text{IRF3N}]/dt &= +K_{75} \cdot [\text{IRF3Na}] \\ &\quad + K_{76} \cdot [\text{IRF3}] \\ &\quad - K_{77} \cdot [\text{IRF3N}]; \end{aligned} \quad (2.41)$$

[IRF3N] is IRF3 concentration in the nucleus,

$$\begin{aligned} d[\text{IFNmRNA1}]/dt &= (K_{82} \cdot F1 - K_{82}) \\ &\quad - K_{83} \cdot [\text{IFNmRNA1}]; \end{aligned} \quad (2.42)$$

[IFNmRNA1] is IFN β mRNA concentration,

$$\begin{aligned}
d [\text{IFN}\beta] / dt &= - K_1 . [\text{IFN}\beta] \\
&+ 0.51 . K_{50} . [\text{IFNmRNA1}] \\
&- K_{15} . [\text{IFNAR}] . [\text{IFN}\beta] \\
&- K_{16} . [\text{IFNAR2}] . [\text{IFN}\beta] \\
&+ K_{17} . [\text{IFNAR2IFN}\beta] \\
&+ K_{27} . [\text{IFNAR2JAKIFN}\beta] \\
&- K_{28} . [\text{IFNAR2JAK}] . [\text{IFN}\beta] \\
&+ K_{29} . [\text{IFNAR2JAKIFN}\beta a] \\
&- K_{30} . [\text{IFNAR2JAK a}] . [\text{IFN}\beta];
\end{aligned} \tag{2.43}$$

[LPS2TLR4] is LPS and dimerized TLR4 receptor concentration.

To model the events at the receptor level, one first needs to clarify how the different parts of the receptor function and how they interact with the ligand. All Type I interferons act through the same receptor complex called as IFNARs composed of two subunits IFNAR1 and IFNAR2. They and the ligand form ternary complex with stoichiometry 1:1:1 (Jaks et al., 2007). These receptor subunits differ in length of their extensions though cytoplasm and on the cell surface. They have different affinities to IFNs, basal turnover and internalization rates. In addition to general idea of accepting IFNAR receptor down-regulation as a means of signal attenuation (Kalie et al., 2008) recently internalization suggested as essential step for full and fast IFN signal transduction (Marchetti et al., 2006). Surface IFNAR2 decay slower and much less dynamic than IFNAR1. Type I interferons can produce immunomodulatory, antiviral and antiproliferative activities (Baig and Fish, 2008). The extent of ISGF3 and antiviral activity are in parallel with the relative affinities of ligands towards IFNAR2 (Jaks et al., 2007). On the other hand the differential antiproliferative potency correlated with relative affinities towards the different receptor subtypes, Jaks et al. (2007), and prolonged IFNAR1 down regulation. According to other findings, while low concentrations, transient activity and weak binding of interferon's cause antiviral activity, prolonged signals with high concentrations and strong binding results with antiproliferative activity (Kalie et al., 2008). In this view total binding affinity to receptor subunits determines occurrence of antiproliferative activity. A broader description of antiproliferative factors is ternary complex stability and rate of complex formation (Kalie et al., 2008). Nonlinearity in pSTAT1 activation and binding affinity dependent nonlinear effects of the antiviral response is strongly correlated with the ternary complex stabilization

on the membrane and the deactivation rate of the signaling complex (Kalie et al., 2008). The specific activity of interferons is a consequence of ternary complex binding affinity rather than its components. By considering these later perspectives, in the model IFNAR1 and IFNARII are taken to be identical for the sake of simplicity and their different internalization rates and affinities are ignored. Antiproliferative activity utilizes pSTAT-independent pathway.

The other main steps in the interferon model are represented by schematics given in Figure 2.6 and can be summarized as: the interferon receptor dimerized either in the presence and in the absence of the ligand, than transformed to JAK bound receptor complex. The activation of the complex yields active ISGF3. Both active and inactive forms of ISGF3 are transported in and out from the nucleus.

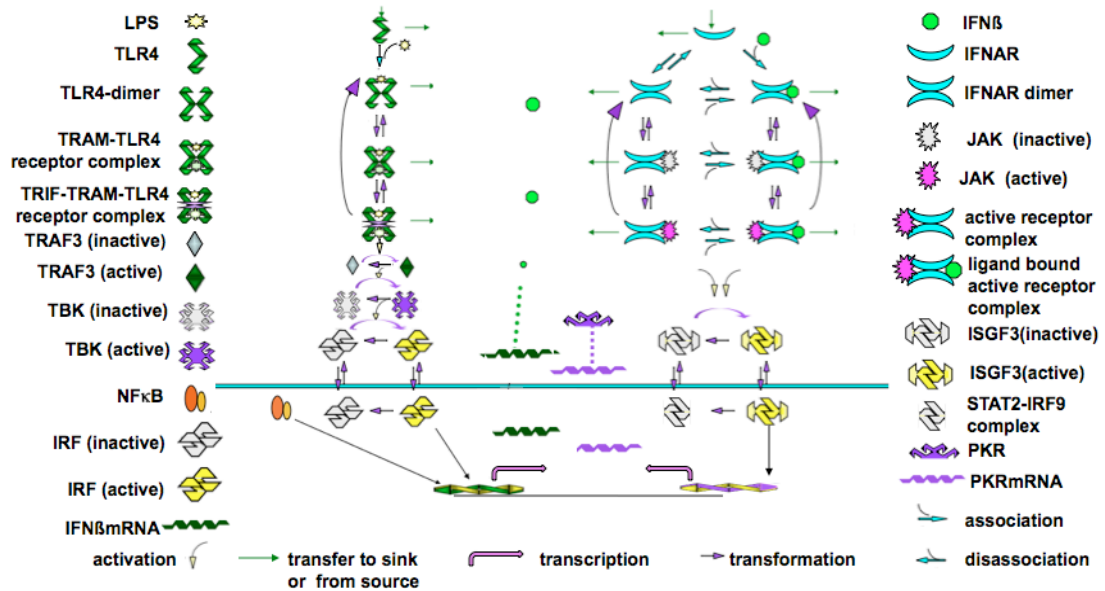


Figure 2.8: The schematics of the TLR4 and IFN β model. The purple arrows indicate direction of the transformation processes, the blue arrows are reserved for reactions, and yellow arrows for activation processes, green arrows indicate internalization, degradation to sink without leading a signaling cascade or synthesis of the complexes. ϕ indicates sources and sinks.

2.5 The PKR Connection

By concerning that only one of the transcription factor seems to function in early and late responses of PKR, we utilized following formulas for PKR synthesis facilitated by either p53 or ISGF3.

$$p53_Fregulatory = \frac{1 + \frac{[p53]}{K_p} f_p}{1 + \frac{[p53]}{K_p}} \quad (2.44)$$

Where $[p53]$ indicates the concentration, f_p is the binding affinity to DNA and K_p is the effective equilibrium dissociation constant.

$$ISGF3_Fregulatory = \frac{1 + \frac{[ISGF3]}{K_{pkr}} f_{pkr}}{1 + \frac{[ISGF3]}{K_{pkr}}} \quad (2.45)$$

Where $[ISGF3]$ indicates the concentration, f_{pkr} is the binding affinity to DNA and K_{pkr} is the effective equilibrium dissociation constant.

To trace the concentration profile, all the factors involved in the concentration changes included in an ODE as given below:

$$\frac{d[PKR]}{dt} = k_p \left(\frac{1 + \frac{[p53]}{K_p} f_p}{1 + \frac{[p53]}{K_p}} - 1 \right) - K_d PKR \quad (2.46)$$

$$\frac{d[PKR]}{dt} = k_{pkr} \left(\frac{1 + \frac{[ISFG3]}{K_{pkr}} f_{pkr}}{1 + \frac{[ISFG3]}{K_{pkr}}} - 1 \right) - K_{d1} PKR \quad (2.47)$$

where K_d , K_{d1} indicates the degradation rate.

To obtain these equation we utilized previously mentioned statistical physics approach based on the binding probability of these molecules, with a difference that only one transcription factor is required in this case. As previously mentioned regulatory factor is obtained by utilizing:

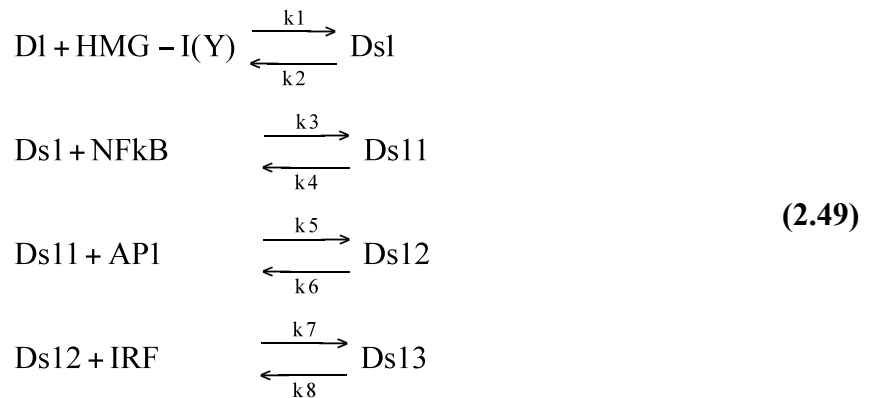
$$P_{bound} = \frac{1}{1 + \frac{N}{PF_{regulatory}} e^{\Delta \epsilon_{pd} / k_B T}} \quad (2.48)$$

where P represents number of RNA polymerases,

$e^{-\epsilon_{pd}^S / k_B T} = P_o$ is the Boltzmann weight (Bintu et al., 2005).

2.6 Method V-Stochastic Modeling of Interferon Pathway

For interferon pathway only reported stochastic models is designed for transcription part of the process, Hu et al. (2007), and there is a need to develop a model for the whole pathway to recapitulate single cell behaviour. Since the role of transcriptional noise in regulation of the IFNB1 in human dendritic cells is investigated and because of the applied approach, it is worth to summarize the reported study here. The idea behind the model is based on that the observed noise is a result of stochasticity in the time onset of transcription and enhancosome formation is very likely the source of dominant part to the stochastic behavior. In the model, four proteins bind DNA by just causing conformational change without interacting with each other, Panne et al., 2004, and so bind in sequential manner. The four proteins are the transcriptional activators NF- κ B and AP-1(ATF-2-c-Jun), interferon regulatory factor IRF and the architectural protein HMG-I(Y) (Yie et al., 1999; Munshi et al., 1999; Munshi et al., 2001; Agalioti et al., 2000; Thanos D. and Munshi, 1992). Since it provides reasonable approximation for sequential, cooperative assembly and consequent stochasticity in the time of transcriptional initiation, for the sake of simplicity possible requirement of more than one IRF and necessity of HMGI-(Y) are ignored. As a result, just four reactions given below are involved in transcription:



D_1 represent promoter region, D_{s13} the bound form of enhosome

$$k_1 = k_3 = k_5 = k_7 = 4.85 \cdot 10^{-5} \text{ nM}^{-1}\text{s}^{-1}$$

$$k_2 = k_4 = k_6 = k_8 = 24.25 \cdot 10^{-4} \text{ nM}^{-1}\text{s}^{-1}$$

and the transcription is represented by :



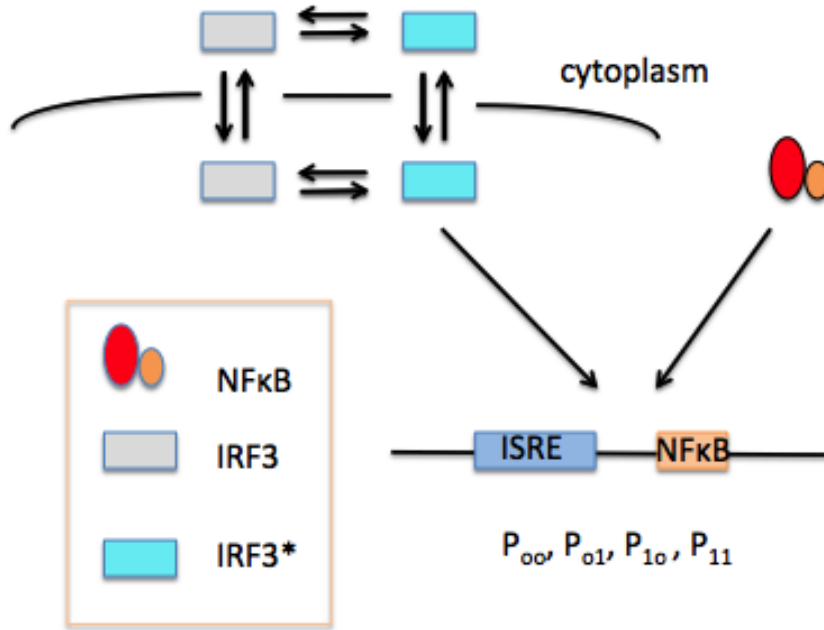
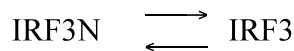
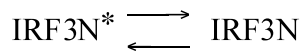
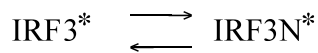
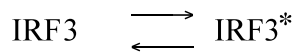


Figure 2.9 : Schematics of interferon mRNA production.

The results obtained by applying Gillespie's algorithm on these reactions and the experiments indicate that indeed the source of the intrinsic and extrinsic noise mainly arise from variations in the formation time of the enhanceosomes.

To match with my previous interferon model utilizing regulation factor in transcription stage, based on the study mentioned above, I decided to develop rather simplified version of stochastic transcription model including the two molecules but with a difference of functioning together as AND gate at transcription as illustrates in Figure 2.9.



(2.51)



The reaction for mRNA:



For this purpose I used the following procedures of **Gillespie algorithm**:

If one considers the present state of a chemical system as an ensemble of $X_1, X_2 \dots X_n$, to determine how system evolves, the time and kind of the next reaction are needed. When the number of molecules is low, these questions are answerable only in probabilistic sense because of the stochastic nature of reactions.

According to Gillespie's algorithm, Gillespie (1977), in such calculations reaction probability density function is give by:

$$P(\tau, \mu) = \begin{cases} a_\mu \exp(-a_0 \tau) & \text{if } 0 \leq \tau < \infty \\ 0 & \text{otherwise} \end{cases} \quad (2.53)$$

Where $a_\mu = h_\mu c_\mu$ $\mu = 1, \dots, M$,

h_μ = number of distinct molecular combinations in the state $(X_1, X_2 \dots X_n)$,

probability of reaction to occur in between this particular combination of molecules.

$c_\mu \equiv c_\mu$ is related to deterministic reaction rate constant with $k_1 = V \cdot c_1 \langle X_1 X_2 \rangle / \langle X_1 \rangle \langle X_2 \rangle$ for the reaction R_1 and V is the volume of the reaction occur.

Since there is no difference in between $\langle X_1 X_2 \rangle$ and $\langle X_1 \rangle \langle X_2 \rangle$ in deterministic approach (the reaction rate constants contains, the equation can simply written as

$k_1 = V \cdot c_1$ and

$$a_0 = \sum_{\mu=1}^M a_\mu = \sum h_\mu c_\mu \quad (2.54)$$

As the main step of the algorithm described above, first initial values c_μ , h_μ are assigned to calculate a_μ and accordingly a_0 is calculated. Two random numbers r_1 and r_2 are used to obtain

$$\tau = \frac{1}{a_0} \ln\left(\frac{1}{r_1}\right) \quad (2.55)$$

and to determine an integer μ as follows:

$$\sum_{v=1}^{M-1} a_v < r_2 a_0 \leq \sum_{v=1}^M a_v \quad (2.56)$$

Then, τ and μ are utilized to update time and molecular population levels and these steps are repeatedly applied to obtain a transcription profile. Reaction kinetic rates of the previously mentioned enhanceosome model were used.

Based on this theory, the algorithm and related formulas for the two transcription factor can be given as:

to trace the active IRF3 in the nucleus

$$\begin{aligned}
 P_{00} &= P_{00} - 1; & \text{IRF3N}^* &= \text{IRF3N}^* - 1; & P_{10} &= P_{10} + 1; \\
 P_{00} &= P_{00} + 1; & \text{IRF3N}^* &= \text{IRF3N}^* + 1; & P_{10} &= P_{10} - 1; \\
 P_{01} &= P_{01} - 1; & \text{IRF3N}^* &= \text{IRF3N}^* - 1; & P_{11} &= P_{11} + 1; \\
 P_{01} &= P_{01} + 1; & \text{IRF3N}^* &= \text{IRF3N}^* + 1; & P_{11} &= P_{11} - 1;
 \end{aligned} \tag{2.57}$$

and for NF κ B in the nucleus

$$\begin{aligned}
 P_{00} &= P_{00} - 1; & \text{NF}\kappa\text{B} &= \text{NF}\kappa\text{B} - 1; & P_{01} &= P_{01} + 1; \\
 P_{00} &= P_{00} + 1; & \text{NF}\kappa\text{B} &= \text{NF}\kappa\text{B} + 1; & P_{01} &= P_{01} - 1; \\
 P_{10} &= P_{10} - 1; & \text{NF}\kappa\text{B} &= \text{NF}\kappa\text{B} - 1; & P_{11} &= P_{11} + 1; \\
 P_{10} &= P_{10} + 1; & \text{NF}\kappa\text{B} &= \text{NF}\kappa\text{B} + 1; & P_{11} &= P_{11} - 1;
 \end{aligned} \tag{2.58}$$

The mRNA synthesis is modeled by:

$$\text{mRNA} = \text{mRNA} + 1; \tag{2.59}$$

and mRNA degradation is:

$$\text{mRNA} = \text{mRNA} - 1; \tag{2.60}$$

where the probability of which reaction will occur is given by

$$\begin{aligned}
 P1 &= k_1 \cdot P_{00} \cdot \text{IRF3N}^*; \\
 P2 &= k_2 \cdot P_{10}; \\
 P3 &= w \cdot k_3 \cdot P_{01} \cdot \text{IRF3N}^*; \\
 P4 &= w \cdot k_4 \cdot P_{11}; \\
 P5 &= k_5 \cdot P_{00} \cdot \text{NF}\kappa\text{B}; \\
 P6 &= k_6 \cdot P_{01}; \\
 P7 &= w \cdot k_7 \cdot P_{10} \cdot \text{NF}\kappa\text{B}; \\
 P8 &= w \cdot k_8 \cdot P_{11}; \\
 P9 &= k_9 \cdot P_{11}; \\
 P10 &= k_{10} \cdot \text{mRNA};
 \end{aligned} \tag{2.61}$$

and the parameters are:

$$k_1 = k_3 = k_5 = k_7 = 4.85 \cdot 10^{-5} \text{ nM}^{-1}\text{s}^{-1}$$

$$k_2 = k_4 = k_6 = k_8 = 24.25 \cdot 10^{-4} \text{ nM}^{-1}\text{s}^{-1}$$

$$w = 5;$$

Developing a stochastic model were not among the initial objective of this PhD thesis at 2008, however, developments in the field was toward the direction of single cell and stochastic studies. I had chance to initiate the study in UCSD Center of Theoretical Biology and presented here because of the link between the subjects and just to exemplify stochastic approach on the system. Rest of the study is reserved for a later model that I am planning to conduct following the PhD degree due to some documentation (i.e., document no: 30.2. ITU. 0.10.10.00-772.02/221) and related permissions issues necessary to visit expert groups during the PhD.

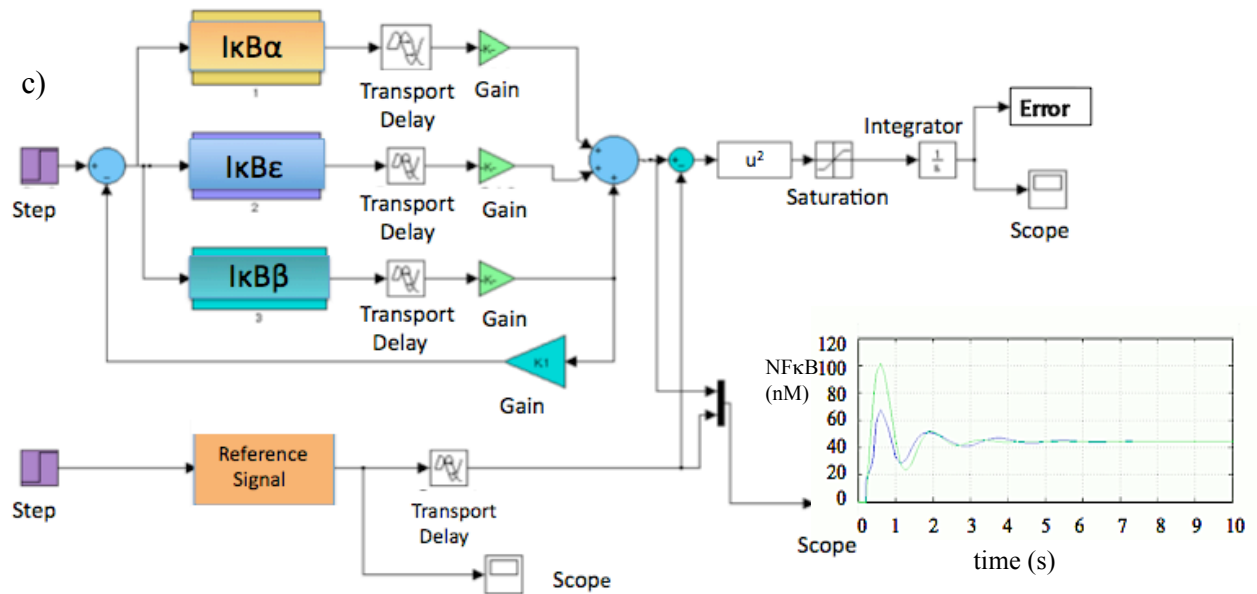
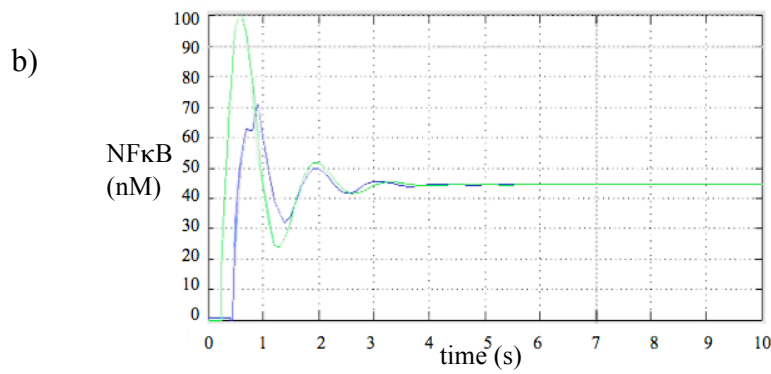
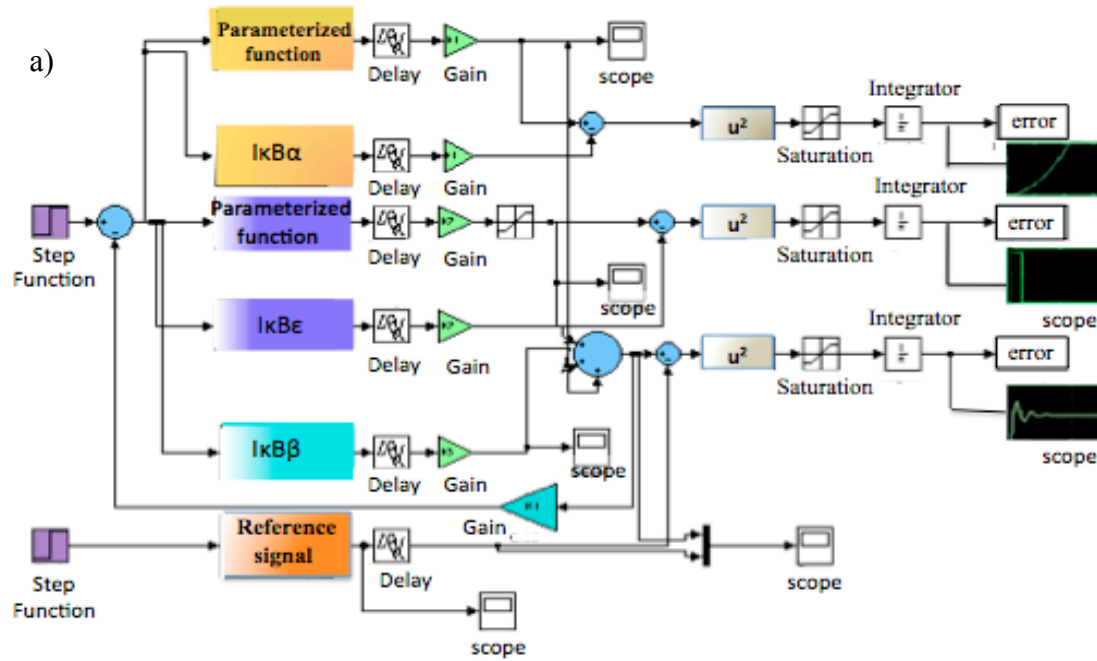
3. RESULTS and DISCUSSION

3.1 Results for the NF κ B-I κ B module

An approach based on the control theory and transfer functions is used to model the NF κ B-I κ B signaling. I attempted to identify model topologies and parameter sets that reproduce the dynamic behaviour of the NF κ B signaling which is seen experimentally and in the ODE models.

After obtaining each transfer function via curve fitting, I have tried to optimize each function as a part of the whole system by minimizing least mean square difference of the each function with its parameterized version. To do so the total value of this difference of all three transfer functions is minimized by use of genetic algorithms. By this way even though the total NF κ B profile of the whole system is attained, the existence of feedbacks and parameterized values of each transfer function in the same model cause the large deviations in individual profiles of the NF κ B that produced only when one of the I κ B isoform is present (Figure 2.1, Figure 2.2 and Figure 3.1-a).

To prevent this I decided to optimize only delays and gains in the system and followed a similar strategy of minimizing the least mean square error, but in this case for just total NF κ B expression level (Figure 3.1). The best result obtained till now is demonstrated in Figure 3.1 b, c. There is a small attenuation in the last peak of the total NF κ B expression. The lower amplitude of the first peak does not necessarily fit since the different cells in a culture can respond with different strength. The most crucial thing is obtaining the main trend in the overall profile matching with realistic values of the parameters. This optimization is performed for the transfer function that scales the over all expression in between 10 second time interval, so I do not expect linear proportionality between these delays with that of real time scaled ones but at least they seems to have similar trends as the real values.



delay1= 0.18834, delay3= 0.34165, gain in the feedback loop = 0.00908

Figure 3.1: Results of optimization for the total NFκB profile, gains and delay in the system.

Transfer functions for real scales were also determined. Throughout this study I have observed that the transfer function methodology is not efficient to apply large systems, if real profile of each system is not well defined for different initial conditions. A function having a right profile for a specific case may not produce the expected one when many conditions change in the system. The determination of right transfer functions requires a well-defined system for different sets of conditions and sometimes it is not possible. On the other hand solving a set of ODEs for system provide flexibility of changing solution for different inputs. Even if the profile of a species can not be known under some conditions, solution of the system ODEs can provide it. If knowledge about some part of the system is very restricted, in place of specific transfer function for each species, sometimes its effective to represent that part by a single transfer function. Such Modeling methods can be very effective to represent vague processes in between two steps at a certain dose of stimuli, especially at the beginning of the pathway. This provides a chance to model the whole system without worrying what is going on in this part. A good example to this is the model developed by Covert et al. in 2005 for LPS stimulated pathway performed by assigning one transfer function for each MyD88 depended and independent pathways to obtain desired profiles of IKK.

In summary, to resolve the whole pathway with transfer functions and guest dose response characteristic of system require a library of data for many species under these circumstances, for many case these kind of empirical data sets not available and hybrid approaches need to be applied. In spite of some progress in these NF κ B-I κ B models, because of not considering this problem scientifically effective any longer, due to the restrictions of the methodology detailed above and having already some models for the systems based on ODEs, I mainly concentrated on ODEs model. We may still use transfer function method to define unknown parts of the systems in single step like Covert et al. did in 2005. According to these developments my model for large system is based on reaction kinetics ODEs.

3.2 Modeling of TLR4 and IFN β Pathways with Ordinary Differential Equation Based Method

Despite the extensive literature on IRF3 and IFN β , the time course expression levels of these species applicable for Modeling purposes are very restricted. We tested the

model based on data that covers the longest time span for these two molecules. IFN β protein production is observed after 2 hours of the treatment in the RAW264.7 cells subjected to 10 ng/mL LPS for up to 12 hours (Qin et al., 2005). The IRF3 profile was obtained from the gel shift assays, Qin et al. (2005), for RAW264.7 cells incubated within 10 ng/mL LPS up to 4 hours (Figure 3.2a, b). To obtain LPS molar concentration, we assumed an average weight of 100kDa for endotoxin (typically endotoxin weight range of between 10kDa and 1000kDa) (Rietschel et al., 1994; Roth et al., 1993). In that case 10 ng/mL endotoxin corresponds to 0.1nM of LPS.

The *in silico* experiments were initiated by LPS stimulation of TLR4 receptor and the signal propagating through the down stream cascade of MyD88 independent pathway (Figure 2.8 left) results with IRF3 and IFN β expression profiles. These profiles were tuned by modulating the parameters to fit the reference empirical data. The list of the parameters and their sources are provided in Table 1 at the end of the section. Figure 3a represents the simulation and empirical results in comparison. According to these data, while IFN β protein peaks at 8 hours with 4ng/mL concentration and then declined to 2ng/mL at 12 hours (the molecular weight of interferon 1a and interferon1b reported by their manufacturers are used in the conversion to molar concentration), IRF3 activation is observed during the first hour and reaches a peak at the second hour (Figure 3.2a). The blue line represents the empirical IRF3 profile, Qin et al. (2005), gathered by Image J program. The red line in the same graph indicates simulations results for IRF3. Having no data about the amplitude of IRF3 expression, it is assumed that active IRF3 in the nucleus have a peak around 0.012 μ M. The peak of the profiles represented with blue and red lines are normalized to one (Figure 3a). The IFN β transcription rate (parameter 50) is highly linked to the parameter IRF3 activation constant (parameter 71). To have more precise values for these parameters we need to have information about the concentration of the IRF3 expression. We have only experimental results for the four time points so the empiric results are discontinuous. Even though the similar tendencies are attained up to 4 hours, the lack of data after that point prevents us from understanding the whole profile. The main trends in the simulation such as having a pick around 2 hours and having a considerable decrease at four hour match with the IRF3 profile estimate calculated by the network component analysis (NCA) (Seok et al., 2009). Our findings and the gel shift data that we used also have similar trends. In accordance

with this IRF3 profile, we suggest the possible IRF3 expressions for different doses of the ligand (Figure 3.2b). These profiles need to be tested by experiments. Interferon production changes with LPS level as shown in Figure 3.2c. Figure 3.2d provides insight to understand how LPS level modulates IRF3 concentration. The colour gradient reflects different IFN β (Figure 3.2c) and IRF3 levels (Figure 3.2d).

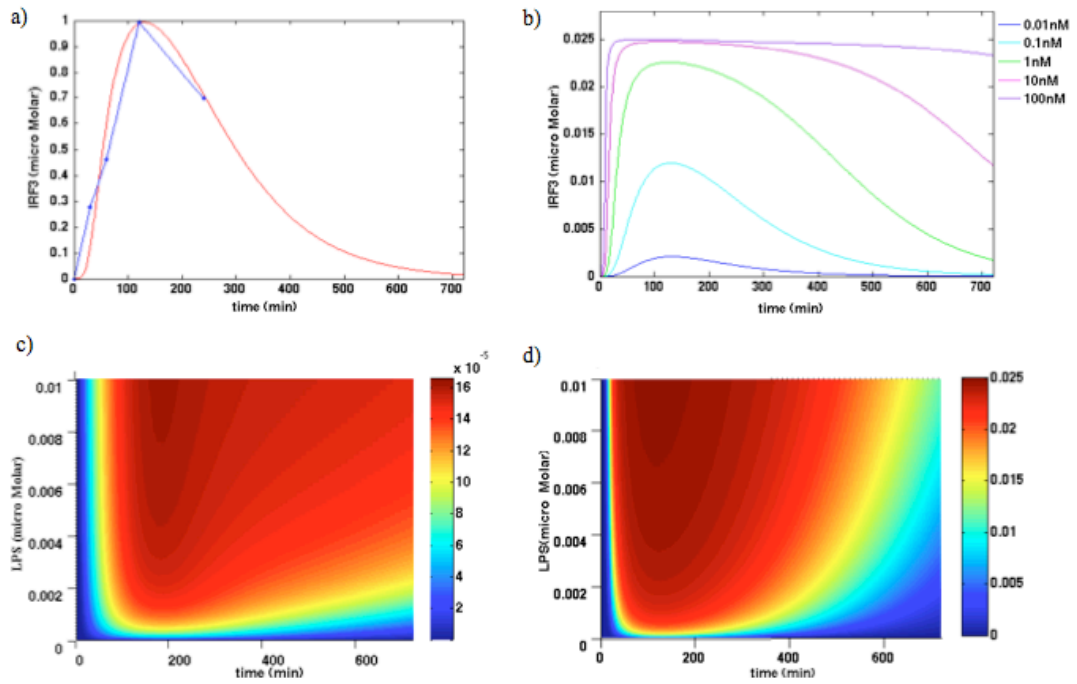


Figure 3.2: *In silico* simulations of the IRF3 expression profile and dose response curves. a) *In silico* IRF3 activation profile (red line) in comparison with empirical results (blue line), the results normalized to one because of the lack of knowledge about amplitude b) IRF3 dose response curves for different concentrations of LPS treatment. The colour code in the left part indicates the LPS doses. c) Colour-plots for IFN β profiles for different doses of LPS treatment, colours represent IRF3 concentration. d) IRF3 expression for doses of LPS, colours indicate IRF3.

The application of reported empirical IRF3 profile represented as in Figure 3.2a and NF κ B expression level shown in Figure 3.3a resulted in the interferon profile represented by the red line in Figure 3.3b. Figure 3.3a depicts LPS induced NF κ B profiles, from literature we have time course data up to 4 hour of LPS treatment for mouse embryonic fibroblast (MEFs), Covert et al., (2005); Lee et al., (2009), and the data from Th1 cells indicate that NF κ B activity persist at high level for the first 12 hours after stimulation and being lost entirely after 24 hours (Sharif, 2007). Figure 3.3b also includes interferon beta time course expression in the same cell line up to 12 hours (Qin et al., 2005). Even though we attain very close profile with the

empirical one (Figure 3.3 b), the deviation in the graph can be an indication of other missed mechanisms such as presence or a lack of time lag between two-transcription factors (resulting from the different sources of NF κ B and IRF3 profile data), possible other intermediates and/or feedbacks. Also one needs to concern differences in between cell cultures and individual cells in a given population. To have an idea about how single cells behave, a stochastic Modeling approach should be employed.

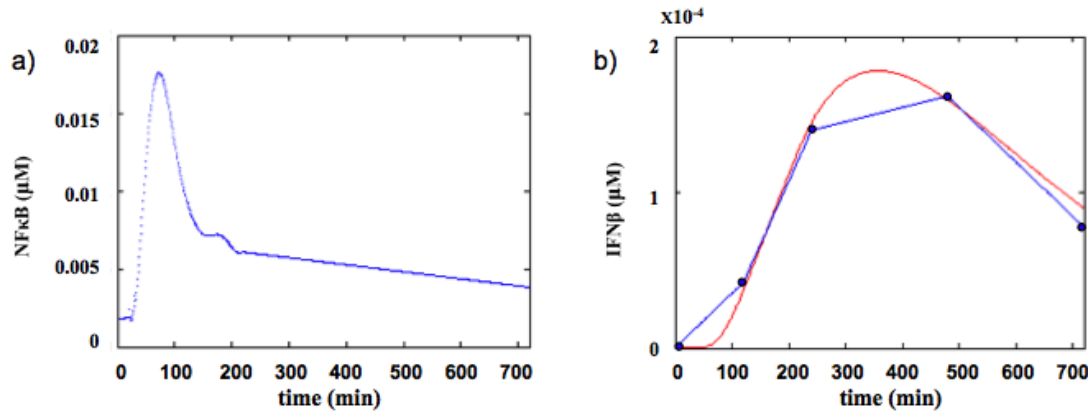


Figure 3.3: The simulation results for IFN β in comparison with experimental values. a) Population average of LPS stimulated NF κ B profile (Lee et al., 2009) (The amplitude is changed to 0.045 μ M as given in Covert et al, (2005) in place of 0.025 μ M.) b) *in silico* IFN β expression results (red line) in comparison with the empirical IFN β profile (blue line).

The regulation of IFN β is a result of a sensitive balance of many mechanisms. In the graphs at Figure 3.3 both empirical and simulation results for interferon begin from zero level. This is based on the fact that IFN β gene expression is constitutively blocked in absence of infection, Nourbakhsh and Hauser (1999); Nourbakhsh et al. (2000), and infection causes a transient activity (Doly et al., 1998). For the different organs of normal human individuals, *in vivo* constitutive production of IFN β mRNA is less than 10^{-4} copy per cell (Tovey et al., 1987). One reason behind the low mRNA production rate is NF κ B repression factor (NRF) (Nourbakhsh and Hauser, 1999; Nourbakhsh and Hauser, 1997). NRF exerts negative feedback on IFN β 3 promoter after positioning on the negative regulatory element (NRE). Infection breaks this feedback without the need of NRF removal from NRE (Nourbakhsh et al., 2000). In response to high doses of LPS (250 μ g/mouse), NRF knockout mice show same LPS induced shock symptoms as unmodified mice (Froese et al., 2006). The virus induced IFN β promoter activity are not only built on NRF but also other sensitive regulatory mechanisms like a protein called as Yin Yang1 (YY1) are involved. YY1

is a transcriptional factor, which can either function as activator or repressor, Lee et al., (1994), depending up on the way of how it interacts with cofactors, from where its acetylated, concomitant different DNA binding affinities, Yao et al. (2001), concentration of both cofactors and YY1 (Weill et al., 2003). Presence of histone deacetylase inhibitors can result with transcription from the IFN β promoter without a need of infection (Shestakova et al., 2001). In addition, both simultaneous presence of IRF3 together with NF κ B, Servant et al. (2002), and right timing and positioning of inducers allow the IFN β promoter to be active (Natoli et al., 2005). In general, location of target side on the nucleosome like being at peripheral part or inner regions is a factor determining transcriptional regulation (Andersaon and Widom, 2000).

It is important to determine biologically significant LPS and interferon doses in the analysis of these two pathways. An interferon concentration around 30 pM is very low for antiproliferative effects for either IFN α and IFN β in WISH cells. Despite IFN α , 300 pM IFN β can produce antiproliferative in the same type of cells (Kalie et al., 2008). 100 pM IFN β application is enough to produce maximal ISGF3 activity in 2fTGH and HL116, B2TB1 cells. For these cell types 1.5 pM IFN β cause half maximal ISGF3 activation and 10pM IFN β result with half maximal (Jaks et al., 2007). By focusing on these data, in our simulations, either a 100pM interferon or the *in silico* interferon produced through TLR4 model with a peak of 180 pM directly applied on the IFN β beta pathway in Figure 3.3b. The LPS concentration determined from reference experimental study, Qin et al. (2005), utilized for interferon curve in Figure 3.4a and b. The amount of *in silico* interferon produced in our TLR4 model is 180 pM and is enough to produce maximal ISGF3 activity, thus antiviral response.

There are other data in literature shed light to the profile of our concern. For example LPS stimulation result with IRF3 Ser-396 phosphorylation at 30 min and show a peak at 60 min (McCoy et al., 2008). It was also reported that IRF3 activation could occur as early as within 7 min, Selvarajoo et al. (2008), or 15-30 min of the stimulation (Doyle et al., 2002). These experimental results appear to be in agreement with Figure 3.1 because IRF3 begins at very early stages of the stimulation and reaches a peak around one and half hour. The deviation from having a peak around 60 min to 90 min can result from the multiple steps in phosphorylation and from the difference in the cell type. Small amounts of TLR3/TLR4 agonists such as 1 ng/ml LPS/lipid treatment can results with an increase exceeding 50-fold in gene

expression (Doyle et al., 2002). A study conducted on murine bone marrow macrophages indicate that 100ng/ml LPS treatment cause IRF3 activation within first 15–30 min of treatment and IFN β shows 100 times increase in concentration with a peak around one hour. During the next 5 hours, it decline more than ten times (Doyle et al., 2002). These data are also consistent with respect to the IRF3 simulation results but the point at where IFN β have a peak strongly deviates from our reference data, which probably results from cell type and organism difference. Application of 1.0 μ g/ml Escherichia coli-type synthetic lipid A on mice peritoneal macrophages, it was shown that mobility shift assay data of IRF3 taken by two hours time intervals of treatment indicated the presence phosphorylated IRF3 at the second and at the fourth hours, with a relative decrease in the concentration at the forth hour (Kawai et al., 2001). Treatment of human monocyte-derived macrophages with 0.5 μ g/ml LPS points out 100 fold change in IFN β mRNA transcription at the first hour and transcription vanishes around six hour. In the same study western blot analysis indicate IRF3 activation both at 45 min and second hour of stimulus (Marson et al., 2004). All these data indicate similar tendencies with our results, within feasible range since the sources are different organisms and cell lines.

In the interferon pathway part of the simulation, the model utilizes the interferon outcome coming from TLR4 pathway and triggers signal transduction resulting the nuclear accumulation of active ISGF3. We tested that the receptor modules of both the interferon and TLR4 models almost have the same outcomes for the same parameter sets. As a result, concerning the number of intermediates up to IRF3 and ISGF3, similar profiles are expected for both transcription factors. We were not able to obtain a consistent ISGF3 time course profile from literature. We were not able to obtain a consistent ISGF3 time course profile from literature, however, we know that ISGF3 activation occurs in the very early stages of signal transduction just after stimulation of Type I interferon receptor (Fu et al., 1992; Levy et al., 1989). IFN α treatment results with ISGF3 localization at the nucleus just half an hour after the treatment, reaching a peak at 1 hour and restoring the basal level around 6,5 hour (Levy et al., 1989). Cytoplasmic extract of HeLa cells indicated the presence of ISGF3 in the first minutes of IFN α treatment before the translocation to the nucleus. In these cell lines ISGF3 begin to appear in the nucleus even just five minute after IFN α (Levy et al., 1989). IFN β application results with ISGF3 both in the nucleus

and cytoplasm of human epithelial cells even with in first 10 min of the treatment (Smieja et al., 2008). All these data are in accord with our simulation results given in Figure 3.4. However the only EMSA data for a time span long enough, Smieja et al., (2008), the profiles seems to have a peak after five hour, which contradicts with our results and the empirical ones indicating a peak around one hour. Therefore, based on the current data, we only proposed here how could the ISGF3 dose response curve looks like. The Figure 3.4 indicates the dose response profiles for different level of LPS and IFN β application. LPS doses are given in colour code in the upper right part of the graph.

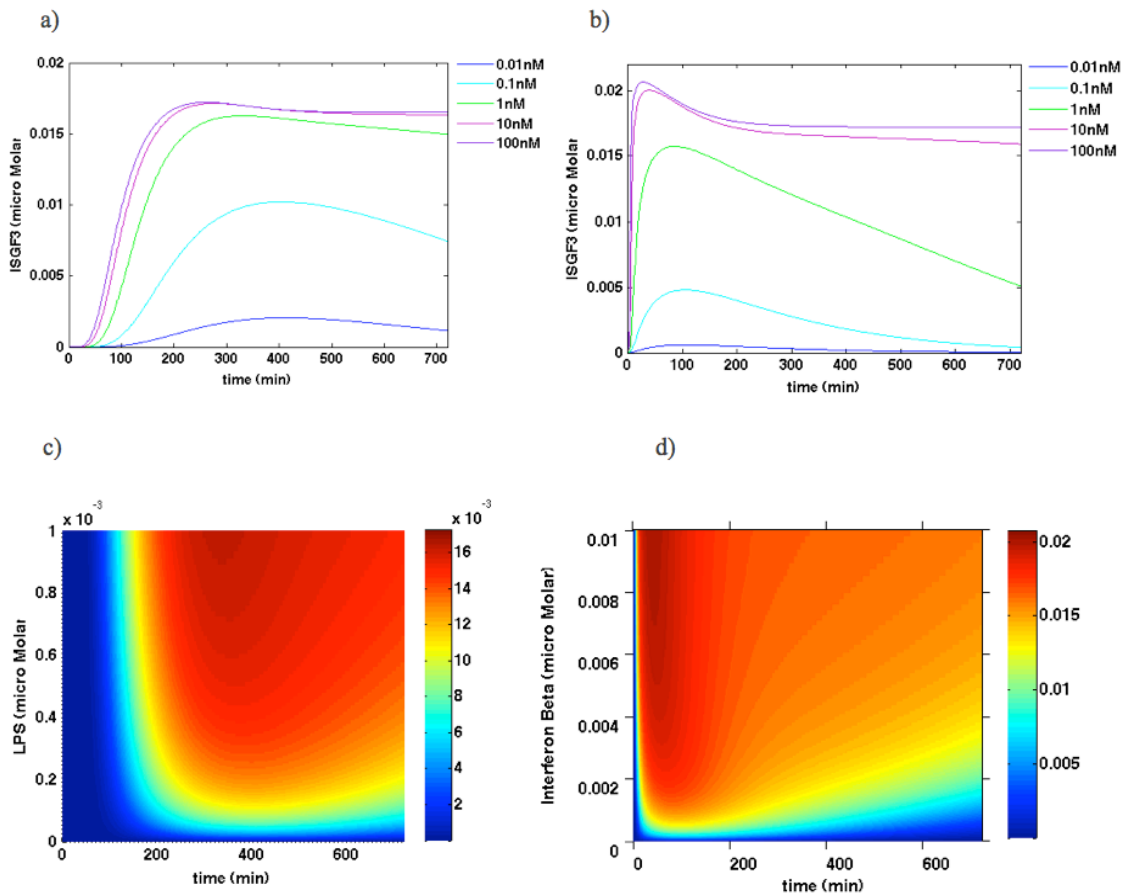


Figure 3.4: The proposed LPS-ISGF3 dose response curves. a) ISGF3 dose response curve for different levels of LPS-the colour codes represent LPS doses. b) IFN β -ISGF3 dose response curve-the colour-codes represent IFN β doses. c) LPS-ISGF3 dose response colour plots- the colours represent different ISGF3 levels indicated by the concentration next to the colour bar. d) IFN β -ISGF3 colour plots- the colours represent different ISGF3 levels indicated by the concentration next to the colour bar.

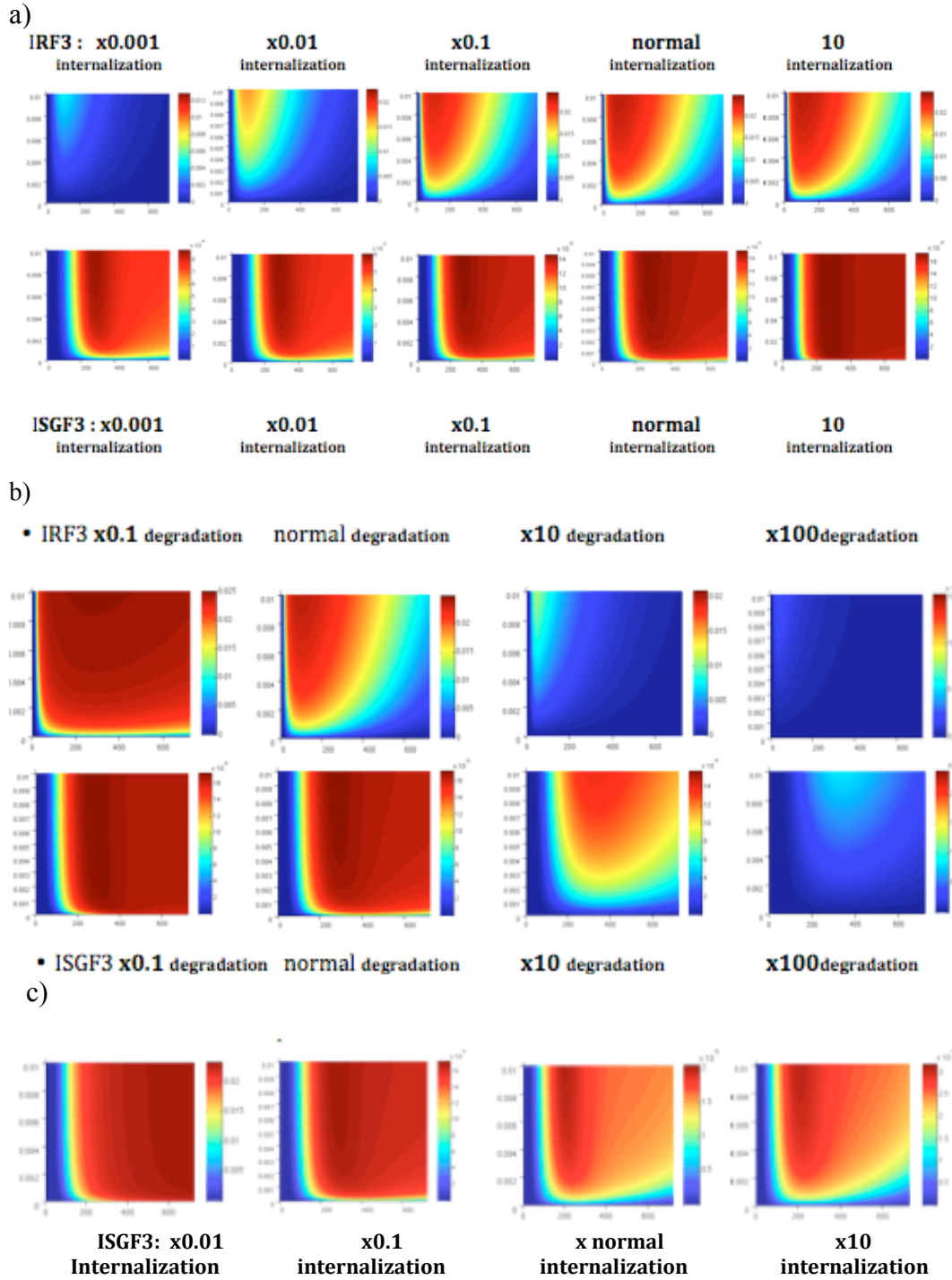


Figure 3.5: The effect of degradation and internalization rate on the transcription factor profile. a) The effect of TLR4 internalization rate (causing the signaling cascade) on the transcription factor profiles. The difference in the IRF3 and ISGF3 is because of the number of the steps in between ligand and the transcription factor, the difference in the rate parameter between two pathways, the number of reaction at the receptor level. b) The effect of TLR4 receptor degradation on the transcription factor profiles. c) The effect of IFN β receptor internalization (indicated as ϕ and not leading signaling cascade) on the transcription factor profiles.

To determine the effect of receptor metabolism on IRF3 and ISGF3 profiles, receptor internalization and degradation rates were changed. The results are illustrated in the Figure 3.5. While an increase in TLR4 internalization rate that result in the initialization of the signaling cascade cause an increase in the strength of both transcription factor (Figure 3.5a), the internalization resulted with direct degradation of receptor or in other words not triggering the signaling cascade cause considerable decrease in the profiles (Figure 3.5b). As easily can be observed from the graphs the receptor concentrations have an important role in the transcription factor activation. Figure 3.5c represent the effect of IFN β receptor degradation .

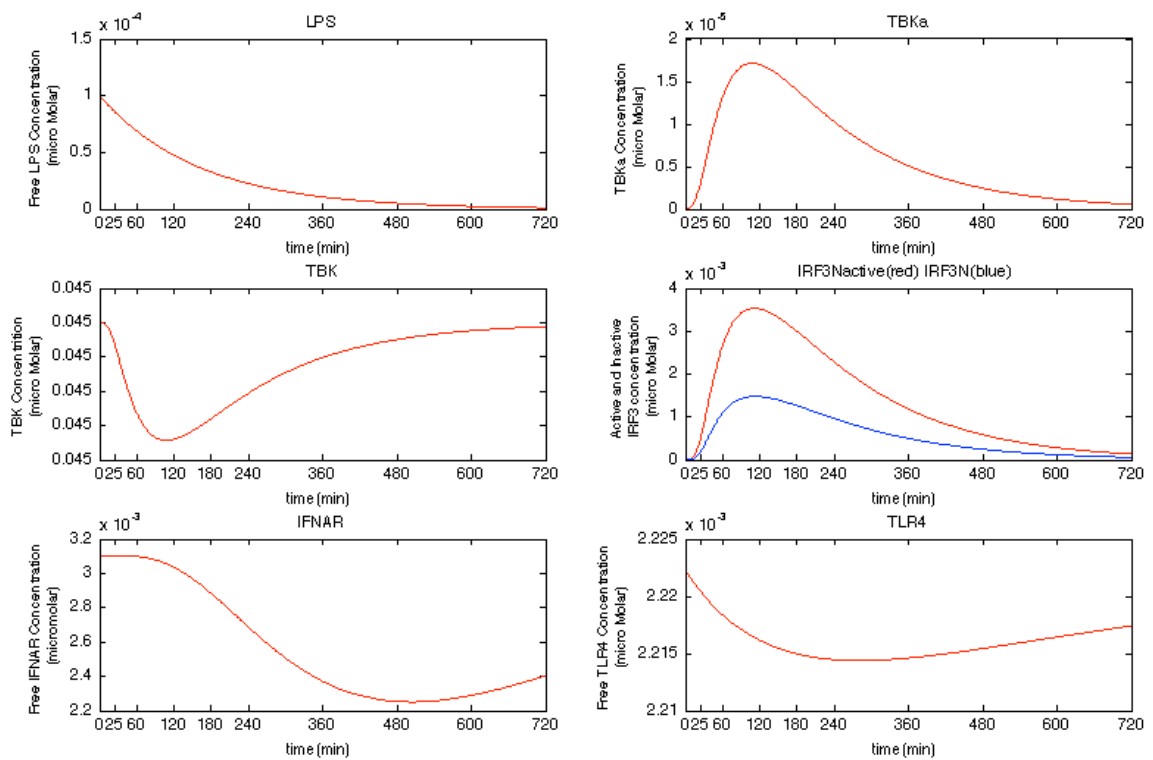


Figure 3.6: Expression profiles of some other reaction species in the model

The expression profile of some other important species in the pathways are given in the Figure 3.6. The first graph indicates how free LPS level change in the in silico environment. The next two graphs indicate free TBKa and TBK profiles. We know experimentally that TBK1 has rapid response to LPS stimulations and TBK1 activity show remarkable increase at the first 15th min after LPS stimulation (Solis et al., 2007). The second graph in the second row represents active and inactive IRF3 profiles in the nucleus. Last two graphs represent the surface receptor concentration change for IFNAR and TLR4. While initially concentration decreases because of degradation and internalization, due to decrease in the ligand, receptor synthesis rate

or recycling back to surface overcome the degradation or internalization rate and surface receptor concentration begins to be recovered by time. These results are in parallel with the experimental results indicating the recovery and recycling of interferon receptor to the surface (Kalie et al., 2008). To obtain receptor concentration, either the number of the receptors can be divided by an average cell volume or titration curve and K_d values can be utilized. It is assumed that on average 100-5000, Novick et al. (1995) and Uze et al. (2007), interferon receptor per cell exist. However for example in Daudi cell this number is around $1.1 \cdot 10^4$ (Cutrone and Langer, 1997). While the calculation for Daudi cells $5.5 \cdot 10^{-3} \mu\text{M}$ receptor, these values varies for different cell types and sizes. A receptor concentration of $4 \cdot 10^{-3} \mu\text{M}$ fulfills the empirical $\text{IFN}\beta$ profile, which remains in the feasible range. From the titration curve and so from K_d value, the concentration for TLR4 is around $1-1.2 \cdot 10^{-2} \mu\text{M}$ obtained (Visintin et al, 2010). Simulations satisfy empirical values around $5.6 \cdot 10^{-3}$ with in viable limits concerning the differentiation in cell types with a value around $3 \cdot 10^{-3} \mu\text{M}$ (Figure 3.6).

The parameter values utilized at the model are in the Table 1 given below. Deterministic Modeling gives population average results, however, the behaviour of single cells can deviate drastically from the population average. Even though we may try to attain some empirical values, results from cell cultures can be deceptive, because of the immortalization process and duration of ex vivo cultivation. A similar problem also exists for in vitro studies because of a loss of natural surroundings, three-dimensional structure with numerous regulatory loops and feedback regulations exerted by extracellular factors or cell-cell signaling (Froese et al., 2006). Therefore, slight deviations from the parameters in the model to some extend can still lead to biologically feasible results for different cell types and cell environment. The model parameters and sources are listed in Table 1.









Colour codes	
	Parameters fit, lighter yellows are the ones that we have some comparison or information.
	Parameters very close to or same with the A20 model for TNFR (Werner et al., 2008).
	The model is very sensitive to these parameters at least in some range. We have references for these values from the literature.
	These values are same with yellow ones, if we know yellows we know these values also
	We know these values from the literature.
	Not active
	Insensitive to these parameters in a wide range.
	We know one of these values for another system.

Table 3.1: The list of model parameters and sources.

Code	Reaction	Category	Location	Values	Source of parameter
1	IFN β →	Protein Degradation	Extra Cellular	0.00115 min ⁻¹	The value is calculated for 10 hr half life.
<p>Insensitive to this parameter in between 2 and 10 hrs. But for around one hour and lower values of half-life interferon level decreases considerably.</p> <p>Interferon-beta (IFN-beta) is biologically unstable under physiologic conditions in vitro and is cleared rapidly from the bloodstream on administration in vivo. Association with sIFNAR-2 (a soluble recombinant form of the type I IFN receptor subunit), IFN-beta is more stable in vitro and exhibits increased efficiency when administered in vivo. The in vitro enhancement is due to the specific interaction of IFN-beta with sIFNAR-2, followed by dissociation of IFN-beta from the complex over time in culture. In vivo, the serum half-life of IFN-beta is extended from minutes to hours when administered intravenously in mice as a sIFNAR-2-associated complex (McKenna S.D., et al., 2004)</p> <p>As reported by manufacturer, after intracellular muscle injection serum levels of AVONEX® (interferon beta) typically peak between 3 and 15 hours and then decline at a rate consistent with a 10 hour elimination half-life.</p>					
2	→IFNAR	Protein Synthesis	Cytoplasm	5.85*10 ⁻⁶ min ⁻¹ . After ligand 1.8e-5 min ⁻¹	100-5000 molecule/cell (Novick D. et al., 1995) 500-5000 molecule/cell (Uze G. et al., 2007) 1.1x10 ⁴ for Daudi cells (Cutrone E. C. et al., 1997)
<p>Obtained by fitting, 2e-7 at the TNF-NFκB model (Werner SL, et al., 2008) used as reference value, which is also a fit to recapitulate amount of TNF receptor at (Watanabe et al., 1988), and we deviate it to fit our system.</p>					
3	IFNAR→	Protein Degradation	Cell Surface	0.0058 min ⁻¹	The value given for TNFAR the TNF-NFκB model (Werner SL, et al., 2008) is used.
4	2IFNAR →IFNAR2	Association	Cell Surface	1*10 ⁻⁷ μM ⁻¹ min ⁻¹	It assumed to have small value relative to parameter 15-16. In the TNF-NFκB model (Werner SL, et al., 2008) its equal to 1e ⁻⁵ μM ⁻¹ min ⁻¹ TNFR receptor. The changes in between 1e ⁻⁵ μM ⁻¹ min ⁻¹ -1e ⁻⁷ μM ⁻¹ min ⁻¹ has no effect on IFNbeta and ISGF3 results.
5	IFNAR2→2IFNAR	Disassociation	Cell Surface	0.104 min ⁻¹	(Kalie E., et.al, 2008) Table 2 half life TNFR disassociation is 0.1 min ⁻¹ in the TNF-NFκB model (Werner SL, et al., 2008) 0.433 min ⁻¹ (Moraga et. al, 2009)
6	IFNAR2→ (Internalization)	Protein Degradation	Cell Surface	0.0058 min ⁻¹ before ligand and 0.01732 after ligand.	It assumed same as parameter 18. Parameter fit
<p>Depends on dose. By concerning the dose dependent change in internalization rate (Kalie E., et.al, 2008) if basal level degradation or internalization assumed as 0, from the graphs of receptor internalization (Kalie E., et.al, 2008 :Figure4), relative to basal level concentration of receptors, the internalization rate obtained as 0.00385 for 30pM and 0.012 for 300pM. These means almost three times change in the internalization rate applied for ten times increase in dose of ligand To apply such a correlation, at least almost 3 times increase in internalization after stimulus, we assumed this value as 0.01732. For another cytokine receptor TNFR, this value is given as 0.0017 in the TNF-NFκB model ((Werner SL, et al., 2008)</p>					
7	IFNAR2 → IFNAR2JAK	Transformation	Cell Surface	100 min ⁻¹ x 8.3 *10 ⁻⁵	TTR and TNFR association rate the TNF-NFκB model (Werner SL, et al., 2008), multiplied by JAK concentration in cytoplasm.
<p>JAK concentration is an as assumption. And the results are insensitive to the values in between 8.3 *10⁻⁵, 10⁻¹ for JAK concentration.</p>					
8	IFNAR2JAK→ IFNAR2	Transformation	Cell Surface	1.66*10 ⁻¹ -1.66*10 ⁻⁵ min ⁻¹	Parameter fit
<p>The value is determined considering the importance of receptor internalization and time lapse recycling back to surface. It can have values between 1.66*10⁻⁵ and 1.66*10⁻¹. However, an increase in this value results with lower levels of ISGF3 and transcriptional activation than physiological feasible values.</p>					
9	IFNAR2JAK→ IFNAR2JAK*	Activation	Cell Surface	30 min ⁻¹	The receptor activation parameter of the TNF-NFκB model (Werner SL, et al., 2008)
10	IFNAR2JAK*→ IFNAR2JAK	Deactivation	Cell Surface	2 min ⁻¹	The receptor deactivation parameter of the TNF-NFκB model (Werner SL, et al., 2008)

Table 3.1 (continued): The list of model parameters and sources.

Code	Reaction	Category	Location	Values	Source of parameter
11	IFNAR2JAK* \rightarrow IFNAR2JAK (SOCS mediated)	Inactive allocated parameter for Deactivation	Cell Surface	$\mu\text{M}^{-1}\text{min}^{-1}$	The model include feedback mechanisms inside for test purposes of their effects but not active for the results presented in this paper.
12	IFNAR2JAK* \rightarrow IFNAR2+JAK	Disassociation	Cell Surface	$1.666*10^{-5} \text{ min}^{-1}$	Same with parameter8
13	IFNAR2JAK \rightarrow (Internalization)	Protein Degradation	Cell Surface	0.01732 min^{-1}	Same with parameter6
14	IFNAR2JAK* \rightarrow (Internalization)	Protein Degradation	Cell Surface	0.01732 min^{-1}	Same with parameter6
15	2IFNAR+IFNbeta \rightarrow IFNAR2IFNbeta	Association	Cell Surface	$12\mu\text{M}^{-1}\text{min}^{-1}$	(JAKs E. et. al, 2007)
16	IFNAR2+IFNbeta \rightarrow IFNAR2IFNbeta	Association	Cell Surface	$12\mu\text{M}^{-1}\text{min}^{-1}$	(JAKs E. et. al, 2007)
17	IFNAR2IFNbeta \rightarrow IFNAR2+IFNbeta	Disassociation	Cell Surface	0.104 min^{-1} 1.5 min^{-1}	(Kalie E., et.al,2008) Table 2 half life (JAKs E. et. al, 2007) Table I
18	IFNAR2IFNbeta \rightarrow (Internalization)			0.01732 min^{-1} Depending on dose of ligand	It assumed same as parameter 6.
19	IFNAR2IFNbeta+JAK \rightarrow IFNAR2JAKIFNbeta	Association	Cell Surface	100 min^{-1} $\times 8.3 * 10^{-5}$	Same as parameter 7
20	IFNAR2JAKIFNbeta \rightarrow IFNAR2IFNbeta+JAK	Disassociation	Cell Surface	$1.666*10^{-5} \text{ min}^{-1}$	Same as parameter 8
21	IFNAR2JAKIFNbeta \rightarrow IFNAR2JAKIFNbeta*	Activation	Cell Surface	30 min^{-1}	Same with parameter 9
22	IFNAR2JAKIFNbeta* \rightarrow IFNAR2JAKIFNbeta	Deactivation	Cell Surface	2 min^{-1}	Same with parameter 10
23	IFNAR2JAKIFNbeta* \rightarrow IFNAR2IFNbetaJAK (SOCS mediated)	Deactivation	Cell Surface	$\mu\text{M}^{-1}\text{min}^{-1}$	For this model it is inactive
24	IFNAR2JAKIFNbeta* \rightarrow IFNAR2IFNbeta+JAK	Disassociation	Cell Surface	$1.666*10^{-5} \text{ min}^{-1}$	Same as parameter 8
25	IFNAR2JAKIFNbeta \rightarrow (Internalization)	Protein Degradation	Cell Surface	0.01732 min^{-1}	Same with parameter6
26	IFNAR2JAKIFNbeta* \rightarrow (Internalization)	Protein Degradation	Cell Surface	0.01732 min^{-1}	Same with parameter6
27	IFNAR2JAKIFNbeta \rightarrow IFNAR2JAK+IFNbeta	Disassociation	Cell Surface	0.104 min^{-1}	Assumed as has the same value with parameter 17
28	IFNAR2JAK+IFNbeta \rightarrow IFNAR2JAKIFNbeta	Association	Cell Surface	$12\mu\text{M}^{-1}\text{min}^{-1}$	Assumed as has the same value with parameter 16
29	IFNAR2JAKIFNbeta* \rightarrow IFNAR2JAK*+IFNbeta	Disassociation	Cell Surface	0.104 min^{-1}	Assumed as has the same value with parameter 17
30	IFNAR2JAK*+IFNbeta \rightarrow IFNAR2JAKIFNbeta*	Association	Cell Surface	$12\mu\text{M}^{-1}\text{min}^{-1}$	Assumed as has the same value with parameter 16
31	ISGF3 \rightarrow ISGF3* (IFNAR2JAK* mediated)	Activation	Cytoplasm	$600\text{-}3000 \mu\text{M}^{-1}\text{min}^{-1}$ molar .	Parameter fit. By Smieja J. et al. this value assumed as STAT1 and STAT2 heterodimer formation: $600 \mu\text{M}^{-1}\text{min}^{-1}$. In the TNF-NFkB model model (Werner SL, et al., 2008) IKK activation parameter is $520\mu\text{M}^{-1}\text{min}^{-1}$
For $600 \mu\text{M}^{-1}\text{min}^{-1}$ maximum $0.012 \mu\text{M}$, for $3000, 0.002 \mu\text{M}$ active ISGF3 accumulate at nucleus in the case of 0.003 micro Molar IFNbeta stimuli. In the case of experimental IFNbeta profile with a peak of $0.00018 \mu\text{M}$ results with about maximum 0.0115 micro Molar active nuclear ISGF3 Graphs in the figure5 is for ISGF3 activation rate $2000 \mu\text{M}^{-1}\text{min}^{-1}$ and because IRF3 also arranged to have a peak around 0.012 micro Molar which is about the value of the plateau in NFkB profile.					

Table 3.1 (continued): The list of model parameters and sources.

Code	Reaction	Category	Location	Values	Source of parameter
32	ISGF3 \rightarrow ISGF3* (IFNAR2/JAK1/IFNbeta* mediated)	Activation	Cytoplasm	600-3000 $\mu\text{M}^{-1}\text{min}^{-1}$	Parameter fit Same with parameter 31
33	ISGF3* \rightarrow ISGF3 (Constitutive)	Deactivation	Cytoplasm	0.7 min^{-1}	Parameter fit
34	ISGF3*N \rightarrow ISGF3N (Constitutive)	Deactivation	Nucleus	0.31 min^{-1}	Parameter fit
35	ISGF3*N \rightarrow ISGF3*	Transportation	Nucleus to Cytoplasm	0.07 min^{-1}	Parameter fit
36	ISGF3* \rightarrow ISGF3*N	Transportation	Cytoplasm to Nucleus	0.9 min^{-1}	Parameter fit
37	ISGF3 \rightarrow ISGF3N	Transportation	Nucleus to Cytoplasm	0.74 min^{-1}	Parameter fit
38	ISGF3N \rightarrow ISGF3	Transportation	Nucleus to Cytoplasm	0.0025 min^{-1}	Parameter fit
39-49	Inactive allocated parameters				
50	\rightarrow IFN β	IFNbeta transcription rate	Nucleus	$7.3 \cdot 10^{-2} \text{min}^{-1}$	Parameter fit
51	LPS \rightarrow	Degradation	Extra Cellular	$0.005776226 \text{min}^{-1}$ (for a half life of two hour)	Less than 1 hour for isolated LPS, 2 hour for CD14 bound, 12 hour lipoprotein bound (Flegel W. A., et al., 1993). While above two it is not sensitive, below this value it became sensitive.
52	\rightarrow TLR4	Protein Synthesis	Cytoplasm	$1.78 \times 10^{-5} \text{min}^{-1}$ After ligand it is assumed $4 \times 10^{-5} \text{min}^{-1}$	Obtained by fitting.
MD-2, TLR4 binding curves for HEK293 cells gives a 12nM Kd, so the concentration of MD-2 and TLR4 value can be assumed as 12nM. We were able to fit the results with a concentration around 18nM for TLR4 and the difference can correspond to cell difference. 2e-7 from the TNF-NF κ B model (Werner SL, et al., 2008) used as reference value, which is also a fit to recapitulate amount of TNF receptor at (Watanabe et al., 1988), and we deviate it to fit our system.					
53	TLR4 \rightarrow	Degradation	Cell Surface	0.0022min^{-1}	Parameter fit In the TNF-NF κ B model (Werner SL, et al., 2008) this value for TNFR is 0.0058.
54	LPSTLR4_2 \rightarrow	Internalization	Cell Surface	Before ligand 0.0022min^{-1} . After ligand 0.031min^{-1}	Close to parameter 6. Parameter fit
55-56	Inactive allocated parameters reserved for feedbacks				
57	2TLR4 + LPS \rightarrow LPSTLR4_2	Association	Cell Surface	$0.18143 \mu\text{M}^{-1}\text{min}^{-1}$	(Shin H. J., 2007:Table1)
58	LPSTLR4_2 \rightarrow	Internalization	Cell Surface	Before ligand 0.0022min^{-1} . After ligand 0.031min^{-1}	Close to 6,13,14,18, 25, 26, Same with 54,65,66.
59	LPSTLR4_2 \rightarrow LPSTRIFF	Transformation	Cell Surface	8.3×10^{-2} (not very sensitive to this parameter)	Same with parameter 7
60	LPSTRIFF \rightarrow LPSTLR4_2	Transformation	Cell Surface	$1.666 \times 10^{-5} \text{min}^{-1}$	Same with parameter 24, 64.
61	LPSTRIFF \rightarrow LPSTRIFF	Transformation	Cell Surface to cytoplasm	30 min^{-1}	Same with parameter 9
64	TRAF3 \rightarrow TRAF3* (LPSTRIFF mediated)	Activation	Cytoplasm	$1.666 \times 10^{-5} \text{min}^{-1}$	Same with parameter 24, 60.

Table 3.1 (continued): The list of model parameters and sources.

Code	Reaction	Category	Location	Values	Source of parameter
65	LPSMyD88→	Internalization	Cell Surface	Before ligand 0.0022 min ⁻¹ . After ligand 0.031 min ⁻¹	Close to 6,13,14,18, 25, 26, Same with 54,65,66.
66	LPSTRIFF →	Internalization		Before ligand 0.0022 min ⁻¹ . After ligand 0.031 min ⁻¹	Close to 6,13,14,18, 25,26, Same with 54,65,66.
67-68	Inactive Allocated Parameters				
69	TBK →TBK*	Activation	Cytoplasm	8.3 min ⁻¹	Parameter Fit
70	TBK*→ TBK	Deactivation	Cytoplasm	0.0389 min ⁻¹	Parameter fit
71	IRF3→ IRF3*	Activation	Cytoplasm	800 min ⁻¹	Parameter fit
72	IRF3*→ IRF3 (Constitutive)	Deactivation	Cytoplasm	0.6 min ⁻¹	Parameter fit
73	IRF3*→IRF3*N	Transportation	Cytoplasm to Nucleus	0.94 min ⁻¹	Parameter fit
74	IRF3*N→IRF3*	Transportation	Nucleus to Cytoplasm	0.03 min ⁻¹	Parameter fit
75	IRF3*N→IRF3N	Deactivation	Nucleus	0.31 min ⁻¹	Parameter fit
76	IRF3→IRF3N	Transportation	Cytoplasm to Nucleus	0.00000000025 min ⁻¹	Parameter fit
77	IRF3N→IRF3	Transportation	Nucleus to Cytoplasm	0.74 min ⁻¹	Parameter fit
78-79	Reserved for feedback mechanisms	Inactive			
82	Regulation factor rate	Transcription	Nucleus	0.00049 min ⁻¹	Parameter fit depends on the value of parameter 83 and IFNbeta expression profile.
83	IFNβmRNA →	Degradation	Nucleus, Cytoplasm	0.0048 min ⁻¹	For constant level of 0.045 μM NFκB application this value becomes 0.0154 min ⁻¹ which exactly in agreement with 45 min half life (Peppel K. and Baglioni C., 1991)
Human interferonβ mRNA was examined in murine C127 cells that carry an expression vector for this mRNA. The mRNA decayed with a 45 min half life in actinomycin D treated cells (Peppel K. and Baglioni C., 1991).					
84	NFκB→	Disassociation from DNA	Nucleus	3 min ⁻¹	IκBα dose dependent This the range reported for NFκB-dissociation facilitated by IκBα (Bergqvist S., et al., 2009)
85	IRF3N*→	Disassociation from DNA	Nucleus	3 min ⁻¹	We assumed the same value with parameter 84.
86	ω	Interaction rate of two transcription factor	Nucleus	2	Parameter Fit
87	f _{AB}		Nucleus	9	Parameter Fit
88	f _{pkr}		Nucleus	3	Parameter Fit

3.3 The Results for the PKR Connection

The ISGF3 outcome and the model are tested for published PKR profiles (Donze et al., 2004; Hsu et al., 2004). PKR is one of the products of the pathway responsible for broad antiviral and anticellular actions and important because several cancer drugs target and modulate PKR action (García et al., 2006; Yoon et al., 2009). Assuming that the late phase activity of PKR arises only because of the synthesis from ISRE site, *in silico* ISGF3 dependent PKR profile and empirical data is compared in Figure 3.7.

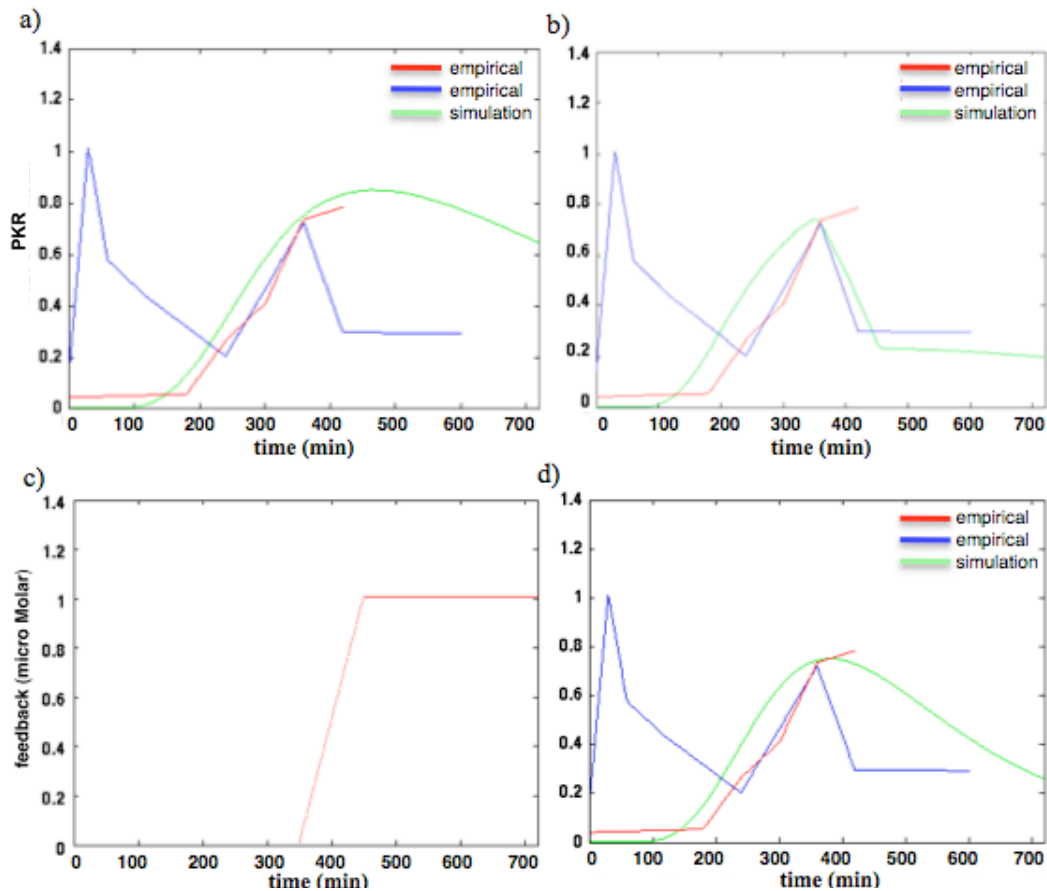


Figure 3.7: a), b), d) NIH3T3 cell extracts immunoblotting results with an anti-PKR antibody (Donze et al., 2004) (The red line in the graph. The Data are normalized). PKR activation under the influence of 100 ng/ml LPS. PKR examined in lysed cells (illustrated by blue), Hsu et al., (2004), the outcome model (green line). c) the profile of proposed molecule inserting negative feedback on PKR. d) PKR negative feedback on its self by inhibiting the phosphorylation of STAT.

Utilization of an empirical IFN β profile, Qin et al (2005), in the system resulted in a PKR expression reflecting similar characteristics in first incline and position of the peak for the late phase activity of PKR. The slight deviation in the position of first

incline is a result of reduction in the steps of ISGF3 production in the model. Since we do not have data about the amplitude of the expression, the highest peak of PKR is normalized to one. The data from NIH3T3 cell, Donze et al. (2004), does not include the profile after 420 min and data from bone-marrow-derived macrophages, Hsu et al. (2006), have a sharper decline which can be a result of a negative feedback on PKR production (Figure 3.7-b and 3.7-d) such as a feedback on itself (Figure 3.7-d), other feedback mechanisms effecting phosphorylated STAT dimmer profiles, Yamada et al. (2003), having a different IFN profile for this cell line, or having a higher receptor internalization rate for this cell type. To determine which mechanisms are responsible for the decline we need to have more data for IFN, PKR data of single cell line.

4. CONCLUSIONS

Notwithstanding the extensive number of experimental data for PAMPs, the correlations among them are unclear and many data are inconsistent. Computational modeling and system biology tools brings these data together and helps to analyse the whole picture for the system of the concern. In this study we utilized some of these methods to explain the mechanisms regulating the NF κ B, and to model TLR4 and IFN β pathways.

The study was initialized with modeling of NF κ B-I κ B signaling module. To recapitulate the expression of each species, corresponding transfer functions were obtained via Matlab curve fitting algorithm. To observe the behavior of each species inside the system, each function was optimized as a part of the whole system by minimizing least mean square difference with their parameterized version. The model was constructed in a way that in addition to the parameters of the transfer function, also parameters related with delays and feedbacks can be optimized. The difference between each transfer function was minimized by use of genetic algorithms and results were refined by use of pattern search algorithm. Even though the first attempts were in the directions of resolving the feedback mechanisms of I κ B isoforms, in spite of large search space and the feedback inputs causing a computationally infeasible model, the chosen method combining optimization techniques, control diagrams and feedbacks in Simulink environment appeared to be unproductive.

ODEs explicitly include many reaction kinetics rates. The direct comparison of these parameters with actual system rate data provides guidance to realize the model, however, the link between transfer function parameters and actual system is difficult to interpret which makes transfer function models difficult to handle. In addition to these handicaps, a library of I κ B isoforms for different doses of stimuli is a must for such a model, because of the fact that each transfer function is a specific solution of the system and in nonlinear systems, dose dependent attributes of individual species can demonstrate large variations under different conditions.

Evaluating the efficiency of the method, problem reduced to the optimization of

some specific parameters and single feedback mechanism due to increased level of NF κ B. This reduction let a simplified model of the system for a well-defined expression profile under some initial conditions. At the end of simulations we were able to attain a NF- κ B profiles that match with the emperical data in main characteristics, except the amplitude of the initial peak within a feasible range caused by cell differentiation and with some deviation of the first peak position. The model can be enlarged to the previously proposed model including the other species only if we know the behaviour of the species under a set of different conditions, and only after that it can be used to determine the behaviour of the remaining other very restricted number of the species and mechanisms. At this stage we are totally restricted by the lack of experimental data. On the other hand, as applied on LPS stimulated pathway, Covert et al., (2005), especially at the initial stage of the cascades, it is very effective tool just to represent a vague part of the signaling pathway and can be used as a link between signal and outcome of a specific step.

As second stage of the study, to determine the mechanisms regulating the NF κ B, we utilized reaction kinetics ODEs. In this context both TLR4 and Interferon Beta pathways are combined in an *in silico* model. Simulation results are validated by empirical expression profiles for IFN β and IRF3. ISGF3 responses for different doses of LPS and interferon treatment are proposed in parallel to the present data in literature. To explain the transcription factors and interferon profiles, receptor metabolism makes use of as an important and determining step as also validated by previous experimental studies (Kagan et al., 2008; Marchetti et al., 2006). In transcriptional regulation of IFN β , to restrict the transcription with a limit, we utilized a hybrid method combining a statistical approach and ODEs. The resultant IFN β initiates IFNAR signaling cascade. The extension of the IFN β pathway in a way including the related gene expressions can enlighten other regulatory mechanisms between the two pathways. The concomitant ISGF3 profile needs to be validated by further experimental gel shift data but concerning the number of steps, similarity to IRF3 profile is an expected result. PKR transcribed by ISGF3 is presumed to have a role in NF κ B regulation. Having a model for PKR production provides the opportunity to model other important factors regulated by PKR. There are published expression profiles for PKR for both early and late responses of the system. Our initial findings indicate very similar profiles with the late phase of

empirical ones. Having a PKR profile could allow us to refine the current NF κ B models.

In addition to being the first study combining the TLR4 and Interferon beta pathways in a single *in silico* model and analyzing how they communicate with each other, the content of this part of the study also can be evaluated and has a value as review of the literature for both pathways and their interactions. This model utilized the TLR4 internalization and other receptor metabolism as important and determining steps in explaining the transcription factors and interferon profiles as already validated by the experimental studies (Kagan et al., 2008; Marchetti et al., 2006). Thus, in aspect and focus, it is different from other LPS models in the literature remaining the mechanism at this stage elusive and bringing about explanations either utilizing the transfer functions, Covert et al. (2005), or suggesting additional unidentified intermediate species (Selvarajoo, 2006). The model was designed to explain two vital pathogen activated pathways and at least it seems to bring about one of the best approaches for interferon beta production through LPS stimulation, both because of involving receptor internalization and because of its efficiency in recapitulation of empirical data. A reported statistical physics method, Bintu et al. (2005), is adopted to simulate the AND gate characteristic exhibited by NF κ B and IRF3 at interferon transcription. This part of the study is also original because of the utilization way of the method in a pathogen activated pathway model to limit transcription and together with detailed model structure, this methodology provided the opportunity to mimic nonlinear dose response relation in the pathway. The same methodology is also applied for PKR transcription but this time for single transcription factor. Simulation results were validated by empirical expression profiles for IFN β and IRF3. ISGF3 responses for different doses of LPS and interferon treatment are proposed in parallel to the present data in literature. The concomitant ISGF3 profile needs to be validated by further experimental gel shift data. At the down stream of ISGF3, PKR is responsible for broad antiviral, anticellular actions of the pathway and hence several cancer drugs target and modulates its activity. Concerning its importance, the model is tested for published PKR profiles. The model also provides a realistic approach in the timing of late phase in the PKR expression profile. While the simulation results are able to recapitulate the experimental expression profiles of IFN β , IRF3, Qin et al. (2005) and PKR, Donze et al. (2004); Hsu et al. (2004), the model is also supported

by literature data related with rate parameters .

To shed light on the whole picture, epigenetics is another factor having a role in the differentiation of specialized immune cells for IFN β regulation. Concerning this factor, in addition to the statistical method used here at transcription level, factors like chromosome folding may be employed to refine the model as a further study.

The deterministic modeling approach in the case of ODEs only produces data about the behaviour of population average. Today it is possible to gather plenty of data from single cell experiments such as conducted by micro-fluidic devices. To explain single cell behaviour I designed a model (at UCSD Centre of Theoretical Biological Physics) and obtained first results for IFN β production. The insertion of this model in the large system is still on process.

The attempts restricted in a single pathway can be possibly misleading because of extensive communication between the parts of immune system. This model developed as a part of a larger model involving other main pathogen activated pathways and the results are planned to be utilized in the regulation of other important transcription factor profiles such as NF κ B.

In addition to communication of Type I interferon and TLR4 pathways, TNF α pathway is important factor effecting the late phase of NF κ B because of the fact that the induction of TNF α through Trif dependent part of TLR4 pathway introduce the system with extra IKK (Lee et al, 2009). Even though insertion of this mechanism in probabilistic sense very effectively to handle the problem of the late phase regulation in a stochastic manner, Lee et al. (2009), the presence of other mechanism effective through TNF α should be also concerned. For example in Multiple Sclerosis (MS) disease, IFN β medication results with a better prognose of the disease by reduction of the relapses (Gayo et al., 1999). This is a result of a decrease in TNF α production under the drug (interferon 1b) treatment (Gayo et al., 1999). It is known that TNF α causes the lost of myelin sheets which is the source of MS. By involving the mechanisms of IFN β dependent TNF α synthesis reduction, I am about to bring in a more realistic approach for the rates of the reported stochastic model, Lee et al. (2009), and improve the model by combining linked TLR4 and IFN β with this system through PKR. This combination will result with a large hybrid model including very important four pathway of innate immune system for the first time in literature and will result with a refinement of the current main well known models of the

distinct pathways.

Even though this study begin by supposing and proposing the late phase activity of LPS stimulated pathway can be explained by defining the behaviour of the each intermediate by transfer functions and later it appears that this method is a not effective tool for such an system. However, with the ODEs model presented here two important pathways regulating to responses to bacterias (LPS-MyD88 pathway) and virus (IFN β pathway) successfully modeled and new insights in to NF κ B regulation are brought and suggested.

Involvement of many cross talk and feedback mechanisms to deal with pathogens makes immune system highly challenging in Modeling aspects, but bacteria and viruses have very effective tools to cope with these complicated challenging mechanisms, mostly based on their easily adaptable basic structures, large numbers and sophisticated decision making strategies to survive. Resolving the mechanisms in both bacterial and immune system site could provide the chance for better therapeutics, but still we are far away to resolve whole mechanism of very primitive structures and many important parts of the immune system is still elusive.

The bacterial decision making sometimes shows similarities with highly developed organisms and can be explained with game theory approaches more sophisticated than the classic game theory problem called as the Prisoner's Dilemma (Schoultz et al., 2009). Under adverse stress conditions 10% of bacteria population chose a state called competence, while 50-70% of the population either die directly or commit to sporulation, which is a stage not able to validate immediate favourable conditions. The bacteria under competence stage can take the advantage of lysed other bacterial cells genetic material to repair itself (Schoultz et al., 2009). In some cases the population survival become only possible by the bacteria's choosing competence mode. Similar rates are also valid in other life-forms. For example, to find food while the most of rats goes to known main food source, the other members of population search for other alternatives. In the cases of insufficiency in the main known food source, the members searching for alternatives can be only hope for the population. The behavioral observations of different life-forms indicating similar rates in searching alternatives can yeild a question: is it posibble use the renormalization methods to understand decision-making strategies of different life-forms regardless of their complexity level? Actually a more important question that can arise is: how logical for a population to prevent the members searching for alternatives or a better

one how logical to prevent young scientist searching for alternatives by isolating intellectually or treat them with mobing methodologies?

Pathogen life forms and immune systems evolves their own strategies in the battle between and the systems gained complex attributes challing the system biologist. Researches conducted in both type of of life forms have great value, to understand life and deal with human sicknesses.

REFERENCES

- Agalioti, T., Lomvardas, S., Parekh, B., Yie, J., Manitas, T. and Thanos, D.,** (2000). Ordered recruitment of chromatin modifying and general transcription factors to the IFN-beta promoter. *Cell*, 103, 667-678.
- Alexopoulou, L., Holt, A.C, Medzhitov, & Flavel, (1995).** Recognition of the Alpha/Beta Interferon-Stimulated Jak/Stat Pathway by the SH2 Domain-Containing Tyrosine Phosphatase SHPTP1. *Mol.Cell. Biol.*, 15, 7050 –7058.
- Alexopoulou, L., Holt, A. C., Medzhitov, R., Flavell, R. A.,** (2001). Recognition of double-stranded RNA and activation of NF- κ B by Toll-like receptor 3. *Nature*, 732-8, 413, PMID: 11607032.
- An, G. C., Faeder, J. R.,** (2009). Detailed qualitative dynamic knowledge representation using a BioNetGen model of TLR-4 signaling and preconditioning. *Mathematical Biosciences*, 217 53–63.
- An, G.,** (2009). A model of TLR4 signaling and tolerance using a qualitative, particle-event-based method: Introduction of Spatially Configured Stochastic Reaction Chambers (SCSRC), *Math Biosci*;217(1):43-52.
- Andersaon, J.D.& Widom, J.,** (2000). Sequence and position-dependence of equilibrium accessibility of nucleosomal DNA target sites. *J. Mol. Biol.*, 296, 979-987.
- Amundson S. A., Myers T. G., Fornace Jr A. J.,** (1998); Roles for p53 in growth arrest and apoptosis: putting on the brakes after genotoxic stress. *Oncogene*, 17(25), 3287-3299.
- April, J., Glover, F., Kelly, J., Laguna, M.,** (2003). Practical introduction to simulation optimization. In: Chick, S.(Ed.) Proceedings of the 2003 Winter Simulation Conference (pp. 71–78). Institute of Electrical and Electronics Engineers, Piscataway.
- Baig E. and Fish E. N.,** (2008). Distinct signature type I interferon responses are determined by the infecting virus and the target cell. *Antiviral Therapy*, 13:409–422.
- Balachandran, S., Kim, C. N., Yeh, W. C., Mak, T. W., Bhalla, K., Barber, G. N,** (1998). Activation of the dsRNA-dependent protein kinase, PKR, induces apoptosis through FADD-mediated death signaling. *EMBO J.*, 17: 6888-6902.
- Balachandran, S., Roberts, P.C., Brown, L. E. , Truong, H., Pattnaik, A. K., Archer, D. R., Barber, G.N.,** (2000). Essential role for the dsRNA-dependent protein kinase PKR in innate immunity to viral infection. *Immunity*. 13: 129–141.

- Barnes, B., Lubyova, B. & Pitha, P. M.**, (2002). On the role of IRF in host defense. *J. Interferon Cytokine Res.*, 22, 59-71.
- Barken, D., Wang, C.C., Kearns, J., Cheong, R., Hoffmann, A., Levchenko, A.**, (2005). Comment on "Oscillations in NF-kappaB signaling control the dynamics of gene expression". *Science*, 308(5718):52.
- Barton, G. M. and Medzhitov, R.**, (2003). Toll-Like Receptor Signaling Pathways. *Science*, 1524, DOI: 10.1126, 1085536.
- Basak, S., Kim, H., Kearns, J. D., Tergaonkar, V., O'Dea, E.L., Werener, S.L., Benedict C.A., Ware, C.F., Ghosh, G., Verma, I.M., Hoffmann A.**, (2007) A fourth I κ B protein within the NF-kB Signaling Module. *Cell*, 128, pp. 369-381.
- Bergqvist, S., Alverdi, V., Mengel, B., Hoffmann, A., Ghosh, G., and Komives, E. A.**, (2009). Kinetic enhancement of NF κ B DNA dissociation by I κ B α . *PNAS*, vol. 106 (46).
- Bintu, L., Buchler, N. E, Garcia, H. G, Gerland, U., Hwa, T., Kondev, J. and Phillips R.**, (2005). Transcriptional regulations by numbers: models. *Current Opinion in Genetics & Development*. 15: 116-124.
- Bintu, L., Buchler, N. E, Garcia, H. G, Gerland, U., Hwa, T., Kondev, J. and Phillips R.**, (2005). Transcriptional regulations by numbers: applications. *Current Opinion in Genetics & Development*. 15: 125–135.
- Brandman, O., Meyer, T.**, (2008). Feedback loops shape cellular signals in space and time. *Science*. 322(5900):390-5.
- Carlos, A. C. C., Gary, B. L., and David, A. V. V.**, (2007). *Evolutionary Algorithms for Solving Multi-Objective Problems. Second Edition*. Springer.
- Carpenter, S., O'Neill, L. A.**, (2007). How important are Toll-like receptors for antimicrobial responses? *Cell Microbiol.*, 9(8), 1891-901.
- Chen, J., Baig, E., Fish, E.N.**, (2004). Diversity and relatedness among the type I interferons. *J Interferon Cytokine Res.*, 24:687–698.
- Cheong, R., Bergmann, A., Werner, S. L.**, (2006). Regal J., Hoffmann A. and Levchenko A., Transient I κ B Kinase Activity Mediates Temporal NF- κ B Dynamics in Response to a Wide Range of Tumor Necrosis Factor- α Doses., *J Biol Chem.*, 281: 2945–2950.
- Cheong, R., Hoffmann, A. and Levchenko, A.**, (2008). Understanding NF- κ B signaling via mathematical modeling., *Molecular Systems Biology*, 4; Article number 192; doi:10.1038/msb.30.
- Cheong, R. and Levchenko, A.**, (2010). Oscillatory signaling processes: the how, the why and the where. *Current Opinion in Genetics and Development*, 20:665–669.
- Cho, K.-H., Shin, S-Y, Lee, H-W, and O.Wolkenhauer**, (2003). Investigations in the Analysis and Modelling of the TNF α Mediated NF- κ B Signaling Pathway. *Genome Research*, 3:2413- 2422.

- Clement, J. F., Bibeau-Poirier, A., Gravel, S. P., Grandvaux, N., Bonneil, E., Thibault, P., Meloche, S., and Servant, M. J., (2008).** Phosphorylation of IRF-3 on Ser 339 Generates a Hyperactive Form of IRF-3 through Regulation of Dimerization and CBP Association. *J. Virol.*, 82, 3984–3996.
- Conrad E., D., 1999: Mathematical models of biochemical oscillation** (Master's Thesis). VirginiaTech, Electronic Thesis and Desertations. (etd-051499-113229).
- Coello Coello C. A., Lamont G. B, Van Veldhuisen D. A., (2007).** Evolutionary Algorithms for Solving Multi-Objective Problems. Springer. ISBN 978-0-387-36797-3.
- Covert, M. W., Leung, T. H., Gaston, J. E., Baltimore, D., (2005).** Achieving stability of lipopolysaccharide-induced NF-kappaB activation. *Science*, 309: 1854–1857.
- Cutrone, E. C., Langer, J. A., (1997).** Contributions of cloned type I interferon receptor subunits to differential ligand binding. *FEBS Letters* 404 197-202.
- Dalpke, A., Heeg, K., Bartz, H., (2008).** Baetzv A. Regulation of innate immunity by suppressor of cytokine signaling (SOCS) proteins. *Immunobiology*, 213, 225–235.
- D'Angello G. J., (1983).** Tutorial on petri nets, *ACM SIGSIM Simulation Digest*, Volume 14 Issue 1-4. doi-10.1145/1102863.1102866
- David, M., Chen, H. E., Goelz, S., Larner, A. C., and Neel, B. G., (1995).** Differential Regulation of the Ternary Interferon-Receptor Complex Rather than the Affinity to the Individual Subunits Dictates Differential Biological Activities. *The Journal Of Biological Chemistry*, Vol. 283, NO. 47, pp. 32925–32936.
- David R. and Alla H., (2005).** Discrete, continuous, and hybrid Petri Nets. Springer, ISBN 9783540224808.
- Deb, K., (2001).** *Multi-Objective Optimization Using Evolutionary Algorithms*, 1st edn. Chichester: Wiley.
- Doly, J., Civas A., Navarro, S., and Uze, G. (1998).** Type I interferons: expression and signalization. *Cell. Mol. Life Sci.*, 54: 1109–1121.
- Donze, O., Deng, J., Curran, J., Sladek, R., Picard, D., and Sonenberg, N., (2004).** The protein kinase PKR: a molecular clock that sequentially activates survival and death programs. *EMBO J.*, 23, 564-571.
- Dorf, R.C and Bishop, R. H., (2008).** Modern Control Systems. *Printice Hall*, eleventh edition, 212-400.
- Doyle, S., Vaidya, S. A., O'Connell R., Dadgostar, H., Dempsey, P. W., Wu T.-T., Rao, G., Sun, R., Haberland, M. E., Modlin, R. L., and Cheng, G., (2002).** IRF3 Mediates a TLR3/TLR4-Specific Antiviral Gene Program. *Immunity*, 17, 251-263.

- Endo, T. A., Masuhara, M., Yokouchi, M., Suzuki, R., Sakamoto, H., Mitsui, K., Matsumoto, A., Tanimura, S., Ohtsubo, M., Misawa, H., Miyazaki T., Leonor N., Taniguchi T., Fujita T., Kanakura Y., Komiya S., Yoshimura A., (1997).** A new protein containing an SH2 domain that inhibits JAK kinases. *Nature.*, 387 (6636): 921-4.
- Flegel, W. A., Baumstark, M. W. , Weinstock, C., Berg, A. , And Northoff H., (1993).** Prevention of Endotoxin-Induced Monokine Release by Human Low- and High-Density Lipoproteins and by Apolipoprotein A-I. *Infection and Immunity*, p. 5140-5146
- Froese, N., Schwarzer, M., Niedick, I., Frischmann, U., Köster, M., Kröger, A., Mueller, P. P., Nourbakhsh, M., Pasche ,B., Reimann, J., Stacheli, P., Hauser, H., (2006).** Innate Immune Responses in NF- κ B-Repressing Factor-Deficient Mice. *Molecular and Cellular Biology*, p. 293–302.
- Fu, X.-Y., Schindler, C., Improt, T., Aebersold, R. and Darnell, J. E., Jr, (1992).** The Proteins of ISGF-3, the Interferon α -Induced Transcriptional Activator, Define a Gene Family Involved in Signal Transduction. *Proc. of the Natl. Acad. Sci. of the United States of America*, Vol. 89, No. 16, pp. 7840-7843.
- Gad, H. H., Dellgren, C., Hamming, O. J., Vends S., Paludan S. R., Hartmann R., (2009).** Interferon- λ is functionally an interferon but structurally related to the interleukin-10 family. *J. Biol. Chem.*, 284, 20869–20875.
- García, M. A., Gil J., Ventoso I., Guerra S., Domingo E., Rivas C., Esteban M., (2006).** Impact of Protein Kinase PKR in Cell Biology: from Antiviral to Antiproliferative Action. *Microbiology And Molecular Biology Reviews*, 70, 1032–1060.
- Gayo, A., Mozo, L., Suárez, A., Tuñón, A., Lahoz, C., and Gutiérrez, C., (1999).** Interferon beta-1b treatment modulates TNF and IFN spontaneous gene expression in MS. *Neurology*, 52:1764
- Gibney, C. A., Foreman, B. E., Nelson, G., See, V., Horton, C. A., Spiller, D. G., Edwards, S. W., McDowell, H. P., Unitt, J. F., Sullivan, E., Grimley, R., Benson, N., Broomhead, D., Kell, D. B., White, M. R., (2004).** Oscillations in NF- κ B signaling control the dynamics of gene expression. *Science*, 306, 704–708.
- Gillespie, D.T., (1977).** Stochastic modelling of coupled chemical reactions. *J.Phys. Chem.* 81, 2340-2361.
- Gioannini, T.L. and Weiss, J.P., (2007).** Regulation of interactions of Gram-negative bacterial endotoxins with mammalian cells. *Immunol Res*; 39:249–60.
- Giordanetto, F. and Kroemer, R.T., (2003).** A three-dimensional model of suppressor of cytokine signalling 1 (SOCS-1). *Protein Eng.*, 16: 115–124.

- Gohda, J., Matsumura, T., Inoue, J.,** (2004). Cutting edge: TNFR-associated factor (TRAF)6 is essential for MyD88-dependent pathway but not toll/IL-1 receptor domain-containing adaptor-inducing IFN-beta (TRIF)-dependent pathway in TLR signaling. *J Immunol.*, 173: 2913–2917.
- Gosu, V., Basith, S., Durai, P., Choi S.,** (2012). Molecular Evolution and Structural Features of IRAK Family Members. *Plos One*, 7(PLoS: e49771. doi:10.1371/journal.pone.004977111)
- Guantes, R. and Poyatos J.F.,** (2006). Dynamical principles of two-component genetic oscillators. *PloS Comput. Biol.* 2 e30.
- Günel, A.,** (2012). Modelling the interactions between TLR4 and IFN β pathways. *Journal of Theoretical Biology*, 307, 137–148
- Hacker, H., Redecke, V., Blagoev B., Kratchmarova, I., Hsu, L.C., Wang, G.G., Kamps, M.P., Raz, E., Wagner, H., Hacker, G., Mann, M., Karin, M.,** (2006). Specificity in Toll-like receptor signalling through distinct effector functions of TRAF3 and TRAF6. *Nature*, 439: 204-207.
- Hajela, P, Lin, C. Y.,** (1992). Genetic search strategies in multicriterion optimal design. *Struct Optimization*, 4(2):99–107.
- Hamidreza, E. and Christopher, D. G.,** (2008). A fast Pareto genetic algorithm approach for solving expensive multiobjective optimization problems, *J. Heuristics*, 14: 203–241.
- Hayot, F. and Jayaprakash, C.,** (2006). NF- κ B oscillations and cell to cell variability. *J. Theor. Biol*, 240(4), 583-91.
- Hayot, F. and Jayaprakash, C.,** (2008). A tutorial on cellular stochasticity and Gillespie's algorithm. Prime Technical Report. Retrieved from http://clip.med.yale.edu/courses/stochastic/Hayot_gillespie.pdf
- Hemmi, H., Takeuchi O., Sato S., Yamamoto M., Kaisho M., Sanjo H., Kawai T., Hoshino K., Takeda K., and Akira S.,** (2004). The roles of two IkappaB kinase-related kinases in lipopolysaccharide and double stranded RNA signaling and viral infection. *J. Exp. Med.*, 199, 1641–1650.
- Hida, S., Ogasawara K., Sato K., Abe M., Takayanagi H., Yokochi T., Sato T., Hirose S., Shirai T., Taki S., and Taniguchi T.,** (2000). CD8+T cell-mediated skin disease in mice lacking IRF-2, the transcriptional attenuator of interferon-alpha/beta signaling. *Immunity*. 13: 643–655.
- Hoffmann, A., and Baltimore, D.,** (2006). Circuitry of NF- κ B Signalling. *Immunological Reviews*, 210, pp.171-186.
- Hoffmann, A., Levchenko, A., Scott, M., Baltimore, D.,** 2002: The NF- κ B- I κ B signaling module: temporal control and selective gene activation. *Science* 298(5596), 1241-1245. DOI: 10.1126/science.1071914.
- Honda, K., Yanai, H., Takaoka, A. and Taniguchi, T.,** (2005). Regulation of the type I IFN induction: a current view. *International Immunology* , Vol. 17, No. 11, pp. 1367–1378.
- Honda, K. et al.,** (2005). IRF-7 is the master regulator of type-I interferon-dependent immune responses. *Nature*, 434, 772–777.

- Hostager, B. S., Catlett, I. M. & Bishop, G. A.,** (2000). Recruitment of CD40 and tumor necrosis factor receptor-associated factors 2 and 3 to membrane micro domains during CD40 signaling. *J. Biol. Chem.* 275, 15392–15398.
- Hsu, L-C, Park, J.M., Zhang, K., Lu, J-L, Maeda, S., Kaufman, R. J., Eckmann, L., Guiney, D.G, Karin, M.,** (2004). The protein kinase PKR is required for macrophage apoptosis after activation of Toll-like receptor 4. *Nature*, 428:341-345.
- Hu, J., Sealfon, S. C., Hayot, F., Jayaprakash, C., Kumar, M., Pendleton, A.C, Ganee, A., Sesma, A.F., Moran, T.M., Wetmur, J.G.,** (2007). Chromosome-specific and noisy IFNB1 transcription in individual virus-infected human primary dendritic cells. *Nucleic Acids Research*, 35(15), 5232-5241.
- Ikonen I., Biles W. E., Kumar A., Wissel J. C., Ragade R. K.,** (1997): A Genetic Algorithm for Packing Three-Dimensional Non-Convex Objects Having Cavities and Holes. In *ICGA '97*, 591-598.
- Isaacs, A., and Lindemann, J.,** (1957). Virus interference. *Proc. R. Soc. Ser. B* 47, 258–267.
- Jaks, E., Gavutis, M., Uzé, G., Martal, J. and Piehler, J.,** (2007) Differential Receptor Subunit Affinities of Type I Interferons Govern Differential Signal Activation. *J. Mol. Biol.* 2007, 366, 525–539.
- Jamaluddin, M., Wang S., Garofalo R., Elliott T., Casola A., Baron S., and Brasier, A. R.,** (2001). IFN- β mediates coordinate expression of antigen processing genes in RSV-infected pulmonary epithelial cells. *Am J Physiol Lung Cell Mol Physiol.*, 280, L248–L257.
- Janssens S., Beyaert R.,** (2003). Functional diversity and regulation of different interleukin-1 receptor-associated kinase (IRAK) family members. *Mol Cell.*, 11(2), 293-302.
- Jiang, H-Y., and Wek, R. C.,** (2005). GCN2 phosphorylation of eIF2 α activates NF- κ B in response to UV irradiation. *Biochem. J.*, 385, 371–380.
- Jones, D.F., Mirrazavi, S.K., Tamiz, M.,** (2002). Multiobjective meta-heuristics: an overview of the current state-of-the-art. *Eur J Oper Res.*, 137(1), 1–9.
- Kagan, J. C., Su, T., Horn, T., Chow, A., Akira, S. and Medzhitov, (2008).** TRAM couples endocytosis of Toll-like receptor 4 to the induction of interferon-beta. *Nature Immunology*, 9(4), 361–368.
- Kagan, J.C. and Medzhitov, R.,** (2006). Phosphoinositide-mediated adaptor recruitment controls Toll-like receptor signaling. *Cell.*, 125, 943–955.
- Kagan, J. C, Su T., Horng T., Chow A., Akira S., Medzhitov R.,** (2008). TRAM couples endocytosis of Toll-like receptor 4 to the induction of interferon-beta. *Nat Immunol.*, 9, 4.
- Kalie, E., Jaitin, D. A., Podoplelova, Y., Piehler, J., and Schreiber, G.,** (2008). The Stability of the Ternary Interferon-Receptor Complex Rather than the Affinity to the Individual Subunits Dictates Differential Biological Activities. *The Journal Of Biological Chemistry*, Vol. 283(47), 32925–32936.

- Katze, M. G.** (1995). Regulation of the interferon-induced PKR: can viruses cope? *Trends Microbiol.*, 3, 75–78
- Katze, M. G., He, Y., Jr, M.G.,** (2002). Viruses and Interferon: A fight for supremacy, *Nature Review Immunology*, 2 (9,) 675-687.
- Kawai, T., Akira, S.,** (2007). Signaling to NF- κ B by Toll-like receptor. *Trends in Molecular Medicine*, Vol.13(11), 460-9.
- Kawai, T., and Akira, S.,** (2009) The roles of TLRs, RLRs and NLRs in pathogen recognition. *International Immunology*, Vol. 21, (4), pp. 317–337.
- Kawai, T., Takeuchi, O., Fujita, T., Inoue, J., Mühlradt, P. F., Sato, S., Hoshino K., Akira, S.,** (2001). Lipopolysaccharide Stimulates the MyD88-Independent Pathway and Results in Activation of IFN-Regulatory Factor 3 and the Expression of a Subset of Lipopolysaccharide-Inducible Genes. *Immunol.*, 167, 5887-5894J.
- Kawai, T., Akira, S.,** (2006). TLR signaling. *Cell Death Differ.* 13: 816-825.
- Kawagoe T, Sato S, Matsushita K, Kato H, Matsui K, et al.,** (2008): Sequential control of Toll-like receptor-dependent responses by IRAK1 and IRAK2. *Nat Immunol*, 9, 684–691.
- Kearns, J. D., Basak, S., Werner, S.L , Huang, C.S., and Hoffmann A.,** (2006). I κ B ϵ provides negative feedback to control NF- κ B oscillations, signaling dynamics, and inflammatory gene expression, *The Journal of Cell Biology*, Vol. 173(5), 659–664.
- Keating, S. E., Moloney, G. M., Moran, E. M., Bowie, A. G.,** (2007). IRAK-2 participates in multiple toll-like receptor signaling pathways to NF κ B via activation of TRAF6 ubiquitination. *J. Biol. Chem.*, 16;282(46):33435-43.
- Kinjyo, I., Hanada, T., Inagaki-Ohara ,K., Mori, H., Aki, D., Ohishi, M., Yoshida, H., Kubo, M., Yoshimura, A.,** (2002). SOCS1/JAB is a negative regulator of LPS-induced macrophage activation. *Immunity*, 17(5), 583-591.
- Kobayashi, K., Hernandez, L. D., Jorge E. Gala, J.D., Janeway C.A., Medzhitov R., and Flavell R. A.,** (2002). IRAK-M Is a Negative Regulator of Toll-like Receptor Signaling. *Cell*, Vol. 110, 191–202.
- Kolda, T. G., Lewis, R.M., and Torczon, V.,** (2003). Optimization by direct search: New perspectives on some classical and modern methods. *SIAM Rev.*, 45, 385-482.
- Konak, A., Coit D. W.,** (2006). Multi-objective optimization using genetic algorithms: A tutorial. *Reliability Engineering and System Safety*, 91 992–1007.
- Krishna, S., Jensen, M. H. and Sneppen, K.,** (2006). Minimal model of spiky oscillations in NF- κ B signaling. *Proc. Natl Acad. Sci. USA*. 103 10840–5.

- Ku., C-L., von Bernuth., H., Picard., C., Zhang. SY., Chang., HH., Yang, K., Chrabieh, M., Issekutz, AC., Cunningham, CK., Gallin, J., Holland , SM., Roifman, C., Ehl, S., Smart, J., Tang, M., Barrat, FJ., Levy, O., McDonald, D., Day-Good, NK., Miller, R., Takada, H., Hara, T., Al-Hajjar, S., Al-Ghonaum, A., Speert, D., Sanlaville, D., Li, X., Geissmann, F., Vivier, E., Maródi, L., Garty, BZ., Chapel, H., Rodriguez-Gallego, C., Bossuyt, X., Abel, L., Puel, A., Casanova, JL., (2007).** Selective predisposition to bacterial infections in IRAK-4-deficient children: IRAK-4-dependent TLRs are otherwise redundant in protective immunity. *JEM*, 204, 2407.
- Kumar, H., Kawai T., Akira S., (2009).** Toll-like receptors and innate immunity. *Biochemical and Biophysical Research Communications*, 388, 621–625.
- Lagarias, J.C., Reeds, J.A., Wright, M.H., Wright, P., (1998).** Convergence properties of the Nelder-Mead simplex algorithm in low dimensions. *SIAM J. Optim.*, 9, 112–147.
- Lawrence, T., Bebie, M., Liu, G. Y., Nizet, V., Karin, M., (2005).** IKK α limits macrophage NF- κ B activation and contributes to the resolution of inflammation. *Nature*, 434, 1138–1143.
- Li, Q. and Verma, I.M., (2002).** NF- κ B regulation in immune system. *Nat.Rev.Immunol.*, 2:725-734.
- Lee, T.K., Denny, E.M., Sanghvi, J.C., Gaston, J.E., Maynard, N.D., Hughey, J.J., Covert, M.W., (2009).** A noisy paracrine signal determines the cellular NF- κ B response to lipopolysaccharide. *Sci Signal.*, 2(93): ra65.
- Lee, E.G., Boone, D.L., Chai, S., Libby, S.L., Chien, M., Lodolce, J.P., Ma, A., (2000).** Failure to regulate TNF-induced NF- κ B and cell death responses in A20-deficient mice. *Science*, 289, 2350–2354.
- Lee, T. C., Zhang, Y. and Schwartz, R. J., (1994).** Bifunctional transcriptional properties of YY1 in regulating muscle actin and c-myc gene expression during myogenesis. *Oncogene*, 9, 1047-1052.
- Levy, D. E., Kessler, D. S., Pine, R. and Damell, J. E., Jr, (1989).** Cytoplasmic activation of ISGF3, the positive regulator of interferon- α -stimulated transcription, reconstituted in vitro. *GenesDev.*, 3, 1362-1371
- Levy, D. A. and Garcia-Sastre A., (2001).** The virus battles: IFN induction of the antiviral state and mechanisms of viral evasion. *Cytokine & Growth Factor Reviews*, 12, 143–156.
- Lipniacki, T., Paszek, P., Brasier, A., R., Luxon, B., Kimmel, M., (2004).** Mathematical model of NF- κ B regulatory module. *Journal of Theoretical Biology*, 228, 195-215.
- Lipniacki, T., Puszynski K., Paszek P., Brasier, A. R. and Kimmel, M., (2007).** Single TNF α trimers mediating NF- κ B activation: Stochastic robustness of NF- κ B signaling. *BMC Bioinformatics*, 8: 376.
- Lu, Y-C., Yeh, W-C. Ohashi, P. S., (2008).** LPS/TLR4 signal transduction pathway. *Cytokine*, 42, 145-151.

- Mancuso, G., Midiri, A., Beninati, C., Biondo, C., Galbo, R., Akira, S., Henneke, P., Golenbock, D., Teti, G., (2004).** Dual role of TLR2 and myeloid differentiation factor 88 in a mouse model of invasive group B streptococcal disease. *J Immunol*, 172, 6324-6329.
- Marchetti, M., Monier, M.N., Fradagrada, A., Mitchell K., Baychelier F., Eid P., Johannes L., Lamaze C., (2006).** Stat-mediated signaling induced by Type I and Type II interferons (IFNs) is differentially controlled through lipid microdomain association and clathrin dependent endocytosis of IFN receptors, *Mol. Biol. Cell.*, vol. 17, 2896–2909.
- Marie, I., E.Durbin, J. and Levy, D. E., (1998).** Differential viral induction of distinct interferon- α genes by positive feedback through interferon regulatory factor-7. *The EMBO Journal* Vol.17(22), 6660–6669.
- Marshall, J. E., Gorecki, H., Walton, K., Korytowski, A., (1992).** *Time-Delay Systems; stability and performance criteria with applications*. West Sussex, England: Ellis Horwood Limited.
- Marson, A., Lawn, R. M., and Mikita, T., (2007).** Oxidized Low Density Lipoprotein Blocks Lipopolysaccharide induced Interferon b Synthesis in Human Macrophages by Interfering with IRF3 Activation. *The Journal Of Biological Chemistry*, Vol. 279 (27), 28781–28788.
- Materi W. and Wishart D. S., (2008).** Computational system biology in drug discovery and development: methods and applications. *Drug Discovery Today*, Vol 12(7/8), pp.295-303
- McCoy, C. E., Carpenter S., Pålsson-McDermott, E. M., Gearing, L. J., and O'Neill, L. A. J., (2008).** Glucocorticoids Inhibit IRF3 Phosphorylation in Response to Toll-like Receptor-3 and -4 by Targeting TBK1 Activation. *The Journal of Biological Chemistry*, vol. 283(21), 14277–14285.
- McQuarrie, D.A., (1967).** Stochastic Approach to Chemical Kinetics. *J. Appl. Prob.*, 4, 413.
- McKenna, S.D., Vergilis, K., Arulanandam, A.R., Weiser, W.Y., Nabioullin, R., Tepper, M.A., (2004).** Formation of human IFN-beta complex with the soluble type I interferon receptor IFNAR-2 leads to enhanced IFN stability, pharmacokinetics, and antitumor activity in xenografted SCID mice. *J Interferon Cytokine Res.*, 24(2):119-29.
- Merika, M., Thanos, D., (2001).** Enhanceosomes. *Curr Opin Genet Dev.*, 11, 205–8.
- Meurs, E. F., Galabru, J., Barber, G. N., Katze, M. G. & Hovanessian, A. G. , (1993).** Tumor suppressor function of the interferon-induced double-stranded RNA-activated 68000- M_r protein kinase, *Proc. Natl Acad. Sci. USA*, 90, 232–236.
- Meylan E, Burns K, Hofmann K, Blancheteau V, Martinon F, Kelliher M, Tschopp J., (2004).** RIP1 is an essential mediator of Toll-like receptor 3-induced NF-kappa B activation. *Nat Immunol.*, 5(5): 503-7.

- Mitsuzawa, H., Nishitani, C., Hyakushima, N., Shimizu, T., Sano, H., Matsushima, N., et al.,** (2006). Recombinant soluble forms of extracellular TLR4 domain and MD-2 inhibit lipopolysaccharide binding on cell surface and dampen lipopolysaccharide-induced pulmonary inflammation in mice. *J Immunol*, 177, 8133–9.
- Miyake, K.,** (2007). Innate immune sensing of pathogens and danger signals by cell surface Toll-like receptors. *Semin Immunol.*, 19: 3–10.
- Mori, M., Yoneyama, M., Ito, T., Takahashi, K., Inagaki, F., and Fujita T.,** (2004). Identification of Ser-386 of Interferon Regulatory Factor 3 as Critical Target for Inducible Phosphorylation That Determines Activation. *J. Biol. Chem.*, 279, 9698–9702
- Munshi N., Agalioti, T., Lomvardas S., Merika M., Chen G., and Thanos D.,** (2001). Coordination of a transcriptional switch by HMG1(Y) acetylation. *Science*, 293, 1133–1136.
- Munshi N., Yie Y., Merika M., Senger K., Lomvardas S., Agalioti T. and Thanos D.,** (1999). The IFN-beta enhancer: a paradigm for understanding activation and repression of inducible gene expression. *Cold Spring Harb. Symp. Quant. Biol.*, 64, 149–159.
- Nakagawa R., Naka T., Tsutsui H., Fujimoto M., Kimura A., Abe T., Seki E., Sato S., Takeuchi O., Takeda K., Akira S., Yamanishi K., Kawase I., Nakanishi K. and Kishimoto T.,** (2002). SOCS-1 Participates in Negative Regulation of LPS Responses. *Immunity*, Volume 17(5), 677–687, 1 doi: 10.1016/ S1074-7613 (02) 00449-1.
- Natoli, G., Saccani S., Bosisio D., and Marazzi I.,** (2005). Interactions of NFkB with chromatin: the art of being at the right place at the right time. *Nat. Immunol.* 6, 439–445.
- Nelder J.A. and Mead R.,** (1995). A simplex method for function minimization. *Computer Journal*, 7, 308–313.
- Nelson, D. E., Ihekweba, A. E., Elliott, M., Johnson, J. R., Gibney, C. A., Foreman, B. E., Nelson, G., See, V., Horton, C. A., Spiller, D. G., Edwards, S. W., McDowell, H. P. , Unitt, J. F., Sullivan, E., Grimley, R., Benson, N., Broomhead, D., Kell, D. B., White, M. R.,** (2004). Oscillations in NF- kB signaling control the dynamics of gene expression. *Science*, 306, 704–708.
- Normey-Rico J.E. and Camacho E.F.,** (2007). *Control of Dead-time Process*. London: Springer-Verlag.
- Nourbakhsh, M., Oumard, A., Schwarzer, M., Hauser, H.,** (2000). NRF, a nuclear inhibitor of NF-kappaB proteins silencing interferon-beta promoter, *Eur Cytokine Netw.*, Sep; 11(3): 500–1.
- Nourbakhsh, M. & Hauser, H.** (1999). Constitutive silencing of IFN-b promoter is mediated by NRF (NFkB-repressing factor), a nuclear inhibitor of NF-kB. *EMBO J.*, 18, 6415–6425.
- Nourbakhsh, M. & Hauser, H.,** (1997). The transcriptional silencer protein NRF: a repressor of NF-kB enhancers. *Immunobiology*, 198, 65–72.

- Novick, D. , Cohen, B., Tal, N. , and Rubinstein, M.,** (1995). Soluble and membrane-anchored forms of the human IFN- α /3 receptor. *Journal of Leukocyte Biology*, 57(5), 712-8.
- Núñez Miguel, R., Wong, J., Westoll, J. F., Brooks, H. J., O'Neill, L. A. J., et al.,** (2007). A dimer of the Toll-like receptor 4 cytoplasmic domain provides a specific scaffold for the recruitment of signalling adaptor proteins. *PLoS ONE*, 2, e788.
- O'Dea E. and Hoffmann A.,** (2009). NF- κ B signalling. *Wires Systems Biology and Medicine*, 1, 107-115.
- Oeckinghaus A. and Ghosh S.,** (2009). The NF- κ B Family of Transcription Factors and Its Regulation. *Cold Spring Harb Perspect Biol*, 1(4): a000034.
- O'Neill, L. A., Bowie, A. G.,** (2007). The family of five: TIR-domain-containing adaptors in Toll-like receptor signaling. *Nat Rev Immunol*, 7, 353–64.
- Oganesyan, G., Saha, S. K., Guo, B., He, J. Q., Shahangian, A., Zarnegar, B., Perry, A., Cheng, G.,** (2006). Critical role of TRAF3 in the Toll-like receptor-dependent and -independent antiviral response. *Nature*, 439, 208–211
- Oshiumi, H., Matsumoto, M., Funami, K., Akazawa, T. and Seya, T.,** (2003). TICAM-1, an adaptor molecule that participates in Toll-like receptor 3-mediated interferon- β induction. *Nat. Immunol.*, 4, 161–167.
- Pahl, H.L.,** (1999). Activators and target genes of Rel/NF-kappaB transcription factors. *Oncogene*, 18:6853-66. PMID 10602461
- Panne, D., Maniatis, T., Harrison, S.,** (2004). Crystal structure of ATF-2/c-Jun and IRF-3 bound to the interferon-beta enhancer. *EMBO J.*, 23, 4384-4393.
- Pareto, V.** (1896). *Cours d'economie politique*. Lausanne: F. Rouge.
- Pauli, E-K, Schmolke, M., Wolff, T., Viemann, D., Roth, J., et al.,** (2008). Influenza A Virus Inhibits Type I IFN Signaling via NF-kB-Dependent Induction of SOCS-3 Expression. *PLoS Pathog.*, 4(11): e1000196. doi:10.1371/journal.ppat.1000196.
- Peppel, K. and Baglioni, C.,** (1991). Deadenylation and Turnover of Interferon β mRNA. *The Journal of Biological Chemistry*, Vol. 266 (11), Issue of April 15, 6663-6666.
- Peng, J., Yuan, Q., Lin, B., Panneerselvam, P., Wang, X., Luan, X. L., Lim, S. K., Leung, B. P., Ho, B. and Ding, J. L.,** (2010). SARM inhibits both TRIF- and MyD88-mediated AP-1 activation. *Eur. J. Immunol.*, 40, 1738–1747.
- Phillips, R. J., and S. Ghosh.,** (1997). Regulation of I κ B β in WEHI 231 mature B cells. *Mol. Cell. Biol.* 17, 4390–4396.
- Rothlin, CV., Gosh, S., Zuniga EL., Oldstone, MB., Lemke, G.,** (2007). TAM receptors are pleiotropic inhibitors of the innate immune response. *Cell*, 131(6), 1124-36.

- Qin, H. Wilson, C. A., Lee, S. J, Zhao X.,and Benveniste, E. N.,** (2005). LPS induces CD40 gene expression through the activation of NF κ B and STAT-1 in macrophages and microglia. *BLOOD*, Vol 106, 9.
- Qin, B. Y., Liu, C., Lam, S.S., Srinath, H., Delston, R., Correia, J.J., Derynck, R., and Lin, K.,** (2003). Crystal structure of IRF3 reveals mechanism of autoinhibition and virus-induced phospho-activation. *Nat. Struct. Biol.*, 10, 913.
- Ogata K.,** (1990). *Modern Control Engineering*. Englewood Cliffs: Prentice- Hall Internatinal Editions., 260-270 ISBN 0-13-598731-8.
- Oppenheim A. V., Willsky A. S. with Nawab S. H.,** (1997). *Signals and Systems*. New Jersey: Prentice- Hall, Inc., ISBN 0-13-814757-4.
- Rietschel, E. T., Kirikae, T., Schade, F. U., Mamat, U., Schmidt, G., Loppnow, H., Ulmer, A. J., Zahringer, U., Seydel, U. and Di Padova, F.,** (1994). Bacterial endotoxin: molecular relationships of structure to activity and function. *FASEB. J.*, 8, 217-225.
- Roth, R., Levin, F. C., Levin, J.,** (1993). Distribution of Bacterial Endotoxin in Human and Rabbit Blood and Effects of Stroma-Free Hemoglobin. *Infection and Immunity*, 61(8), 3209-3215.
- Sato, S., Sugiyama, M., Yamamoto, M., Watanabe, Y., Kawai, T., Takeda, K., Akira, S.,** (2003). Toll/IL-1 receptor domain-containing adaptor inducing IFN-beta (TRIF) associates with TNF receptor-associated factor 6 and TANK-binding kinase 1, and activates two distinct transcription factors, NF-kappa B and IFN-regulatory factor-3, in the Toll-like receptor signaling. *J Immunol.*, 171(8), 4304-10.
- Schmitz, J., Weissenbach, M., Haan, S., Heinrich, P. C., and Schaper, F.,** (2000). SOCS3 Exerts Its Inhibitory Function on Interleukin-6 Signal Transduction through the SHP2 Recruitment Site of gp130. *The Journal of Biological Chemistry*, Vol. 275(17), Issue of April 28, 12848 –12856.
- Schultz, D., Wolynes, P. G., Ben Jacob, E., Onuchic, J. N.,** (2009). Deciding fate in adverse times: Sporulation and competence in *Bacillus subtilis*, *Proceedings of the National Academy of Sciences of the United States of America*, 106, Iss: 50, 21027-21034.
- Selvarajoo, K., Takada, Y., Gohda, J., Helmy, M., Akira, S., et al.,** (2008). Signaling Flux Redistribution at Toll-Like Receptor Pathway Junctions. *Plos One*, 3(10): e3430. doi: 10.1371/journal.pone.0003430.
- Selvarajoo, K.,** (2006). Discovering differential activation machinery of the Toll-like receptor 4 signaling pathways in MyD88 knockouts. *Febs Letters*, 580, Issue 5, 1457-1464.
- Selvarajoo K., Tomita M. & Tsuchiya M.,** (2009). Can complex cellular processes be governed by simple linear rules? *J of Bioinformatics and Comp Biol.*, 7(1):243-268.

- Seok, J., Xiao, W., Moldawer, L. L., Davis, R. W. and Covert, M. W.,** (2009). A dynamic network of transcription in LPS-treated human subjects. *BMC Systems Biology*, 3, 78. doi: 10.1186/1752-0509-3-78.
- Servant M. J., Grandvaux N., Hiscott J.,** (2002). Multiple signaling pathways leading to the activation of interferon regulatory factor 3. *Biochem Pharmacol.*, 64, 985–992
- Shin, H. J., Lee, H., Park, J. D., Hyun, H. C., Sohn, H. O., Lee, D. W., and Kim, Y. S. ,** (2007). Kinetics of Binding of LPS to Recombinant CD14, TLR4, and MD-2 Proteins. *Mol. Cells*, Vol. 24, (1), 119-124 .
- Schrodinger E.,** (1944). *What is Life?* Cambridge University Press.
- Schrodinger E.,** (1967). *What is Life? With Mind and Matter and Autobiographical Sketches.* With a Forward by Roger Penrose. Cambridge University Pres, Canto Edition.
- Smieja, J., Jamaluddin, M., Brasier, A. R. and Kimmel, M.,** (2008). Model-based analysis of Interferon- β induced signaling pathway. *Bioinformatics*, 24(20), 2363–2369. doi:10.1093/bioinformatics/ btn400.
- Song, M. M. and Shuai, K.,** (1998). The Suppressor of Cytokine Signaling (SOCS) 1 and SOCS3 but Not SOCS2 Proteins Inhibit Interferon Mediated Antiviral and Antiproliferative Activities. *The Journal of Biological Chemistry*, 273, (52), Issue of December 25, 35056–35062.
- Solis, M., Romieu-Mourez, R., Goubau, D., Grandvaux, N., Mesplede, T., Julkunen, I., Nardin, A., Salcedo, M., and Hiscott, J.,** (2007). Involvement of TBK1 and IKK in lipopolysaccharide-induced activation of the interferon response in primary human macrophages. *Eur. J. Immunol.*, 37, 528–539
- Srinivas, N. and Deb, K.,** (1994). Multiobjective optimization using nondominated sorting in genetic algorithms. *Journal of Evolutionary Computation*, 2(3) 221-248.
- Starr, R., Willson, T.A., Viney, E.M., Murray, L.J., Rayner, J.R., Jenkins, B.J., Gonda, T.J., Alexander, W.S., Metcalf, D., Nicola, N.A, Hilton D.J.,** (1997). A family of cytokine-inducible inhibitors of signalling. *Nature*. 387 (6636): 917-21.
- Suyang, H., R. Phillips, R., Douglas, I., and Ghosh, S.,** (1996). Role of unphosphorylated, newly synthesized I kappa B beta in persistent activation of NF-kappa B. *Mol. Cell. Biol.*, 16, 5444–5449.
- Suzuki, N., Suzuki, S., Duncan, G. S., et al.,** (2002). Severe impairment of interleukin-1 and Toll-like receptor signalling in mice lacking IRAK-4. *Nature*; 416:750–756.
- Taketa, K., Akira S.,** (2004). TLR4 signaling pathways. *Seminars in Immunology*, 16, 3-9.
- Takeda, K., Kaisho, T., Akira, S.,** (2003). Toll-like receptors. *Annu Rev Immunol*; 21, 335-376.
- Taniguchi, T. and Takaoka, A.,** (2001). A weak signal for strong responses: interferon- α/β revisited. *Nat. Rev. Mol. Cell Biol.*, 2, 378–386.

- Tay, S., Hughey, J. J., Lee, T. K., Lipniacki T., Quake, S. R., Covert, M. W.,** (2010). Single cell NF- κ B dynamics reveal digital activation and analogue information processing. *Nature*, 466, 267-271. doi:10.1038/nature09145.
- Thanos, D. and Maniatis, T.,** (1992). The High Mobility Group protein HMG I (Y) is required for NF κ B dependent virus induction of the human IFN β gene. *Cell*, 71, 777-789.
- Thanos D, Maniatis T.,** (1995). Virus induction of human IFN beta gene expression requires the assembly of an enhanceosome. *Cell*, 83(7), 1091–1100.
- Tiana G., Krishna S., Pigolotti S., Jensen M. H., Sneppen K.** (2007). Oscillations and temporal signalling in cells. *Phys. Biol.*, 4 R1 doi: 10.1088/1478-3975/4/2/R01.
- Tobias, P. S, Soldau, K. Ulevitch, R. J.** (1986). Isolation of a lipopolysaccharide-binding acute phase reactant from rabbit serum. *J Exp Med.*, 164, 777–93.
- Tsuchida, T., Kawai, T. and Akira, S.,** (2009). Inhibition of IRF3- dependent antiviral responses by cellular and viral proteins. *Cell Research*, 19, 3-4.
- Url-1**<http://itc.virginia.edu/research/talks/matlab_gads.pdf>, accessed at 10.9.2010.
- Url-2** <<http://www.matworks.com/company/webinars>>, accessed at 8.07.2008.
- Url-3** <<http://www.wikipedia.org/wiki/Avonex>>, accessed at 10.09.2010.
- Url-4** < <http://www.drugbank.ca/drugs/DB00060> >, accessed at 29.06.2006.
- Uzé, G., Schreiber, G., Piehler, J. and Pellegrini, S.,** (2007). The Receptor of the Type I Interferon Family. *Curr Top Microbiol Immunol.*, 316, 71-95.
- Villunger A, Michalak EM, Coultas L, Müllauer F, Böck G, Ausserlechner MJ, et al.,** (2003). p53- and drug-induced apoptotic responses mediated by BH3-only proteins Puma and Noxa. *Science*, 302:1036–1038.
- Visintin A., Halmen, K. A., Latz, E., Monks, B. G. and Golenbock, D. T.,** (2005). Pharmacological Inhibition of Endotoxin Responses Is Achieved by Targeting the TLR4 Coreceptor MD-2. *J. Immunol.*, 175, 6465-6472.
- Vivarelli, M.S., McDonald, D., Miller, M., Cusson, N., Kelliher, M., Geha, R.S.,** (2004). RIP links TLR4 to Akt and is essential for cell survival in response to LPS stimulation. *J. Exp. Med.*, 200 (3), 399–404.
- Wang CY., Mayo MW., Korneluk RG., Goeddel DV., Baldwin Jr AS.,** (1998). NF-kappaB antiapoptosis: induction of TRAF1 and TRAF2 and c-IAP1 and c-IAP2 to suppress caspase-8 activation. *Science*, 281, 1680-1683.
- Wathelet, M.G., Lin, C.H., Parekh, B.S., Ronco, L.V., Howley, P.M. and Maniatis, T.,** (1998). Virus infection induces the assembly of coordinately activated transcription factors on the IFN β enhancer in vivo. *Mol. Cell*. 1998, 1, 507–518.

- Watanabe, N., Kuriyama, H., Sone, H., Neda, H., Yamauchi, N., Maeda, M. and Niitsu, Y.,** (1998). Continuous internalization of tumor necrosis factor receptors in a human myosarcoma cell line. *The Journal of Biological Chemistry*, 263, 10262-10266.
- Wellstead P.,** (2005). Schroedinger's Legacy: Systems and Life. E.T.S. Walton Lecture, A part of W.R. Hamilton Bi-Centenary Lecture Series, Royal Irish Academy. Retrived from <http://www.hamilton.ie/peter/schroedinger.pdf>
- Werner, S. L., Kearns, J.D, Zadorozhnaya, V., Lynch, C., O'Dea, E., Boldin, M P, Ma, A., Baltimore, D, Hoffmann, A.,** (2008). Encoding NF-kappaB temporal control in response to TNF: distinct roles for the negative regulators IkappaBalpha and A20. *Genes Dev.*, 22 (15): 2093-101.
- Werner, S.L, Barken, D., Hoffmann, A.,** (2005). Stimulus Specificity of Gene Expression Programs Determined by Temporal Control of IKK Activity., *Science*, 309(5742), 1857-61.
- Wertz, IE., O'Rourke, KM., Zhou, H., Eby, M., Aravind, L., Seshagiri, S., Wu, P., Wiesmann, C., Baker, R., Boone, DL., Ma, A., Koonin, EV, Dixit, VM.,** (2004). De-ubiquitination and ubiquitin ligase domains of A20 downregulate NF-kappaB signalling. *Nature*, 430(7000), 694-9.
- Wetter, M., Wrigth , J.,** (2003). Comparison of a generalized pattern search and a genetic algorithm optimization method. *Proc. 8 th International Building Performance Simulation Association Conference*, 3, 1401-1408.
- Wormald, S. and Hilton, D.J.,** (2004). Inhibitors of Cytokine Signal Transduction. *J Biol Chem*, 279(2), 821–824.
- Wright, S. D., Tobias, P. S., Ulevitch, R. J., Ramos, R. A.,** (1989). Lipopolysaccharide (LPS) binding protein opsonizes LPS-bearing particles for recognition by a novel receptor on macrophages. *J Exp Med*, 170, 1231–41.
- Wright, S. D., Ramos, R. A., Tobias, P. S., Ulevitch, R. J., Mathison, J. C,** (1990). CD14, a receptor for complexes of lipopolysaccharide (LPS) binding protein. *Science*, 249, 1431–3.
- Xu, Y., Cheng, G. and Baltimore, D.,** (1996). Targeted disruption of TRAF3 leads to postnatal lethality and defective T-dependent immune responses. *Immunity*, 5, 407–415.
- Yamada, S., Shiono, S., Joo, A., Yoshimura, A.,** (2003). Control mechanism of JAK/STAT signal transduction pathway. *FEBS Letters*, 534, 190-196.
- Yamamoto, M., Sato S., Hemmi H., Hoshino K., Kaisho T., Sanjo H., Takeuchi O., Sugiyama M., Takeuchi O., Sugiyami M., Okabe M., Takede K., Akira S.,** (2003). Role of Adaptor TRIF in the MyD88-Independent Toll-Like Receptor Signaling Pathway. *Science*, 301, 640-643.

- Yang, H., Ma G., Lin C. H., Orr M., Wathelet M. G.,** (2004). Mechanism for transcriptional synergy between interferon regulatory factor (IRF)-3 and IRF-7 in activation of the interferon-gene promoter. *Eur. J. Biochem*, 271, 3693–3703.
- Yao, Y.-L., W.-M. Yang, and E. Seto.,** (2001). Regulation of transcription factor YY1 by acetylation and deacetylation. *Mol. Cell. Biol.*, 21, 5979–5991.
- Yasukawa, H., Misawa, H., Sakamoto, H., Masuhara, M., Sasaki, A., et al.** (1999). The JAK-binding protein JAB inhibits janus tyrosine kinase activity through binding in the activation loop. *EMBO J.*, 18, 1309–1320.
- Yoon C.-H., Lee E.-S., Lim D.-S., Bae Y.-S.,** (2009). PKR, a p53 target gene, plays a crucial role in the tumor-suppressor function of p53. *Proc Natl Acad Sci USA*, 106, 7852–7857.
- Yie J., Merika M., Munshi N., Chen G. and Thanos D.,** (1999). The role of HMG χ (Y) in the assembly and function of the IFN- β enhanceosome. *The EMBO Journal*, 18 (11), 3074–3089.
- Zhang SY., Jouanguy E., Ugolini, S., Smahi, A., Elain, G., Romero, P., Segal, D, Sancho-Shimizu, V., Lorenzo, L., Puel A, Picard C, Chapgier A, Plancoulaine, S., Titeux, M., Cognet, C., von Bernuth, H., Ku, CL., Casrouge, A., Zhang, XX., Barreiro, L., Leonard, J., Hamilton, C., Lebon, P., Héron, B., Vallée, L., Quintana-Murci, L., Hovnanian, A., Rozenberg, F., Vivier, E., Geissmann, F., Tardieu, M., Abel, L., Casanova, JL.,** (2007). TLR3 deficiency in patients with herpes simplex encephalitis. *Science*, 317(5844):1522-7.
- Zitzler, E., Deb, K., Thiele, L.,** (2000). Comparison of multi-objective evolutionary algorithms: empirical results. *Evol Comput*, 8(2): 173–95.
- Zurawski R. and Zhou M.,** (2004). Petri Nets and Industrial Applications: A Tutorial. *IEEE Transactions on Industrial Electronics*, 41(6).

APPENDICES

APPENDIX A : Codes

APPENDIX B : Data

APPENDIX A

A1-)The Code Calling the File in Figure 3.1c

```
-  
function z=yeniseri37u(x)  
global k1 k2 k3 a1 a3 K1%The global variables should also defined in  
command window.  
k1=x(1);  
k2=x(2);  
k3=x(3);  
a1=x(4);  
a3=x(5);  
K1=x(6);  
sim('yeniseri301u');  
z= hata(101);
```

A2-) The Optimization Code

(this code calls the yeniseri37u and yeniseri37u calls yeniseri301u)

```
-  
function [x,fval,exitflag,output,population,score] =  
yeniseri37u(nvars,lb,ub,PopulationSize_Data)  
% This is an auto generated M-file from Optimization Tool.  
% Start with the default options  
options = gaoptimset;  
% Modify options setting  
options = gaoptimset(options,'PopulationSize', 40);  
options = gaoptimset(options,'SelectionFcn', {  
@selectiontournament [] });  
options = gaoptimset(options,'HybridFcn',      { @patternsearch  
[] });  
options = gaoptimset(options,'Display', 'off');  
[x,fval,exitflag,output,population,score] = ...  
ga(@yeniseri37u,6,[],[],[],[],[],[0 0 0 0 0 0],[1 1 1 1 1  
1],options);
```

A3-) The Simulink Code in Figure 3.1c

-----			LibraryLinkDisplay	"none"
Model {			Widelines	off
Name	"yeniseri301u"		ShowLineDimensions	off
Version	7.4		ShowPortDataTypes	off
MdlSubVersion	0		ShowLoopOnError	on
GraphicalInterface	{		IgnoreBidirectionalLines	off
NumRootInputs	0		ShowStorageClass	off
NumRootOutputs	0		ShowTestPointIcons	on
ParameterArgumentNames	"		ShowSignalResolutionIcons	on
ComputedModelVersion	"1.48"		ShowViewerIcons	on
NumModelReferences	0		SortedOrder	off
NumTestPointedSignals	0		ExecutionContextIcon	off
}			ShowLinearizationAnnotations	on
SaveCharacterEncoding	"windows-1254"		BlockNameDataTip	off
SaveDefaultBlockParams	on		BlockParametersDataTip	off
ScopeRefreshTime	0.035000		BlockDescriptionStringDataTip	off
OverrideScopeRefreshTime	on		ToolBar	on
DisableAllScopes	off		StatusBar	on
DataTypeOverride	"UseLocalSettings"		BrowsersShowLibraryLinks	off
MinMaxOverflowLogging	"UseLocalSettings"		BrowserLookupUnderMasks	off
MinMaxOverflowArchivemode	"Overwrite"		SimulationMode	"normal"
MaxMdlFileInLength	120		LinearizationMsg	"none"
Created	"Thu Apr 17 11:39:25 2008"		Profile	off
Creator	"REGAL"		ParamWorkspaceSource	"MATLABWorkspace"
UpdateHistory	"UpdateHistoryNever"		AccelSystemTargetFile	"accel.tlc"
ModifiedByFormat	"%<Auto>"		AccelTemplateMakefile	"accel_default_tmf"
LastModifiedBy	"aylingunel"		AccelMakeCommand	"make_rtwt"
ModifiedDateFormat	"%<Auto>"		TryForcingSFcnDF	off
LastModifiedDate	"Tue Dec 11 16:26:31 2012"		RecordCoverage	off
RtWModifiedDateStamp	276895188		CovPath	"/"
ModelVersionFormat	"1.%<AutoIncrement:48>"		CovSaveName	"covdata"
ConfigurationManager	"None"		CovMetricSettings	"dw"
SampleTimeColors	off		CovNameIncrementing	off
SampleTimeAnnotations	off		CovHtmlReporting	on

CovForceBlockReductionOff	on	Simulink.ConfigSet {
covSaveCumulativeToWorkspaceVar	on	\$ObjectID
CovSaveSingleToWorkspaceVar	on	Version
CovCumulativeVarName	"covCumulativeData"	Array {
CovCumulativeReport	off	Type
CovReportOnPause	on	Dimension
CovModelRefEnable	"Off"	Simulink.SolverCC {
CovExternalEMLEnable	off	\$ObjectID
ExtModeBatchMode	off	Version
ExtModeEnableFloating	off	StartTime
ExtModeEnableFloating	on	StopTime
ExtModeTrigType	"manual"	AbsTol
ExtModeTrigMode	"normal"	FixedStep
ExtModeTrigPort	"1"	InitialStep
ExtModeTrigElement	"any"	MaxNumMinSteps
ExtModeTrigDuration	1000	MaxOrder
ExtModeTrigDurationFloating	"auto"	ZcThreshold
ExtModeTrigHoldOff	0	ConsecutiveZCsStepRelTol
ExtModeTrigDelay	0	MaxConsecutiveZCs
ExtModeTrigDirection	"rising"	ExtrapolationOrder
ExtModeTrigLevel	0	NumberNewtonIterations
ExtModeArchiveMode	"off"	MaxStep
ExtModeAutoInconesShot	off	MinStep
ExtModeIncdIrWhenArm	off	MaxConsecutiveMinStep
ExtModeAddSuffixToVar	off	RelTol
ExtModeWriteAllDataTOWS	off	SolverMode
ExtModeArmWhenConnect	on	Solver
ExtModeSkipDownloadWhenConnect	off	SolverName
ExtModelLogAll	on	ShapePreserveControl
ExtModeAutoUpdateStatusClock	off	ZeroCrossControl
BufferReuse	on	ZeroCrossAlgorithm
ShowModelReferenceBlockVersion	off	AlgebraicLoopSolver
ShowModelReferenceBlockIO	off	SolverResetMethod
Array {		PositivePriorityOrder
Type	"Handle"	AutoInsertRateTranBlk
Dimension	1	

```

SampleTimeConstraint    "Unconstrained"
InsertRTBMode           "Whenever possible"
}
Simulink.DataIOCC {
    $ObjectID            3
    Version              "1.6.0"
    Decimation           "1"
    ExternalInput        "[t, u]"
    FinalStateName       "xFinal"
    InitialState         "xInitial"
    LimitDataPoints      on
    MaxDataPoints        "1000"
    LoadExternalInput   off
    LoadInitialState     off
    SaveFinalState       off
    SaveCompleteFinalSimState off
    SaveFormat           "Array"
    SaveOutput           on
    SaveState            off
    SignalLogging        on
    InspectsSignalLogs  off
    SaveTime             on
    ReturnWorkspaceOutputs off
    StatesSaveName       "xout"
    TimesSaveName        "tout"
    OutputSaveName       "yout"
    SignalLoggingName     "logout"
    OutputOption         "RefineOutputTimes"
    OutputTimes          "[]"
    ReturnWorkspaceOutputsName "out"
    Refine               "1"
}
Simulink.OptimizationCC {
    $ObjectID            4
    Version              "1.6.0"

```

```

    Array {
        Type           "Cell"
        Dimension      4
        Cell "ZeroExternalMemoryAtStartup"
        Cell "ZeroInternalMemoryAtStartup"
        Cell "NoFixptDivByZeroProtection"
        Cell "OptimizeModelRefInitCode"
        PropName       "DisabledProps"
    }
    BlockReduction      on
    BooleanDataType     on
    ConditionallyExecuteInputs on
    InlineParams        off
    UseIntDivNetslope   off
    InlineInvariantSignals off
    OptimizeBlockIOStorage on
    BufferReuse          on
    EnhancedBackFolding off
    StrengthReduction   off
    EnforceIntegerDowncast on
    ExpressionFolding   on
    BooleanASBitfields  off
    EnableMemory        on
    MemoryThreshold     64
    PassReuseOutputArgsAs "Structure reference"
    ExpressionDepthLimit 2147483647
    FoldNonRolledExpr   on
    LocalBlockOutputs   on
    RollThreshold       5
    SystemCodeInlineAuto off
    StateBitsets        off
    Databitsets         off
    UseTempVars         off
    ZeroExternalMemoryAtStartup on
    ZeroInternalMemoryAtStartup on

```

InitFltsAndDbIsToZero	on	SolverPfmCheckMsg	"warning"
NoFixptDivByZeroProtection	off	InheritedTsInSrcMsg	"warning"
EfficientFloat2IntCast	off	DiscreteInheritContinuousMsg	"warning"
EfficientMapNaN2IntZero	on	MultiTaskDSMsg	"error"
OptimizeModelRefInitCode	off	MultiTaskConDecSysMsg	"error"
LifeSpan	"inf"	MultiTaskRateTransMsg	"error"
BufferReusableBoundary	on	SingleTaskRateTransMsg	"none"
SimCompilerOptimization	"Off"	TaskSwitchSamePriorityMsg	"warning"
AccelerVerbseBuild	off	SigSpecEnsuresamplerTimeMsg	"warning"
		CheckMatrixSingularityMsg	"none"
		IntegerOverflowMsg	"warning"
Simulink.DebuggingCC {		Int32ToFloatConvMsg	"warning"
\$ObjectID	5	ParameterDowncastMsg	"error"
Version	"1.6.0"	ParameterOverflowMsg	"error"
RTPrefix	"error"	ParameterUnderflowMsg	"none"
ConsistencyChecking	"none"	ParameterPrecisionLossMsg	"warning"
ArrayBoundsChecking	"none"	ParameterTunabilityLossMsg	"warning"
SignalInfnAnchoring	"none"	FixptConstUnderflowMsg	"none"
SignalRangeChecking	"none"	FixptConstOverflowMsg	"none"
ReadBeforeWriteMsg "UseLocalSettings"		FixptConstPrecisionLossMsg	"none"
WriteAfterWriteMsg "UseLocalSettings"		UnderspecifiedDataTypeMsg	"none"
WriteAfterReadMsg "UseLocalSettings"		UnnecessaryDataTypeConvMsg	"none"
AlgebraicLoopMsg	"warning"	VectorMatrixConversionMsg	"error"
ArtificialAlgebraicLoopMsg	"warning"	InvalidFcnCallConvMsg	"Use local settings"
SaveWithDisabledLinksMsg	"warning"	FcnCallInpInsideContextMsg	"none"
SaveWithParameterizedLinksMsg	"none"	SignalLabelMismatchMsg	"warning"
ChecksInitialOutputMsg	on	UnconnectedInputMsg	"warning"
UnderspecifiedInitializationDetection	"Classic"	UnconnectedOutputMsg	"warning"
MergeDetectMultiDrivingBlocksExec	"none"	UnconnectedLinkMsg	"warning"
CheckExecutionContextPrestartOutputMsg	off	SFCCompatibilityMsg	"none"
CheckExecutionContextRuntimeOutputMsg	off	UniqueDataStoreMsg	"none"
SignalResolutionControl	"UseLocalSettings"	BusObjectLabelMismatch	"warning"
BlockPriorityViolationMsg	"warning"	RootOutputRequireBusObject	"warning"
MinStepsizeMsg	"warning"	AssertControl	"UseLocalSettings"
TimeAdjusmentMsg	"none"	EnableOverflowDetection	off
MaxConsecutiveZCMsg	"error"		


```

ModelReferenceIOMsg          "none"
ModelReferenceVersionMismatchMessage "none"
ModelReferenceIOMismatchMessage "none"
ModelReferenceCSMismatchMessage "none"
UnknownTsInSupMsg           "warning"
ModelReferenceDataLoggingMessage "warning"
ModelReferenceSymbolNameMessage "warning"
ModelReferenceExtraNoncontSigs  "error"
StateNameClashWarn          "warning"
SimStateInterfaceChecksMismatchMsg "warning"
StrictBusMsg                "warning"
LoggingUnavailablesignals    "error"
BlockIODiagnostic           "none"
}

Simulink.HardwareCC {
  $ObjectID          6
  Version            "1.6.0"
  ProdBtPerChar      8
  ProdBtPerShort     16
  ProdBtPerInt       32
  ProdBtPerLong      32
  ProdIntDivRoundTo  "Undefined"
  ProdEndianness     "Undefined"
  ProdWordSize       32
  ProdShiftRightIntArith on
  ProdHWDviceType "32-bit Generic"
  TargetBtPerChar    8
  TargetBtPerShort   16
  TargetBtPerInt     32
  TargetBtPerLong    32
  TargetShiftRightIntArith on
  TargetIntDivRoundTo "Undefined"
  TargetEndianness   "Unspecified"
  TargetWordSize     32
  TargetTypeEmulationWarnSuppressLevel 0
}

Simulink.SFSimCC {
  $ObjectID          8
  Version            "1.6.0"
  SFSimEnabledDebug on
  SFSimOverflowDetection on
  SFSimEcho          on
  SimBlas            on
  SimCtrlC           on
  SimExtrIntrinsic on
  SimIntegrity       on
  SimUseLocalCustomCode off
  SimBuildMode       "sf_incremental_build"
}

Simulink.RTWCC {
  $BackupClass      "Simulink.RTWCC"
  $ObjectID         9
  Version           "1.6.0"
  Array {
    Type           "Cell"
    Dimension      1
  }
  Cell "IncludeHyperlinkInReport"
}

```

PropName	"DisabledProps"	Dimension	2
	}	Simulink.CodeAppCC {	
	SystemTargetFile	\$ObjectID	10
		Version	"1.6.0"
GenCodeonly	off	Array {	
MakeCommand	"make_rtw"	Type	"Cell"
GenerateMakefile	on	Dimension	16
TemplateMakefile	"grt_default_tmf"	Cell	
GenerateReport	off	Cell	"IgnoreCustomStorageClasses"
SaveLog	off	Cell	"InsertBlockDesc"
RTWVerbose	on	Cell	"SFDataObjDesc"
RetainRTWFile	off	Cell	"SimulinkDataObjDesc"
ProfileTLC	off	Cell	"DefineNamingRule"
TLCDebug	off	Cell	"SignalNamingRule"
TLCCoverage	off	Cell	"ParamNamingRule"
TLCAssert	off	Cell	"InlineDPrmAccess"
ProcessScriptMode	"Default"	Cell	"CustomSymbolStr"
ConfigurationMode	"Optimized"	Cell	"CustomSymbolStrGlobalVar"
ConfigAtBuild	off	Cell	"CustomSymbolStrType"
RTWUseLocalCustomCode	off	Cell	"CustomSymbolStrField"
RTWUseSimCustomCode	off	Cell	"CustomSymbolStrFcn"
IncludeHyperlinkInReport	off	Cell	"CustomSymbolStrBlkIO"
LaunchReport	off	Cell	"CustomSymbolStrTmpVar"
TargetLang	"C"	Cell	"CustomSymbolStrMacro"
IncludeBusHierarchyInRTWFile	off	PropName	"DisabledProps"
BlockHierarchyMap	off	}	
IncludeERTFirstTime	off	ForceParamTrailComments	off
GenerateTraceInfo	off	GenerateComments	on
GenerateTraceReport	off	IgnoreCustomStorageClasses	on
GenerateTraceReports1	off	IgnoreTestpoints	off
GenerateTraceReportsf	off	InchierarchyInIds	off
GenerateTraceReportEm1	off	MaxIdLength	31
GenerateCodeInfo	off	PreserveName	off
RTWCompilerOptimization	"Off"	PreserveNameWithParent	off
CheckMdlBeforeBuild	"Off"	ShowEliminatedStatement	off
Array {		IncAutoGenComments	off
Type	"Handle"		


```

    FontAngle "normal"
    UsedDisplayTextasClickCallback off
}
}
LineDefaults {
    FontName "Arial"
    FontSize 9
    FontWeight "normal"
    FontAngle "normal"
}
BlockParameterDefaults {
    Block {
        BlockType Fcn
        Expr "sin(u[1])"
        SampleTime "-1"
    }
    Block {
        BlockType Gain
        Gain "1"
        Multiplication "Element-wise(K.*u)"
        ParamMin "[]"
        ParamMax "[]"
        ParameterDataTypeMode "Same as input"
        ParameterDataType "fixdt(1,16,0)"
        ParameterScalingMode "Best Precision: Matrix-wise"
        ParameterScaling "[]"
        ParamDataTypeStr "Inherit: Same as input"
        OutMin "[]"
        OutMax "[]"
        OutDataTypeMode "Same as input"
        OutDataType "fixdt(1,16,0)"
        OutScaling "[]"
        OutDataTypeStr "Inherit: Same as input"
        LockScale off
        RndMeth "Floor"
        SaturateOnIntegerOverflow on
    }
    SampleTime "-1"
}
}
Block {
    BlockType Integrator
    ExternalReset "none"
    InitialConditionSource "internal"
    InitialCondition "0"
    LimitOutput off
    UpperSaturationLimit off
    LowerSaturationLimit "-inf"
    ShowSaturationPort off
    ShowStatePort off
    AbsoluteTolerance "auto"
    IgnoreLimit off
    ZeroCross on
    ContinuousStateAttributes ""
}
}
Block {
    BlockType Mux
    Inputs "4"
    DisplayOption "none"
    UseBusObject off
    BusObject "BusObject"
    NonVirtualBus off
}
}
Block {
    BlockType Saturate
    UpperLimit "0.5"
    LowerLimit "-0.5"
    LinearizeAsGain on
    ZeroCross on
    SampleTime "-1"
    OutMin "[]"
    OutMax "[]"
    OutDataTypeMode "Same as input"
}

```

```

        OutDataType      "fixdt(1,16,0)"
        OutScaling        "[]"
        OutDataTypeStr    "Inherit: Same as input"
        LockScale         off
        RndMeth            "Floor"
    }

    Block {
        BlockType
        ModelBased         scope
        TickLabels          off
        ZoomMode            "OneTimeTick"
        Grid               "on"
        TimeRange           "auto"
        YMin               "-5"
        YMax               "5"
        SaveToWorkspace    off
        SaveName            "ScopedData"
        LimitDataPoints    on
        MaxDataPoints      "5000"
        Decimation         "1"
        SampleInput        off
        SampleTime         "-1"
    }

    Block {
        BlockType
        Time              Step
        Before            "1"
        After             "0"
        SampleTime        "1"
        VectorParamsID    "-1"
        ZeroCross         on
    }

    Block {
        BlockType
        IconShape         Sum
        "rectangular"
    }

        Inputs            "++"
        CollapseMode      "All dimensions"
        CollapsedDim      "1"
        InputSameDr       on
        AccumDataTypesStr "Inherit: Inherit via
        internal rule"

        OutMin            "[]"
        OutMax            "[]"
        OutDataTypeMode   "Same as first input"
        OutDataType        "fixdt(1,16,0)"
        OutScaling        "[]"
        OutDataTypeStr    "Inherit: Same as first input"
        LockScale         off
        RndMeth            "Floor"
        SaturateOnIntegerOverflow on
        SampleTime        "-1"
    }

    Block {
        BlockType
        VariableName      ToWorkspace
        MaxDataPoints     "simulink_output"
        Decimation        "1000"
        SampleTime        "1"
        FixptAsFl         "0"
    }

    Block {
        BlockType
        TransferFcn       off
        Numerator          "[]"
        Denominator        "[1 2 1]"
        AbsoluteTolerance "auto"
        ContinuousStateAttributes ""
        Realization        "auto"
    }

    Block {
        BlockType
        TransportDelay
    }

```

```

        DelayTime          "1"
        InitialOutput      "0"
        BufferSize          "1024"
        FixedBuffer        off
        TransDelayFeedthrough off
        PadeOrder           "0"
    }
}
System {
    Name                    "yeniseri301u"
    Location                [-187, 477, 808, 1067]
    Open                    on
    ModelBrowserVisibility  off
    ModelBrowserWidth       200
    ScreenColor             "white"
    PaperOrientation        "landscape"
    PaperPositionMode       "auto"
    PaperType               "A4"
    PaperUnits              "centimeters"
    TiledPaperMargins       [0.500000, 0.500000, 0.500000,
0.500000]
    TiledPagescale         1
    ShowPageBoundaries     off
    ZoomFactor              "80"
    ReportName              "simulink-default.rpt"
    SIDHighWatermark       25
    Block {
        BlockType          TransferFcn
        Name                "1"
        SID                 1
        Position            [190, 129, 295, 191]
        BackgroundColor     "yellow"
        Numerator            [39.89 216.318 516.102 0]
        Denominator          [1 0.4784 12.938 0]
    }
}

```

```

        Block {
            BlockType      TransferFcn
            Name            "2"
            SID             2
            Position        [190, 232, 295, 288]
            BackgroundColor "[0.501961, 0.501961, 1.000000]"
            Numerator        [16.52 393.71028 -10.44]
            Denominator      " [1 4.086 0]"
        }
    }
    Block {
        BlockType          TransferFcn
        Name                "3"
        SID                 3
        Position            [190, 329, 300, 381]
        BackgroundColor     "cyan"
        Numerator            [-30.2 736]
        Denominator          "[1 8]"
    }
    Block {
        BlockType          Fcn
        Name                "Fcn"
        SID                 4
        Position            [620, 240, 680, 270]
        Expr                "u^2"
    }
}
    Block {
        BlockType          Gain
        Name                "Gain1"
        SID                 5
        Position            [425, 145, 450, 175]
        BackgroundColor     "[0.501961, 1.000000, 0.501961]"
        Gain                "k1"
        ParameterDataTypeMode "Inherit via internal rule"
        ParameterDataType    "sfix(16)"
        ParameterScaling      "2^0"
    }
}

```

```

ParamDataTpeStr "Inherit: Inherit via internal rule"
OutDataTpeMode "Inherit via internal rule"
OutDataTpe "sfix(16)"
OutScaling "2^0"
OutDataTpeStr "Inherit: Inherit via
internal rule"
SaturateOnIntegerOverflow off
}
Block {
  BlockType Gain
  Name "Gain2"
  SID 6
  Position [425, 245, 455, 275]
  BackgroundColor [0.501961, 1.000000, 0.501961]
  Gain "K2"
  ParameterDataTpeMode "Inherit via internal rule"
  ParameterDataTpe "sfix(16)"
  ParametersScaling "2^0"
  ParamDataTpeStr "Inherit: Inherit via internal rule"
  OutDataTpeMode "Inherit via internal rule"
  OutDataTpe "sfix(16)"
  OutScaling "2^0"
  OutDataTpeStr "Inherit: Inherit via internal rule"
  SaturateOnIntegerOverflow off
}
Block {
  BlockType Gain
  Name "Gain3"
  SID 7
  Position [425, 340, 455, 370]
  BackgroundColor [0.501961, 1.000000, 0.501961]
  Gain "K3"
  ParameterDataTpeMode "Inherit via internal rule"
  ParameterDataTpe "sfix(16)"
  ParameterScaling "2^0"
}

ParamDataTpeStr "Inherit: Inherit via internal rule"
OutDataTpeMode "Inherit via internal rule"
OutDataTpe "sfix(16)"
OutScaling "2^0"
OutDataTpeStr "Inherit: Inherit via internal rule"
SaturateOnIntegerOverflow off
}
Block {
  BlockType Gain
  Name "Gain4"
  SID 8
  Position [445, 428, 495, 472]
  BlockMirror on
  BackgroundColor "cyan"
  Gain "K1"
  ParameterDataTpeMode "Inherit via internal rule"
  ParameterDataTpe "sfix(16)"
  ParametersScaling "2^0"
  ParamDataTpeStr "Inherit: Inherit via internal rule"
  OutDataTpeMode "Inherit via internal rule"
  OutDataTpe "sfix(16)"
  OutScaling "2^0"
  OutDataTpeStr "Inherit: Inherit via internal rule"
  SaturateOnIntegerOverflow off
}
Block {
  BlockType Integrator
  Name "Integrator"
  SID 9
  Ports [1, 1]
  Position [785, 240, 815, 270]
}
Block {
  BlockType Mux
  Name "Mux"

```



```

    SID
    10
    Ports
    [2, 1]
    Position
    [620, 441, 625, 479]
    ShowName
    off
    Inputs
    "2"
    DisplayOption
    "bar"
}
Block {
    BlockType
    Name
    Saturate
    "Saturate2"
    SID
    11
    Position
    [700, 240, 730, 270]
    UpperLimit
    "10"
    LowerLimit
    "0"
}
Block {
    BlockType
    Name
    Scope
    "Scope"
    SID
    12
    Ports
    [1]
    Position
    [700, 529, 730, 561]
    Floating
    off
    Location
    [552, 421, 1172, 708]
    Open
    off
    NumInputPorts
    "1"
    List {
        ListType
        AxesTitles
        axes1
        "%<SignalLabel>"
    }
    TimeRange
    "10"
    YMin
    "0"
    YMax
    "120"
    DataFormat
    "StructureWithTime"
    SampleTime
    "0"
}

```

```

    Block {
        BlockType
        Name
        Scope
        "Scope1"
        SID
        13
        Ports
        [1]
        Position
        [875, 264, 905, 296]
        Floating
        off
        Location
        [695, 91, 1019, 331]
        Open
        off
        NumInputPorts
        "1"
        List {
            ListType
            AxesTitles
            axes1
            "%<SignalLabel>"
        }
        TimeRange
        "10"
        YMin
        "0"
        YMax
        "0.025"
        SaveName
        "ScopeData1"
        DataFormat
        "StructureWithTime"
        SampleTime
        "0"
    }
    Block {
        BlockType
        Name
        Scope
        "Scope2"
        SID
        14
        Ports
        [1]
        Position
        [430, 589, 460, 621]
        Floating
        off
        Location
        [410, 533, 734, 772]
        Open
        off
        NumInputPorts
        "1"
        List {
            ListType
            AxesTitles
            axes1
            "%<SignalLabel>"
        }
    }
}

```

```

TimeRange      "10"
YMin           "0"
YMax           "100"
SaveName       "Scopedata2"
DataFormat     "StructureWithTime"
SampleTime     "0"
}
Block {
  BlockType    Step
  Name         "Step1"
  SID          15
  Position     [50, 500, 80, 530]
  BackgroundColor "[0.607843, 0.443137, 0.756863]"
  Time         "0"
  SampleTime   "0"
}
Block {
  BlockType    Step
  Name         "Step2"
  SID          16
  Position     [50, 245, 80, 275]
  BackgroundColor "[0.607843, 0.443137, 0.756863]"
  Time         "0"
  SampleTime   "0"
}
Block {
  BlockType    Sum
  Name         "Sum"
  SID          17
  Ports        [2, 1]
  Position     [580, 245, 600, 265]
  BackgroundColor "cyan"
  ShowName     off
  IconShape    "round"
  Inputs       "|+-"
}

```

```

InputSameDT    off
OutDataTTypeMode "Inherit via internal rule"
OutDataTType    "fixdt(1, 16)"
OutScaling      "2^0"
OutDataTTypeStr "Inherit; Inherit via internal rule"
SaturateOnIntegerOverflow off
}
Block {
  BlockType    Sum
  Name         "Sum2"
  SID          18
  Ports        [2, 1]
  Position     [105, 245, 135, 275]
  BackgroundColor "lightBlue"
  ShowName     off
  IconShape    "round"
  Inputs       "|+-"
  InputSameDT  off
  OutDataTTypeMode "Inherit via internal rule"
  OutDataTType    "sfix(16)"
  OutScaling      "2^0"
  OutDataTTypeStr "Inherit; Inherit via internal rule"
  SaturateOnIntegerOverflow off
}
Block {
  BlockType    Sum
  Name         "Sum3"
  SID          19
  Ports        [3, 1]
  Position     [515, 235, 555, 275]
  BackgroundColor "lightBlue"
  ShowName     off
  IconShape    "round"
  Inputs       "|+++"
  InputSameDT  off
}

```



```

        DstBlock      "Transport\ndelay4"
        DstPort      1
    }
}
Line {
    SrcBlock
    SrcPort
    Points
    DstBlock
    DstPort
    1
}
Line {
    SrcBlock
    SrcPort
    DstBlock
    DstPort
    1
    "3"
    1
    "Transport\ndelay3"
    1
}
Line {
    SrcBlock
    SrcPort
    Points
    Branch {
        Points
        DstBlock
        DstPort
        1
        "Gain3"
        [75, 0]
    }
    Points
    DstBlock
    DstPort
    1
    "Gain4"
    [0, 95]
}
Branch {
    DstBlock
    DstPort
    3
    "Sum3"
}
}
Line {
    SrcBlock
    SrcPort
    Points
    1
    "Sum2"
    [10, 0]
}
}
Branch {
    Points
    Branch {
        DstBlock
        DstPort
        1
        "2"
    }
    Branch {
        Points
        DstBlock
        DstPort
        1
        [-5, 0; 0, 95]
        "3"
    }
}
}
Branch {
    Points
    DstBlock
    DstPort
    1
    [-5, 0; 0, -100]
    "1"
}
}
Line {
    SrcBlock
    SrcPort
    Points
    Branch {
        Points
        DstBlock
        DstPort
        1
        "Sum3"
        [-1, 1; 6, -1]
    }
    Points
    DstBlock
    DstPort
    1
    [5, 1; 0, 194]
    "Mux"
}
}
Branch {
    DstBlock
    DstPort
    1
    "Sum"
}
}
Line {
    SrcBlock
    SrcPort
    Points
    1
    "Transport\ndelay4"
}
}

```

[illegible]

```

SrcPort      1
Points      [-319, 0]
DstBlock    "Sum2"
DstPort      2
}
Line {
  SrcBlock   "Gain1"
  SrcPort    1
  Points     [50, 0]
  DstBlock   "Sum3"
  DstPort    1
}
Line {
  SrcBlock   "Gain2"
  SrcPort    1
  Points     [25, 0; 0, 12]
  DstBlock   "Sum3"
  DstPort    2
}
Line {
  SrcBlock   "Transport\ndelay3"
  SrcPort    1
  DstBlock   "Gain3"
  DstPort    1
}
Line {
  SrcBlock   "Sum"
  SrcPort    1
  DstBlock   "Fcn"
  DstPort    1
}
Annotation {
  Position   [371, 559]
}
}
}
}

```

APPENDIX B

IRF3 DATA

0	$2.76571428 \times 10^{-1}$	$4.62628571 \times 10^{-1}$	$9.92685714 \times 10^{-1}$	$6.96685714285 \times 10^{-1}$
0 min	30 min	60 min	120 min	240 min

The IRF3 data are gathered by Image J program from IRF3 gel shift assay (Qin et al., 2005) and indicates relative amount of IRF3. The IRF3 data and the simulation results are given in normalized form in Figure 3.

IFN β DATA

0 μ M	$0.42 \times 10^{-4} \mu$ M	$1.4 \times 10^{-4} \mu$ M	$1.62 \times 10^{-4} \mu$ M	$0.78 \times 10^{-4} \mu$ M
0 min	120 min	240 min	480 min	720 min

The Data obtained from by data capture (Figure 4d of Qin et al, 2005). According to these data, while IFN β protein peaks at 8 hours with 4ng/mL concentration and then declined to 2ng/mL at 12 hours (the molecular weight of interferon 1a and interferon1b reported by their manufacturers are used in the conversion to molar concentration)

PKR DATA

PKR (NIH3T3 cell extracts immunoblotting results (Donze et al, 2004))		PKR (bone-marrow-derived macrophages (Hsu et al. 2004))	
min	normalized	min	normalized
0	4.11600×10^{-2}	0	$1.39804875 \times 10^{-1}$
180	5.4432×10^{-2}	30	1.00
240	2.6438126×10^{-1}	60	$5.769054375 \times 10^{-1}$
300	4.0655009×10^{-1}	120	$4.34244125 \times 10^{-1}$
360	7.3498169×10^{-1}	240	$2.04262275 \times 10^{-1}$
420	7.8272241×10^{-1}	360	7.221298×10^{-1}
		420	$2.959473125 \times 10^{-1}$
		600	$2.930598125 \times 10^{-1}$

The data are gathered by *Image J* program from gel shift assays (Donze et al, 2004; Hsu et al. 2004). The original data from gel shift assays only include data about relative amounts. All PKR data normalized and characteristics of profiles compared with each other.

NF κ B DATA

NF κ B value is obtained by fitting a function recapitulating experimental profile (Lee et al., 2009) up to 224 min plus extrapolation up to 720 min. for the time interval between 0 and 223:

$$\text{NF}\kappa\text{B} = \text{NF}\kappa\text{B}^*$$

$$\begin{aligned} \text{NF}\kappa\text{B}^* = & -0.17364 - 0.0348 \cdot \cos(0.01408 t) + 0.22 \cdot \cos(0.02816 t) \\ & + 0.03934 \cdot \cos(0.04224 t) + 0.3238 \cdot \sin(0.01408 t) \\ & + 0.0512 \cdot \sin(0.02816 t) - 0.11668 \cdot \sin(0.04224 t) \\ & - 0.04262 \cdot \cos(0.05632 t) - 0.02422 \cdot \sin(0.05632 t) \\ & - 0.006856 \cdot \cos(0.0704 t) + 0.00658 \cdot \sin(0.0704 t); \end{aligned}$$

to extrapolate the function up to 720 min, for the time interval between 223 and 720 it is defined as:

$$\text{NF}\kappa\text{B} = \text{NF}\kappa\text{B} - 0.45 \cdot 10^{-5};$$

The function given above can be directly applied to simulation but it includes a small oscillation between 0-25 minutes and does not exactly reflect the reported experimental profile. Even though this oscillation does not affect the simulation results, to obtain the function given in Figure 4 of the main text, we defined NFκB piecewise in the interval between 0 and 224 as given below:

$$\begin{aligned} \text{NF}\kappa\text{B} &= 0.0018 + 0.000097272 \cdot (t/20)^2 \text{ in between 0 and 20 minutes,} \\ \text{NF}\kappa\text{B} &= \text{NF}\kappa\text{B}^* + 0.002 \cdot (t-20)^{-0.5} \text{ in between 20 and 31 minutes,} \\ \text{NF}\kappa\text{B} &= \text{NF}\kappa\text{B}^* \text{ in between 31 and 223 minutes.} \end{aligned}$$

In that function it is assumed that about 0.0018 μM basal level of NFκB exist to get 0 basal value 0.0018 can be subtracted from the equations and this is also has no effect on the simulation results.

CURRICULUM VITAE



Name-Surname : Aylin GÜNEL
Place and Date of Birth : K.D.Z Eregli
E-mail : aylingunel@yahoo.com
B.S : Middle East Technical University,
Department of Physics Education
Minor Program at Department of Biology
M.Sc. : Izmir Institute of Technology, Department of Physics
Thesis: Electrical and Structural Characterization of
Metallic Superconductor MgB₂
List of Publications :
2011 Gunel A., Modelling the interaction between TRL4 and IFN β
Pathways. Journal of Theoretical Biology, 307, 137-148 (2012).
2004 M. Egilmez, A. Gunel, S.Okur, M. Tanoglu and L. Ozyuzer
Key Engineering Materials, 264, 1197 (2004).

Professional Experience and Rewards:

Istanbul Technical University (ITU)
2010 - 2011 Research Assistant,
Istanbul Technical University Institute of Informatics
2008 - 2009 Affiliate graduate visiting student at University of California
San Diego
2004 - 2010 Research Assistant,
Istanbul Technical University Department of Physics
2000 - 2003 Research Assistant
Izmir Institute of Technology
Space Camp Turkey
2000 - 2000 Conducting training programs.
Likom Project and Consultancy
1998 - August 1999: Organizing and Conducting training programs for 1950 Health
Ministry employees and the operational test for Core Health
Resource Management System program.
DomiNet (Internet serves provider)
1997 - August 1998 Turkiye Coordinator of Internet Vendors.
Middle East Technical University (METU)
1994 - 1995 Teaching Assistant of fourth years biophysics courses of the
Department of Biology at METU.
Rewards:
2008 - 2009 The Scientific and Technological Research Council of Turkey

(TUBITAK).

1991- Ministry of Education of Turkey Scholarship Award, because of registering METU Department of Physics Education as first rank student of the department due to results of nationwide university entrance exam. (because of obligatory duty, I preferred not to utilize it)

Presentations on Thesis:

2011 SBHD 2011
Harvard Medical School –Boston-Poster Presentation
(Hybrid Modeling Of Crosstalk Mechanism Between Innate Immune Response Against Bacteria And Viruses)

2010 ICSB2010 – Edinburgh- Poster Presentation
(Modeling of Interferon Beta Pathway)

2008 HIBIT08 - Istanbul - Poster Presentation
(A Control Theory Approach to NF κ B - I κ B module)

Other Interests:

Painting, cycling, paragliding, hiking, chess, diving.